UC Irvine

UC Irvine Electronic Theses and Dissertations

Title

Investigating microglial regulation of the extracellular matrix in health and neurodegenerative disease

Permalink

https://escholarship.org/uc/item/32x0p5jc

Author

Crapser, Joshua D

Publication Date

2021

Copyright Information

This work is made available under the terms of a Creative Commons Attribution-NonCommercial-NoDerivatives License, availalbe at https://creativecommons.org/licenses/by-nc-nd/4.0/

Peer reviewed|Thesis/dissertation

eScholarship.org Powered by the California Digital Library
University of California

UNIVERSITY OF CALIFORNIA,
IRVINE

Investigating microglial regulation of the extracellular matrix in health and neurodegenerative disease

DISSERTATION

submitted in partial satisfaction of the requirements
for the degree of

DOCTOR OF PHILOSOPHY

in Biological Sciences

by

Joshua Daniel Crapser

Dissertation Committee:
Professor Kim Green, Vice Chair
Professor Leslie Thompson
Associate Professor Jorge Busciglio

2021

Figure 1 and portion of text in Introduction reused from Trends in Immunology, 41 (9), Green et al., 2020, *To Kill a Microglia: A Case for CSF1R Inhibitors*, Copyright 2020, with permission from Elsevier.
Figures and text in Chapter 1 reused from Brain, 143 (1), Crapser et al., 2020, *Microglial depletion prevents extracellular matrix changes and striatal volume reduction in a model of Huntington's disease*, Copyright 2020, with permission from Oxford University Press.
Figures and text in Chapter 2 reused from EBioMedicine, 58, Crapser et al., 2020, *Microglia facilitate loss of perineuronal nets in the Alzheimer's disease brain,* Copyright 2020, with permission from Elsevier.
All other materials © 2021 Joshua Daniel Crapser

DEDICATION

To my dad, for teaching me to be confident, and to my mom, for teaching me when it was appropriate to be so. To both, for resolutely supporting me in every endeavor.

I would also like to dedicate this to my grandpa, whose incredible spirit and humanity could not be eclipsed even by Alzheimer's disease, and to my grandma, who took care of him till the very end.

TABLE OF CONTENTS

LIST OF FIGURES AND TABLES

LIST OF ABBREVIATIONS

A disintegrin and metalloproteinase with thrombospondin motifs (ADAMTS)
Adult-onset leukoencephalopathy with axonal spheroids and pigmented glia (ALSP)
Alzheimer's disease (AD)
Amyloid-β (Aβ)
Blood-brain barrier (BBB)
Cathepsin B (Ctsb)
Cathepsin S (Ctss)
Central nervous system (CNS)
Chondroitinase ABC (ChABC)
Chondroitin sulfate proteoglycan (CSPG)
Colony stimulating factor 1-receptor (CSF1R)
Colony stimulating factor 1-receptor inhibition (CSF1Ri)
Extracellular Matrix (ECM)
Fluorescence-activated cell sorting (FACS)
Glial fibrillary acidic protein (GFAP)
Heparan sulfate proteoglycan (HSPG)
Huntington's disease (HD)
Immunohistochemistry (IHC)
Interferon (IFN)
Knockout (KO)
Nontransgenic (NT)
Perineuronal net (PNN)
Reads Per Kilobase of transcript per Million mapped reads (RPKM)
Wisteria floribunda agglutinin (WFA)
Wild-type (WT)

ACKNOWLEDGEMENTS

None of this work would have been possible without the unwavering support of my mentor and good friend, Dr. Kim Green. It goes without saying – though it still must be said – that he is an incredibly intelligent, passionate, and diligent scientist, whose benevolence and open-mindedness both within and outside of lab is understood by anyone that has the pleasure of working with him. Little else could motivate or enthuse me more than our countless conversations on all things related to (or wholly unrelated to) science, many of which would continue until the early hours of the morning. These served as the springboard for multiple projects, and more importantly, much laughter, without which this thesis would not have been possible.

I am exceedingly grateful to my committee members, Drs. Leslie Thompson and Jorge Busciglio, for their wisdom and kindness over the years. I could not have asked for a better committee.

I thank Dr. Louise McCullough for welcoming me into her lab as an undergraduate all those years ago, and for always offering her wisdom and support. With guidance unfettered by nicety or formality, she expected of me things I did not expect of myself, and provided me the means to accomplish much, even before I had earned anything resembling such confidence. It is for these reasons I could accomplish more than I had ever hoped.

Thanks also to the many friends I have made along the way. Dr. Allison Najafi, Dr. Elizabeth Dominguez, Dr. Lindsay Hohsfield, Dr. Monica Elmore, Rafael Lee, Miguel Arreola, Steve Kim, Edna Hingco, Emily Miyoshi, and everyone else in or associated with the Green lab who have been like a family to me since I arrived in California, and who helped me at and away from the bench more times than I can count. For the same reasons I am grateful to my former McCullough lab friends from Connecticut, Dr. Brett Friedler, Monica Spychala, and Dr. Rodney Ritzel, who continue to check up on me.

Special thanks also to Jan Frankowski, Rianne Campbell, Nicolas Grantham, Luke Hanna, Sennite Meche, and many others who are unaffiliated with work and therefore had no obligation to put up with me, and yet still chose to do so anyway.

I would like to thank my family – my mom, Terrie, my dad, Robert, and my sister, Nicole, and everyone else – who I love more than anything in this world, and who made me who I am.

This work was supported in parts by R01NS083801 (NINDS), R01AG056768 (NIA), and U54 AG054349 (NIA Model Organism Development and Evaluation for Late-onset Alzheimer's Disease (MODEL-AD)) to K.N.G., R01NS090390 (NINDS) to L.M.T., and F31NS108611 (NINDS) to J.D.C. I thank Elsevier and Oxford University Press for permission to include copyrighted figures and text as part of my dissertation.

CURICULUM VITAE

Joshua Crapser

EDUCATION:

Doctor of Philosophy, **Biological Sciences** (May 2021)
University of California, Irvine
GPA 4.0/4.0

Bachelor of Science, **Biological Sciences** (May 2013)
University of Connecticut
GPA: 4.0/4.0

RESEARCH EXPERIENCE:

Graduate Student Researcher (March 2016 – Current): Department of Neurobiology and Behavior, University of California, Irvine
Mentorship: Dr. Kim Green

- Research focus: Investigation of the role of microglia in Huntington's and Alzheimer's disease pathology and symptom development via CSF1R inhibition, with particular focus on the involvement of the extracellular matrix. Characterizing dynamics of microglial repopulation following elimination induced by CSF1R inhibition.

Research Assistant (January 2012 – August 2015): Neuroscience Department, University of Connecticut Health Center
Mentorship: Dr. Louise McCullough

- Research focus: Investigation of the role of aging and inflammation in stroke outcome, particularly pertaining to gut permeability and bacterial translocation from the gut as a source of post-stroke infection.

PUBLISHED WORK:

Peer-Reviewed Articles: *(Asterisk denotes co-first authorship)*

1) Green, K.N.*, **Crapser, J.D.***, Hohsfield, L.A.* (2020). To Kill a Microglia: A Case for CSF1R Inhibitors. *Trends in Immunology* 41, 771-784.

2) **Crapser, J.D.**, Spangenberg, E.E., Barahona, R.A., Hohsfield, L.A., Green, K.N. (2020). Microglia facilitate loss of perineuronal nets in the Alzheimer's disease brain. *EBioMedicine* 58, 102919.
    - Commentary: Reichelt, A.C. (2020). Is loss of perineuronal nets a critical pathological event in Alzheimer's disease? *EBioMedicine* 59, 102946.
3) **Crapser, J.D.**, Ochaba, J., Soni, N., Reidling, J.C., Thompson, L.M., Green, K.N. (2019). Microglial depletion prevents extracellular matrix changes and striatal volume reduction in a model of Huntington's disease. *Brain* 143, 266-288.
4) Spangenberg, E., Severson, P.L., Hohsfield, L.A., **Crapser, J.**, Zhang, J., Burton, E.A., Zhang, Y., Spevak,W., Lin, J., Phan, N.Y., et al. (2019). Sustained microglial depletion with CSF1R inhibitor impairs parenchymal plaque development in an Alzheimer's disease model. *Nature Communications* 10, 3758.
5) Ritzel R.M., Al Mamun A., **Crapser J.**, Verma R., Patel A.R., Knight B.E., Harris N., Mancini N., Roy-O'Reilly M., Ganesh B.P., Liu F., McCullough L.D. (2019). CD200-CD200R1 inhibitory signaling prevents spontaneous bacterial infection and promotes resolution of neuroinflammation and recovery after stroke. *J. Neuroinflammation* 16, 40.
6) Morozko E.L., Ochaba J., Hernandez S.J., Lau A., Sanchez I., Orellana I., Kopan L., **Crapser J.**, Duong J.H., Overman J., Yeung S., Steffan J.S., Reidling J., Thompson L.M. (2018). Longitudinal Biochemical Assay Analysis of Mutant Huntingtin Exon 1 Protein in R6/2 Mice. *J. Huntingtons Dis.* 7, 321-335.
7) Najafi A.R., **Crapser J.**, Jiang S., Ng W., Mortazavi A., West B.L., Green K.N. (2018). A limited capacity for microglial repopulation in the adult brain. *Glia* 66, 2385-2396.
8) Ritzel R.M., Lai Y.J., **Crapser J.D.**, Patel A.R., Schrecengost A., Grenier J.M., Mancini N.S., Patrizz A., Jellison E.R., Morales-Scheihing D., Venna V.R., Kofler J.K., Liu F., Verma R., McCullough L.D. (2018). Aging alters the immunological response to ischemic stroke. *Acta Neuropathol.* 136, 89-110.
9) Verma R., Ritzel R.M., **Crapser J.**, Friedler B.D., McCullough L.D. (2018). Evaluation of the Neuroprotective Effect of Sirt3 in Experimental Stroke. *Transl. Stroke Res.* 10, 57-66.
10) Ritzel R.M., Patel A.R., Spychala M., Verma R., **Crapser J.**, Koellhoffer E.C., Schrecengost A., Jellison E.R., Zhu L., Venna V.R., McCullough L.D. (2017). Multiparity improves outcomes after cerebral ischemia in female mice despite features of increased metabovascular risk. *PNAS*. 114, 5673-5682.
11) **Crapser, J.***, Ritzel, R.*, Verma, R., Venna, V.R., Liu, F., Chauhan, A., Koellhoffer, E., Patel, A., Ricker, A., Maas, K., Graf, J., and McCullough, L.D. (2016). Ischemic stroke induces gut permeability and enhances bacterial translocation leading to sepsis in aged mice. *Aging* 8, 1049-1063.

12) Ritzel, R.M., **Crapser, J.**, Patel, A.R., Verma, R., Grenier, J.M., Chauhan, A., Jellison, E.R., and McCullough, L.D. (2016). Age-Associated Resident Memory CD8 T Cells in the Central Nervous System Are Primed To Potentiate Inflammation after Ischemic Brain Injury. *J. Immunol*. 196, 3318-3330.
13) Ritzel, R.M., Pan, S.J., Verma, R., Wizeman, J., **Crapser, J.**, Patel, A.R., Lieberman, R., Mohan, R., and McCullough, L.D. (2016). Early retinal inflammatory biomarkers in the middle cerebral artery occlusion model of ischemic stroke. *Mol. Vis.* 22, 575-588.
14) Verma, R., Harris, N.M., Friedler, B.D., **Crapser, J.**, Patel, A.R., Venna, V., and McCullough, L.D. (2016). Reversal of the Detrimental Effects of Post-Stroke Social Isolation by Pair-Housing is Mediated by Activation of BDNF-MAPK/ERK in Aged Mice. *Sci. Rep.* 6, 25176.
15) Friedler, B.*, **Crapser, J.***, and McCullough, L. (2015). One is the deadliest number: the detrimental effects of social isolation on cerebrovascular diseases and cognition. *Acta Neuropathol*. 129, 493-509.
16) Ritzel, R.M., Patel, A.R., Grenier, J.M., **Crapser, J.**, Verma, R., Jellison, E.R., and McCullough, L.D. (2015). Functional differences between microglia and monocytes after ischemic stroke. *J. Neuroinflammation* 12, 106-015-0329-1.
17) Ritzel, R.M., Patel, A.R., Pan, S., **Crapser, J.**, Hammond, M., Jellison, E., and McCullough, L.D. (2015). Age- and location-related changes in microglial function. *Neurobiol. Aging* 36, 2153-2163.
18) Venna, V.R., Verma, R., O'Keefe, L.M., Xu, Y., **Crapser, J.**, Friedler, B., and McCullough, L.D. (2014). Inhibition of mitochondrial p53 abolishes the detrimental effects of social isolation on ischemic brain injury. *Stroke* 45, 3101-3104.

RESEARCH ABSTRACTS:

1) **Crapser, J.,** Ochaba, J., West, B., Reidling, J., Thompson, L., Green, K. (2017). Microglial elimination reduces pathology and delays motor symptoms in a mouse model of HD. Research and Education in Memory Impairments and Neurological Disorders (ReMIND) 8th Annual Emerging Scientists Symposium at the University of California, Irvine. Irvine, California, USA.
2) **Crapser, J.**, Ritzel, R., Doran, S., Koellhoffer, E., Patel, A., Friedler, B., Verma, R., McCullough, L. (2015). Worsening of stroke outcome with age is associated with increased intestinal permeability and peripheral inflammation. International Stroke Conference. Nashville, TN.

3) Verma, R., Harris, N., Friedler, B., **Crapser, J.**, Patel, A., Venna, V., McCullough, L. (2015). Pair housing reverses the detrimental effect of social isolation and restores BDNF and MBP in aged mice after stroke. International Stroke Conference. Nashville, TN.
4) **Crapser, J.**, Ritzel, R., Doran, S., Koellhoffer, E., Patel, A., Friedler, B., McCullough, L. (2014). Age-related changes in intestinal permeability and gut microbiota after ischemic stroke. XII International Congress of Neuroimmunology (ISNI). Mainz, Germany.
5) Ritzel, R., Patel, A., **Crapser, J**., McCullough, L. (2014). CD8 T cell recruitment in the normal aging CNS. XII International Congress of Neuroimmunology (ISNI). Mainz, Germany.
6) **Crapser, J.**, Verma, R., McCullough, L. (2014). SIRT3 is upregulated during stroke and contributes to ischemic damage by depressing the transcription of nuclear genes. International Stroke Conference. San Diego, CA.

ACADEMIC AWARDS:

- Allergan Foundation Graduate Award
- Ruth L. Kirschstein F31 National Research Service Award (2019)
- William D. Redfield Graduate Fellowship Award (2019)
- UCI BioSci Graduate Fellowship (2015)
- UCI Graduate Dean's Recruitment Fellowship (2015)
- Babbidge Scholar Award (2010-2013)
- MassMutual Scholars Scholarship (2009-2012)
- American Heart Association Student Summer Fellowship (2013)

TEACHING EXPERIENCE:

- Teaching Assistant, Neurobiology Lab (undergraduate senior course) (2017-2018), University of California, Irvine. Prepared and presented lecture and course material; prepared and graded assignments and exams; conducted laboratory section.
- Teaching Assistant, Neurobiology and Behavior (undergraduate senior course) (2017-2018), University of California, Irvine. Prepared and graded test material; met with students to discuss course material.
- Teaching Assistant, DNA to Organisms (undergraduate freshman course) (2016), University of California, Irvine. Prepared and presented lecture and course material; prepared and graded assignments and exams.

ABSTRACT OF THE DISSERTATION

Investigating microglial regulation of the extracellular matrix in health and neurodegenerative disease

By

Joshua Daniel Crapser

Doctor of Philosophy in Biological Sciences

University of California, Irvine, 2021

Professor Kim Green, Vice Chair

Microglia are the primary immune cells of the central nervous system (CNS) parenchyma, and have evolved conceptually from silent sentinels awaiting pathogenic or injurious disturbance to active and central regulators of brain homeostasis and disease (Prinz et al., 2019). Their functional repertoire equips microglia to perform immune as well as non-immune roles, but less is known about the latter. As exacerbated or, on the other hand, deficient microglial function may contribute to brain dyshomeostasis, shedding light on such functions may provide insight into mechanisms underlying disease etiology and pathogenesis. The development of microglial depletion paradigms via inhibition of colony-stimulating factor 1 receptor (CSF1R), expressed in the brain by microglia and required for their survival (Elmore et al., 2014), provides unprecedented capacity for functional investigation by allowing researchers to observe and draw conclusions from the consequences of microglial absence (up to 99% depletion) on CNS processes for virtually any duration of time (Green et al., 2020). Such methods have suggested that microglia dynamically regulate the dendritic spines of neuronal circuits in the adult homeostatic brain (Rice et al., 2017; Rice et al., 2015), for instance, as well as amyloid plaque

compaction and deposition in the context of Alzheimer's disease (AD) (Casali et al., 2020; Huang et al., 2021; Spangenberg et al., 2019).

The aim of my thesis is to identify and elucidate the role of microglia in the regulation of the brain extracellular matrix (ECM) – the perisynaptic and synaptic manifestations of which serve as the fourth and most recently addended component of the contemporary model of the quad- or tetra-partite synapse, also consisting of pre- and post-synaptic elements and associated glia (Dityatev and Schachner, 2003; Dityatev et al., 2010). While the ECM is divided into several separate compartments in the brain, one particularly salient instance is the perineuronal net (PNN), a specialized reticular formation that surrounds neuronal subsets and proximal synapses to provide synaptic stability, physical and chemical protection, and other unique physiological properties (Fawcett et al., 2019; Reichelt et al., 2019). Not only are PNNs associated with long-term memory storage (Shi et al., 2019a; Thompson et al., 2018; Tsien, 2013), they protect against oxidative stress and amyloid-β (Cabungcal et al., 2013; Miyata et al., 2007), underscoring their particular relevance to disorders like AD. Among other changes, I found that these ECM structures are reduced in Huntington's disease (HD) and AD, two brain disorders with disparate etiologies, pathologies, and microglial activation phenotypes. Importantly, I found that early microglial depletion with CSF1R inhibitors prevented PNN loss in both cases. Surprisingly, elimination of microglia also induced dramatic upregulation of PNN density throughout the brains of healthy adult mice. These results define a novel role of microglia in the regulation of PNNs in the homeostatic CNS, which may in turn go awry in neurodegenerative diseases where microglia adopt dyshomeostatic phenotypes.

INTRODUCTION

A small cell with many hats: The emerging complexity of microglia

Far from acting simply as a structural glue that holds neuronal networks together, as suggested by the Greek word from which the name “glia” is derived, it is now readily apparent that microglia and macroglia (astrocytes, oligodendrocytes) are important determinants of brain development and health (Kierdorf and Prinz, 2017). Microglia in particular have been the focus of further reappraisal as their functional repertoire has extended from the classically immune – detecting and resolving injury and invasive pathogens – to more non-immune roles in the homeostatic brain (Li and Barres, 2018; Prinz et al., 2019; Salter and Beggs, 2014). These findings have occurred across a backdrop of increasingly elegant methodological advances including single cell analyses (Hammond et al., 2019; Li et al., 2019; Masuda et al., 2019), microglial ablation paradigms (Bruttger et al., 2015; Elmore et al., 2014; Green et al., 2020; Han et al., 2017; Rojo et al., 2019; Waisman et al., 2015), and *in vivo* imaging techniques (Liu et al., 2019; Miyamoto et al., 2016; Nimmerjahn et al., 2005; Stowell et al., 2019), that together have characterized the dynamic influence microglia have on virtually all major CNS cell-types over the lifespan of an organism. However, this increased functional complexity suggests greater opportunity for dysfunction and dyshomeostasis should microglia fail to properly perform their cellular roles at the appropriate times, as supported by a growing body of evidence implicating microglia as drivers of disease pathogenesis (Salter and Stevens, 2017). Therefore, taking stock of the homeostatic functions performed by these cells – at this critical juncture of glial biology research – may provide insight into what goes wrong in disease and how such deficits may be best targeted in the clinic.

Microglia and other resident tissue macrophages display considerable diversity across organs at the gene expression and chromatin levels (Gautier et al., 2012; Lavin et al., 2014), reflecting the varying developmental and functional roles they play in each tissue (Li and Barres, 2018; Schafer and Stevens, 2015; Sieweke and Allen, 2013; Varol et al., 2015). The recent wave of studies characterizing microglia at single cell resolution indicate extensive transcriptional heterogeneity during development and disease, with a more homogenous population evident in the homeostatic adult brain (Hammond et al., 2019; Li et al., 2019; Masuda et al., 2019; Mrdjen et al., 2018; Tay et al., 2018). If an empty niche is available in the tissue myeloid compartment, cues from the local microenvironment can reprogram infiltrating bone marrow-derived monocytes or ontogenically foreign macrophages into microglia-like phenotypes (Bennett et al., 2018; Cronk et al., 2018; Ginhoux and Guilliams, 2016; Lund et al., 2018; Shemer et al., 2018). The extent of transcriptional reprogramming appears to depend on the yolk-sac or hematopoietic origin of the cell in question (Bennett et al., 2018; Bruttger et al., 2015; Shemer et al., 2018), at least in the CNS where the adult resident macrophage population derives from yolk-sac erythromyeloid progenitors (Ginhoux et al., 2010; Gomez Perdiguero et al., 2015; Hoeffel et al., 2015; Kierdorf et al., 2013). The capacity for macrophage re-education, combined with the diverse transcriptional profiles of resident macrophages in different organs and stages of life, emphasizes the complexity of homeostatic functions performed by tissue myeloid cells, even in the adult.

Research into microglia in development has revealed numerous essential functions not directly related to immunity but essential for proper brain organization and tissue health (Frost and Schafer, 2016; Kierdorf and Prinz, 2017; Li and Barres, 2018; Schafer and

Stevens, 2015). Additional investigation into early microglial functions has drawn some to label these cells “architects” of the developing CNS (Frost and Schafer, 2016; Kierdorf and Prinz, 2017), with top-down roles in the spatial organization and survival of both neuronal and non-neuronal cell types. In the perinatal period, microglia orchestrate spatial patterning of neurons through a variety of regulatory mechanisms that dictate neuronal/neuronal precursor cell (NPC) survival, i.e. signaling through soluble/membrane-bound microglial factors (glutamate, reactive oxygen species, TNF-α) that induce programmed cell death prior to microglial phagocytosis of debris, reported phagocytosis of live cells (“phagoptosis”), and secretion of pro-survival factors (e.g. insulin-like growth factor; IFG-1) (Li and Barres, 2018; Schafer and Stevens, 2015). Microglia continue to regulate neurogenesis in the adult brain by phagocytic maintenance of the hippocampal NPC pool (Sierra et al., 2010). A major re-evaluation of microglial effector functions in the brain was spurred by the discovery of synaptic engulfment and pruning by postnatal microglia that occurs in an activity- and complement-dependent manner to refine the neural circuitry (Paolicelli et al., 2011; Schafer et al., 2012; Stevens et al., 2007) that continues to some extent in the adult during memory processing (Wang et al., 2020).

Extensive work in recent years has elucidated the regulation of other glial cells by microglia, and vice versa, particularly when it comes to astrocytes (Han et al., 2021; Liddelow and Barres, 2017; Liddelow et al., 2017; Liddelow et al., 2020; Vainchtein et al., 2018; Vainchtein and Molofsky, 2020). Microglia induce a neurotoxic phenotype in astrocytes (termed “A1” astrocytes) following LPS via release of microglial IL-1α, TNF-α, and C1q that promotes neuronal and oligodendrocyte death; loss of these factors (i.e.

Il1α$^{-/-}$*Tnf*$^{-/-}$*C1qα*$^{-/-}$ triple knock-out mice) or microglia themselves (*Csf1r*$^{-/-}$ mice) blocks A1 astrocyte formation (Liddelow et al., 2017). Detrimental gain-of-function properties in neurotoxic astrocytes are accompanied by a loss of beneficial properties, including their support of neuronal outgrowth and synaptogenesis (Liddelow et al., 2017). Subsequent studies determined that blocking these regulatory microglial factors by genetic or pharmacologic means ameliorates such neurotoxic astrocyte reactivity and/or neuronal death in models of amyotrophic lateral sclerosis (ALS) (Guttenplan et al., 2020b), Parkinson's disease (Yun et al., 2018), optic nerve crush (Guttenplan et al., 2020a), glaucoma (Guttenplan et al., 2020a; Sterling et al., 2020), and aging (Clarke et al., 2018). In addition to affecting oligodendrocyte number via the cytotoxic effects of reactive astrocytes (Liddelow et al., 2017), microglia also choreograph oligodendrocyte patterning directly in disease conditions and under homeostatic conditions (Li and Barres, 2018; Miron, 2017). Postnatal microglia are required for early oligodendrocyte precursor cell (OPC) maintenance and maturation and continue to support the OPC pool in adulthood (Hagemeyer et al., 2017), and minocycline-based inhibition of postnatal microglial activation impairs oligodendrocyte differentiation (Shigemoto-Mogami et al., 2014). Furthermore, early microglia promote developmental myelinogenesis (Hagemeyer et al., 2017) at least in part through production of myelinogenic IGF-1 by a CD11c^{+} microglial subpopulation (Wlodarczyk et al., 2017), and myelin in the adult brain is phagocytosed by microglia, where it accumulates with age (Safaiyan et al., 2021; Safaiyan et al., 2016). Interactions with oligodendrocytes in disease are multifaceted, such that microglia can support remyelination in certain cases, as in the secretion of activin A to promote OPC proliferation and differentiation (Miron et al., 2013), and persistently disrupt

OPC/oligodendrocyte population dynamics and myelination in others (Gibson et al., 2019).

Thus, despite traditional classifications of microglia as immune cells first, mounting data tells us that they are intricately entwined in the complex process of brain tissue development and adult brain homeostasis, interacting with virtually every cell type in the brain to orchestrate non-immune as well as classically immune-related processes. Microglial cellular functionality may be perturbed in one of two ways: through 1) toxic gain-of-function, as exemplified by chronically activated microglia that fail to resolve ongoing pro-inflammatory cytokine and neurotoxin production (e.g. plaque-associated microglia in Alzheimer's disease, (Yin et al., 2017)) or 2) loss of beneficial or protective function. An example of the latter may be seen in the failure to appropriately prune neuronal synapses in development, which may contribute to autism spectrum disorders (Kim et al., 2017; Xu et al., 2020; Zhan et al., 2014). The extent to which these changes contribute to brain disease depends on a multitude of contextual factors, including brain age, existing disease pathology, and disease-relevant genetic and environmental risk factors, among others.

Pharmacological depletion of microglia: CSF1R inhibitors

To gain insight into the roles they play, microglia may be depleted via toxin-, genetic-, and pharmacological-based methods, and we have recently reviewed the comparative advantages, disadvantages, and caveats of these different approaches (Green et al., 2020). To serve as an illustration, our lab has previously developed pharmacological paradigms of microglial depletion with inhibitors to CSF1R, signaling through which microglia are dependent for survival (Dai et al., 2002; Elmore et al., 2014; Erblich et al.,

2011; Rice et al., 2015; Rojo et al., 2019; Spangenberg et al., 2016). Formulation of CSF1R inhibitor PLX3397 in rodent chow at a dosage of 290ppm allowed for a non-invasive method of CSF1R inhibition, with subsequent CNS inhibitor concentrations in the low μM range resulting in 50% depletion of microglia within 3 days of treatment, and up to 99% depletion by 3 weeks in adult WT mice. Increasing the dose of PLX3397 in chow to 600ppm induced a ~99% depletion of microglia within 7 days (Najafi et al., 2018)(Figure 1). Of clinical relevance, PLX3397, or pexidartinib, has been granted US FDA approval as a drug treatment for tenosynovial giant cell tumors (Tap et al., 2015), making it an ideal candidate for its application in other disorders involving myeloid dysfunction. However, limitations of this compound include its relatively poor CNS penetrance (~5%; (Elmore et al., 2014)) and potential off-target effects on related receptor tyrosine kinases c-Kit and fms-like tyrosine kinase 3 (FLT3) (Tap et al., 2015).

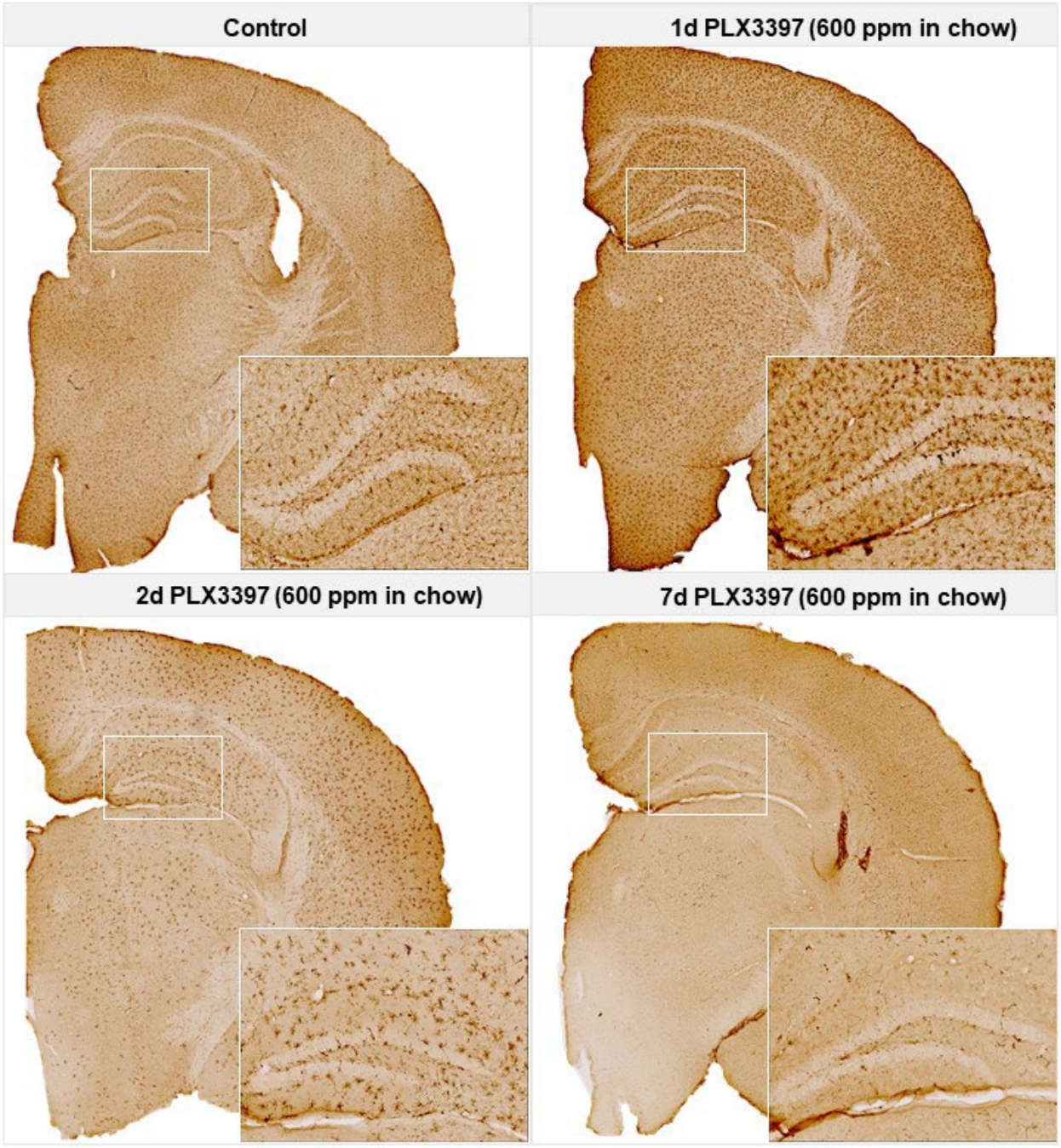

Figure 1. Widespread Depletion of Murine Microglia with Orally Administered Colony-Stimulating Factor 1 Receptor (CSF1R) Inhibitors. For illustrative purposes, wild-type mice aged 2 months were treated with the CSF1R inhibitor PLX3397 (600 ppm in chow) for 1, 2, or 7 days. Controls were treated for 7 days with vehicle chow. To visualize microglial depletion, representative micrographs of brain sections stained via chromogenic immunohistochemistry using the common microglial marker ionized calcium binding adaptor molecule 1 (IBA1) are shown. Higher-resolution images are provided as insets. Scale bar, 120 µm.

Additional inhibitor screening led to the identification of PLX5622, which exhibits both a higher specificity for CSF1R and improved brain penetrance (20%) than PLX3397, with delivery in chow at 1200ppm inducing the depletion of >80% of microglia within 3 days in adult mice (Spangenberg et al., 2019). Research utilizing these inhibitors has reported microglial loss throughout the CNS, including the murine brain parenchyma, spinal cord, and retina (Bellver-Landete et al., 2019; Okunuki et al., 2018; Paschalis et al., 2018), due to microglial cell death (Elmore et al., 2014) rather than downregulation of microglial markers (Spangenberg et al., 2016). Inhibitor-induced depletion of microglia occurs in the absence of behavioral deficits, cytokine storm, brain pathology, or replacement by peripheral myeloid cells (Elmore et al., 2014), and appears to be indefinitely maintainable as long as inhibition is continued (at least 6 months) (Spangenberg et al., 2019).

Restoring CSF1R signaling by inhibitor withdrawal induces full repopulation of the microglial niche via proliferation of surviving microglia (Elmore et al., 2014; Najafi et al., 2018), which may be exploited to correct dysfunctional microglial phenotypes by replacing the old with new cells. This aspect of microglial biology has been utilized to promote brain recovery after traumatic brain injury (TBI) (Henry et al., 2020), neuronal lesion (Rice et al., 2017), and aging (Elmore et al., 2018) by resolving chronically activated or otherwise dyshomeostatic microglia *in vivo*. Thus, by eliminating microglia and observing the consequences of their absence and/or renewal on brain physiology in homeostasis and disease, and whether these processes normalize injury- or disease-associated deficits, we may make inferences about their function in the brain.

Microglia and the extracellular matrix in health and disease

Perhaps more aptly considered the 'glue' of the nervous system than glia themselves, the ECM is a highly complex and dynamic molecular meshwork with roles in plasticity, biophysical protection, and cell signaling (Dityatev and Schachner, 2003; Dityatev et al., 2010; Fawcett et al., 2019; Reichelt et al., 2019). While its role as an extracellular scaffold is well-known, less appreciated is the ability of the ECM to limit, and thus functionally compartmentalize, the diffusion and localization of key molecules (Dityatev et al., 2010), including neurotransmitters (Bikbaev et al., 2015; Nicholson and Syková, 1998), ions (Bekku et al., 2010; Hrabětová et al., 2009; Morawski et al., 2015), and membrane receptors (Cingolani et al., 2008; Favuzzi et al., 2017; Frischknecht et al., 2009; Groc et al., 2007). Furthermore, matrix molecules such as the abundant chondroitin sulfate proteoglycans (CSPGs), which consist of glycosaminoglycan side chains attached to a core protein, may inhibit neurite and axon growth (Fisher et al., 2011; Monnier et al., 2003; Ohtake et al., 2016; Pearson et al., 2018; Properzi et al., 2005; Shen et al., 2009), myelination and remyelination by oligodendrocytes/OPCs (Keough et al., 2016; Lau et al., 2013; Pendleton et al., 2013), and neural stem cell migration (Galindo et al., 2018). This has been classically illustrated in astrocytic glial scars that form after injury (e.g. spinal cord injury) and serve as a physicochemical barrier to neuronal recovery and axonal regrowth, thought to be due in large part to the consequent deposition of matrix components such as CSPGs into the interstitial ECM by reactive astrocytes (Davies et al., 1999; Davies et al., 1997; Lau et al., 2013; Silver and Miller, 2004; Yiu and He, 2006). This interpretation is complicated with the discovery that certain glial scar components (such as specific CSPG subtypes (Nakanishi et al., 2006; Schäfer and Tegeder, 2018)),

and the glial scar as a whole (Anderson et al., 2016; Liddelow and Barres, 2016), both appear to facilitate axon regeneration and neurite outgrowth. Additionally, disruption of injury-induced astrocyte responses upstream to scar formation impedes recovery by impairing injury containment, BBB repair, and inflammation resolution (Bradbury and Burnside, 2019; Bush et al., 1999; Faulkner et al., 2004; Herrmann et al., 2008), and astrocytes themselves may adopt multiple reactive phenotypes that likely exist on a functional spectrum (Liddelow and Barres, 2017; Zamanian et al., 2012) and which may in turn be influenced by proteoglycans (Bradbury and Burnside, 2019; Silvestri et al., 1981). Whatever new findings future studies may hold, it is clear that the ECM has profound influence on brain health and disease.

In terms of composition, the brain ECM is made up largely of proteoglycans, such as CSPGs and heparan sulfate proteoglycans (HSPGs), glycoproteins, such as laminins and tenascins, and glycosaminoglycans, such as the abundant hyaluronan (Dityatev and Schachner, 2003; Dityatev et al., 2010), among other molecules (e.g. collagens), that together constitute roughly 20% of overall brain volume (Nicholson and Syková, 1998; Syková, 1997). The structural molecules that constitute the brain ECM, and the proteases that are secreted to remodel it, are produced by neurons, astrocytes, microglia, and oligodendrocyte lineage cells with varying degrees of overlap in terms of cellular origin depending on the molecule in question (Fawcett et al., 2019; Jones and Tuszynski, 2002; Lau et al., 2013; Song and Dityatev, 2018). The ECM can be partitioned into structural subtypes based on organization composition, which generally include: 1) the basement membrane of the BBB, 2) the diffuse ECM found in interstitial and perisynaptic spaces, 3) the condensed, reticular ECM that ensheathes neuronal subsets and their perisomatic

synapses to form structures known as perineuronal nets (PNNs), and 4) the perinodal ECM that surrounds nodes of Ranvier within axons and that display compositional resemblance to PNNs (Fawcett et al., 2019; Lau et al., 2013). Along with synaptic terminals and glial cells, the diffuse perisynaptic matrix and the synaptic ECM of PNNs constitute the fourth compartment and most recent addition to the conventional model of synaptic function, the tetrapartite synapse (Dityatev and Schachner, 2003; Dityatev et al., 2010).

Perineuronal Nets

Discovered by Camillo Golgi and dismissed by Ramón y Cajal as a fixation artifact, perineuronal nets are specialized ECM structures that condense in a reticular fashion around the soma and proximal neurites (dendrites and axon initial segment) of neurons throughout the brain during development (Fawcett et al., 2019; Vitellaro-Zuccarello et al., 1998). Although PNNs are associated primarily with fast-spiking parvalbumin (PV)-expressing GABAergic interneurons, particularly in the cortex of the brain (Lensjø et al., 2017a; Rossier et al., 2015), they are evident throughout the CNS and across a variety of neuronal subsets (Carstens et al., 2016; Fawcett et al., 2019; Lensjø et al., 2017a; Morikawa et al., 2017; Reichelt et al., 2019; Wegner et al., 2003) and are generally (but not always) labeled with the lectin *Wisteria floribunda* agglutinin (Fawcett et al., 2019). These formations serve as a molecular scaffold to stabilize and regulate the synapses they surround, and reach adult levels during the closure of critical periods of neuroplasticity (Pizzorusso et al., 2002; Reichelt et al., 2019), and the genetic or enzymatic removal of PNNS or their components is capable of reinstating critical period-like plasticity (Boggio et al., 2019; Lensjø et al., 2017b; Pizzorusso et al., 2002; Rowlands

et al., 2018). In line with their role as a synaptic scaffold, PNNs have been proposed as the molecular basis of long-term memory storage (Tsien, 2013), and their experimental removal disrupts consolidation (Banerjee et al., 2017; Shi et al., 2019a) and recall (Shi et al., 2019a; Thompson et al., 2018) of various types of remote fear memories. Thus, the heightened plasticity afforded by PNN loss may impair long-term memory fidelity due to interference from new memory traces (Carulli et al., 2020; Christensen et al., 2021; Reichelt et al., 2019). Physiologically, PNNs also protect host cells from neurotoxins such as $A\beta_{1\text{-}42}$ and oxidative stress (Cabungcal et al., 2013; Miyata et al., 2007), regulate neuronal excitability (Balmer, 2016; Dityatev et al., 2007), and augment neuronal firing by reducing membrane capacitance akin to myelin sheaths (Tewari et al., 2018), thereby influencing excitatory-inhibitory balance. Furthermore, the removal of PNN components alters synaptic transmission (Blosa et al., 2015), synaptic ion channel/neurotransmitter receptor localization (Favuzzi et al., 2017), and synapse number (Geissler et al., 2013; Gottschling et al., 2019). While future experiments will determine whether some of these effects at least partly result from changes to the perisynaptic matrix rather than the PNN proper, particularly in the case of brevican modifications (Frischknecht and Seidenbecher, 2012), these findings taken together underscore the truly multimodal effects that the brain ECM in general, and PNNs specifically, exert on the cells they enwrap.

PNN deficits/decreases have also been observed across more diverse diseases still, many if not all of which are also generally associated with microglial activation, including multiple sclerosis (Gray et al., 2008a), stroke (Dzyubenko et al., 2018; Härtig et al., 2017; Hobohm et al., 2005; Karetko-Sysa et al., 2011; Quattromani et al., 2018), traumatic brain injury (Vita et al., 2020; Wiley et al., 2016), spinal cord injury (Sánchez-Ventura et al.,

2021), epilepsy (McRae et al., 2012; Rankin-Gee et al., 2015), obesogenic high fat and high sugar diet consumption (Reichelt et al., 2021), glioma (Tewari et al., 2018), Alzheimer's disease (Baig et al., 2005; Cattaud et al., 2018; Kobayashi et al., 1989), and schizophrenia (Bitanihirwe and Woo, 2014; Mauney et al., 2013; Pantazopoulos and Berretta, 2016; Pantazopoulos et al., 2010).

Perisynaptic matrix

The vast majority (98%) of CSPGs within the CNS are found in the general diffuse ECM, including the perisynaptic matrix, as opposed to the highly specialized manifestations of the brain ECM that are PNNs (Fawcett et al., 2019). Many key molecules coexist in both the perisynaptic matrix and in PNNs, and so it is inherently difficult to tease apart the effects of their manipulations as resulting from changes to one or another ECM structure, particularly in the case of global genetic ECM knock-out models. For instance, while aggrecan is a requisite component of the PNN backbone (Matthews et al., 2002; Morawski et al., 2012; Rowlands et al., 2018), the shorter CSPG brevican may be considered a reciprocally critical molecule to the perisynaptic ECM (Frischknecht and Seidenbecher, 2012; Jäger et al., 2013; Morawski et al., 2012) and accumulates in synaptic fractions following biochemical fractionation of brain tissue (Li et al., 2004; Seidenbecher et al., 1995). However, these CSPGs can be found across both structures, and so additional research will likely be required to determine where and how they exert their effects on neuronal and synaptic physiology, and the extent to which interactions exist between ECM compartments. Interestingly, neuroglycan C (a.k.a. CSPG-5) appears to localize to perisynaptic regions of glutamatergic and GABAergic terminals, and is often observed at the edges of PNNs (Pintér et al., 2020), and its loss results in presynaptic

functional deficits and premature elimination of synapses during development (Jüttner et al., 2013).

Several approaches exist to study the perisynaptic vs. perineuronal matrix. Mice deficient in link proteins HAPLN1 and HAPLN4, which serve to stabilize interactions between hyaluronan and CSPGs in the ECM (Dityatev et al., 2010), have overall unchanged CSPG levels but fail to incorporate these molecules into PNNs (Bekku et al., 2012; Carulli et al., 2010; Fawcett et al., 2019), and therefore may provide a means of studying the effects of disrupting these structures without affecting the perisynaptic matrix and diffuse ECM at large. Microinjections of chondroitinase ABC (ChABC) near dendrites have also been successfully used to locally degrade perisynaptic CSPGs while leaving PNNs intact (Orlando et al., 2012). Alternatively, studies elucidating the function of the perisynaptic ECM could focus on regions that naturally lack PNNs (Lendvai et al., 2012), and vice versa in regions densely enriched with PNNs (Blosa et al., 2013), although the effects of the perisynapic matrix would not be entirely absent – just relatively minimized – in the latter case.

Research by several groups in the past decade has begun to shed light on the comparative composition of perisynaptic and PNN matrices in the CNS as well as the organizational frameworks that distinguish them (Blosa et al., 2013; Blosa et al., 2015; Brückner et al., 2008; Faissner et al., 2010; Jäger et al., 2013; Lendvai et al., 2012; Lendvai et al., 2013; Mitlöhner et al., 2020). The discovery of axonal coats (ACs) serves as one such example of a well-characterized perisynaptic matrix structure that exists as a separate entity from classical PNNs (Brückner et al., 2008). These round structures of aggrecan- and brevican-based ECM enwrap individual synaptic boutons contacting

neuronal dendrites and somata and sometimes co-mingle with PNN components on associated neurons (Brückner et al., 2008; Jäger et al., 2013; Lendvai et al., 2012), with hypothesized roles at the synapse in restricting neurotransmitter spillover and receptor localization (Blosa et al., 2013; Dityatev et al., 2010; Jäger et al., 2013). Several studies suggest that ACs are synthesized by the presynaptic neuron (Brückner et al., 2008; Jäger et al., 2013; Lendvai et al., 2012; Lendvai et al., 2013), which may have implications in the microglial trogocytosis of presynaptic synapses (Weinhard et al., 2018), in that this process might necessarily involve concurrent remodeling of the presynaptically-generated ECM that supports synapses in these instances and a mechanism in place to allow such preferential targeting by microglia.

Although there is some degree of overlap, perisynaptic ECM can be found around neuronal subsets lacking PNNs (Brückner et al., 2008; Lendvai et al., 2012), as is the case for dopaminergic neurons and glutamatergic principal neurons in the substantia nigra and thalamus, respectively, on which presynaptic ACs make contact (Brückner et al., 2008). Additionally, activation of dopamine receptors and subsequent neuronal activity was shown in an elegant study to induce proteolysis of perisynaptic brevican and aggrecan in the ECM around excitatory synapses which, at least for brevican, was mediated by ADAMTS-4/5 (Mitlöhner et al., 2020). Thus, changes in upstream perisynaptic ECM could lead to downstream signaling-dependent changes in synaptic ECM and plasticity in an increasingly complex, circuit-level process. It has also been shown that targeted perisynaptic matrix degradation induces structural plasticity of dendritic spines (e.g. enhanced spine motility and formation of spine head protrusions) (Orlando et al., 2012) and similar structural changes are associated with increased

functional plasticity as measured by LTP (de Vivo et al., 2013), and thus CSPGs appear to restrict plasticity in either case.

Collectively, these results underscore the far-reaching effects that the brain ECM in the form of the perisynaptic matrix and PNNs exert on the functions of synapses with which they are associated. The microglial modulation of the tetrapartite synapse at the level of the pre- and post-synapse (Schafer and Stevens, 2015; Wake et al., 2013) and glia – both astrocytes (Han et al., 2021; Liddelow and Barres, 2017; Liddelow et al., 2020; Vainchtein and Molofsky, 2020) and oligodendrocyte lineage cells (Miron, 2017) – are, at this time, well reported. This thesis will address the influence of microglia on the fourth component, namely the brain ECM, in health and disease.

CHAPTER ONE

Dyshomeostatic microglia and the ECM in Huntington's disease

Introduction

The cause of Huntington's disease (HD), an autosomal dominant neurological disorder, is well established as an abnormal expansion of CAG triplet repeats in exon 1 of the ubiquitously expressed *huntingtin* (*htt*) gene, resulting in an elongated polyglutamine (Q) tract in the mutant huntingtin protein (mHTT)(1993). While the unaffected population ranges on average 16-20 triplet repeats at this locus, affected patients contain ≥40 CAGs, with the age of symptom onset in general inversely correlating with repeat length (Duyao et al., 1993; Labbadia and Morimoto, 2013). Disease symptoms include progressive movement abnormalities (chorea, dystonia) and cognitive-behavioral impairments, accompanied by selective striatal medium spiny neuron (MSNs) death and cortical atrophy (Ross and Tabrizi, 2011). Pathologically, mHTT accumulates in many cells types, and in multiple forms, due at least in part to the failure of protein quality control networks, as reflected by an accumulation of ubiquitin and other post-translationally-modified proteins (Ochaba et al., 2016) and disruptions in autophagy (Kurosawa et al., 2015). Despite HD's deceivingly simple monogenic origin, the contributions of specific cell types in the brain is only beginning to be elucidated.

Microglia, resident myeloid phagocytes comprising ~12% of cells in the brain, sample the entire parenchymal milieu every 24 hours for deviations from homeostasis (Nimmerjahn et al., 2005). That microglia are potent modulators of neurodegeneration and injury is by now clear (Li and Barres, 2018), and investigation into the full functional spectrum and uniqueness of microglia among related immune cells continues to elucidate critical roles

in development, aging, and disease (Bennett et al., 2018; Mrdjen et al., 2018). Previously, we developed a pharmacological method to eliminate virtually all (~99%) microglia from the murine brain for several months at a time (Dagher et al., 2015; Elmore et al., 2014), based on inhibition of colony-stimulating factor 1 receptor (CSF1Ri). Microglial CSF1R signaling is essential to their survival and has become a thoroughly tested and highly replicated model for targeted elimination of microglia (Acharya et al., 2016; Asai et al., 2015; Bennett et al., 2018; Dagher et al., 2015; Elmore et al., 2014; Feng et al., 2016; Li et al., 2017; Rice et al., 2015; Spangenberg et al., 2016; Stafford et al., 2016; Szalay et al., 2016). By formulating inhibitors in chow, we can ensure non-invasive, uninterrupted drug delivery and elimination of these cells for the duration of treatment.

In HD, microglial activation is detected years before the onset of clinical symptoms and correlates with striatal neuron dysfunction in subclinical (Tai et al., 2007) as well as clinical stages of the disease (Pavese et al., 2006; Politis et al., 2011). Postmortem HD brains contain elevated densities of reactive microglia in regions of neuronal loss (Sapp et al., 2001) and this microgliosis is mirrored in mouse models of the disease (Simmons et al., 2007). While microglia conventionally react to stress signals and exogenous toxins in neurodegeneration, the presence of endogenous mHTT alone alters their transcriptional landscape through increased expression of the myeloid lineage-determining factor Pu.1 (Crotti et al., 2014), resulting in enhanced production of IL-6 and TNFα transcripts as well as increased neurotoxicity in the context of a secondary immune challenge. Furthermore, intrastriatal engraftment of mHTT-expressing human glial progenitor cells in immunodeficient mice results in neuronal hyperexcitability in the striatum along with motor impairments (Benraiss et al., 2016; Osipovitch et al., 2019). We aimed to further extend

these findings by eliminating microglia from a mouse model of HD via sustained CSF1Ri and assessing the impact on disease pathogenesis.

In this study we treated transgenic R6/2 mice, expressing exon 1 of the human *huntingtin* (*HTT*) gene containing ~120 CAG repeats, or nontransgenic (NT) littermates with the clinically utilized and FDA-approved CSF1R inhibitor, PLX3397 (Pexidartinib) (Tap et al., 2014), or vehicle. The R6/2 line is a short-lived and rapidly progressing mouse model of HD that displays motor and behavioral deficits beginning around 7 weeks of age and progressing until an early death at 11-13 weeks (Mangiarini et al., 1996). We find that CSF1Ri and resultant microglial depletion in R6/2 mice is accompanied by ameliorated grip strength and memory deficits, mHTT species accumulation, and protein clearance system pathway dysfunction. At the transcriptional level, we report impaired neuronal and neurite development pathways in addition to an interferon (IFN) signature in the R6/2 striatum that is similarly overrepresented in human HD, aspects of which are diminished following microglial depletion. Additionally, despite a reduction in R6/2 caudoputamen volume, we observed increased neuronal and neurite cytoskeletal element densities in the R6/2 striatum at 11 weeks. This was concomitant with astrogliosis and massive brain-wide deposition of the major extracellular matrix (ECM) chondroitin sulfate proteoglycans (CSPGs), a key component of glial scars (Hsu et al., 2008) and a negative axon guidance cue (Ohtake et al., 2016). In parallel, we observed a disease-related loss of CSPG-containing perineuronal nets (Fawcett et al., 2019), specialized interneuron-associated ECM structures the degradation of which contributes to seizures (Tewari et al., 2018), dampened inhibitory tone, and changes in plasticity (Banerjee et al., 2017). CSF1Ri and the depletion of microglia abrogated each of these changes, including disease-associated

striatal volume loss, underscoring their role as coordinators of brain ECM remodeling that in turn appears to contribute to neurodegeneration in HD. Interestingly, microglial elimination in NT littermates also resulted in brain-wide increases in PNN density, suggesting that microglia tightly regulate PNN formation in health as well as disease.

Materials and Methods

Compounds: CSF1R inhibitor PLX3397 (Pexidartinib) was provided by Plexxikon Inc. and formulated in AIN-76A standard chow by Research Diets Inc. at 275 mg/kg.

Animals: All animal experiments were performed in accordance with animal protocols approved by the Institutional Animal Care and Use Committee (IACUC) at the University of California, Irvine, an American Association for Accreditation of Laboratory Animal Care (AAALAC)-accredited institution. R6/2 mice have been described elsewhere in detail (Mangiarini et al., 1996; Ochaba et al., 2016). For this study, 5-week-old R6/2 male mice were purchased from Jackson Laboratories and housed in groups of up to five animals/cage under a 12-hr light/dark cycle with *ad libitum* access to control chow and water during baseline testing, and then AIN-76A chow (containing vehicle or PLX3397) starting at week 6. Brain tissue from 22-week-old mixed sex wild-type mice on a C57BL/6J congenic background treated for 10 weeks (from week 6) with the more selective CSF1R inhibitor PLX5622 (Plexxikon Inc.) formulated in standard chow by Research Diets Inc. at 1200mg/kg was utilized for additional investigation of perineuronal nets. Assignment of animals to treatment groups was conducted in a random fashion. Researchers were blinded to genotype and treatment group for behavioral tasks and in the analysis of behavioral, histological, stereological, and biochemical assays. CAG repeat sizing of tail samples was performed by Laragen.

Behavioral Testing: Baseline behavioral characterization was performed at 5 weeks of age via Rotarod and grip strength as described previously (Morozko et al., 2018; Ochaba et al., 2016) and again during treatment at regular intervals. Briefly, animals were tested for latency to fall from an accelerating rotarod over three 5-minute interval trials averaged together on weeks 5, 7, and 9. Forelimb grip strength was assessed with a meshed force gauge that records peak force applied (IITC Life Science instrument, Woodland Hills, CA) over 5 trials averaged together on weeks 5, 7, 9, 10, and 11. Body weights were obtained daily from 5-11 weeks of age. Open Field (OF) and Novel Object Recognition (NOR) were assessed on week 11 and were analyzed with EthoVision. For OF, mice were placed in an empty chamber and recorded while roaming freely for 5 minutes. For NOR, mice were placed in a chamber for 5 minutes with two identical objects on day 1, and one familiar and one novel object on day 2, and memory for the familiar object was measured as the time spent investigating the novel object as percentage of total time exploring (i.e. discrimination index). Exclusionary criteria are as follows: If mice did not spend time investigating both objects during training, or either object during testing, the testing data was excluded from analysis, as it cannot be confirmed they spent enough time exploring to learn/discriminate. All behavioral tests were conducted and analyzed in a blinded fashion.

Tissue Collection: After final behavioral measurements on week 11, mice were euthanized with administration of Euthasol followed by transcardial perfusion with ice-cold 1X phosphate-buffered saline. Brains were isolated and divided hemispherically; one hemisphere per animal was drop-fixed in 4% paraformaldehyde (Thermo Fisher Scientific, Waltham, MA) for 48hrs, cryopreserved in 30% sucrose, and sectioned at 40um

on a freezing microtome for immunohistochemistry (IHC), while the other hemisphere was used to extract, flash freeze, and store striatal tissue at -80 ^{o}C for later biochemical analyses. Frozen striatal tissue was split into protein and RNA fractions.

Immunohistochemistry and Confocal Microscopy: Fluorescent immunolabeling followed a standard indirect technique as described previously (Elmore et al., 2014; Spangenberg et al., 2016). Brain sections were stained with antibody to IBA1 (1:1000; 019-19741, Wako and ab5076, Abcam) (Elmore et al., 2014; Smith et al., 2013), HTT (EM48) (1:500; MAB5374, Millipore), DARPP32 (1:500; SC-11365, Santa Cruz) (Morozko et al., 2018), CD68 (1:200; MCA1957GA, BioRad), NeuN (1:500; MAB377, Millipore), IB4 (1:200; 121414, ThermoFisher) (Elmore et al., 2018), Olig2 (1:200; MABN50, Millipore), MAP2 (1:200; ab32454, Abcam) (Elmore et al., 2014), Tau (1:500; A0024, DAKO) (Julien et al., 2012), p62 (1:500; BML-PW9860, Enzo) (Paine et al., 2013), MBP (1:100; MAB386, Millipore) (Cardoso et al., 2015), S100β (1:200; ab52642, Abcam) (Illouz et al., 2019), CD44 (1:200; ab157107, Abcam) (Koga et al., 2018), CSPG (1:200; ab11570, Abcam) (Park et al., 2017), *Wisteria floribunda agglutinin* (WFA) lectin (1:1000; B-1355, Vector Labs) (Yutsudo and Kitagawa, 2015), parvalbumin (1:500; MAB1572, Millipore) (McNamara et al., 2014), c-Kit (1:100; ab25022, Abcam) (Trias et al., 2018), and Flt3 (1:100; ab73019, Abcam) (Svensson et al., 2015). Immunostained sections were mounted and coverslipped with Fluoromount-G with DAPI (00-4959-52, SouthernBiotech). High resolution fluorescent images were obtained using a Leica TCS SPE-II Confocal microscope, and whole-brain stitches using a ZEISS Axio Scan.Z1. Cell and EM48^{+} puncta quantities, area, and intensity were determined using the spots module in Imaris v9.2. Percent area coverage and integrated density measurements were

determined in ImageJ (NIH) at a constant threshold for each stain using 20X confocal images for striatal and dentate gyrus quantifications and regions of interest in whole-brain stitches for cortical analyses.

Western Blotting: Striatal tissue fractionation, gel electrophoresis, and immunoblotting was performed as previously described (Morozko et al., 2018; Ochaba et al., 2016; Ochaba et al., 2018). Briefly, striatal tissue was first homogenized in lysis buffer containing 10 mM Tris (pH 7.4), 1% Triton X-100, 150 mM NaCl, 10% glycerol, and 0.2 mM PMSF. Tissue was lysed on ice for 60 minutes before centrifugation at 15,000 × g for 20 min at 4°C. Supernatant was collected as the detergent-soluble fraction. The pellet was washed 3× with lysis buffer and centrifuged at 15,000 × g for 5 min each at 4°C. The pellet was resuspended in lysis buffer supplemented with 4% SDS, sonicated 3×, boiled for 30 min, and collected as the detergent insoluble fraction. Protein concentration was determined using Lowry Protein Assay (Bio-Rad).

Detergent-soluble fractions were resolved on 4–12% Bis-Tris Poly-Acrylamide gels (PAGE), insoluble fractions on 3–8% Tris-Acetate Poly-Acrylamide gels, and oligomeric species determined by Agarose Gel Electrophoresis (AGE) using a 1%, 375 mM Tris-HCl, pH 8.8, 1% SDS agarose gels. Insoluble mHTT fibrils were detected using a modified filter retardation assay where insoluble fractions were loaded onto a dot blot apparatus (BioRad) and blotted onto a 0.2μm Cellulose Acetate membrane (Morozko et al., 2018). Membranes were blocked in StartingBlock (Invitrogen) or 5% milk in TBST (for fibrils) at room temperature and incubated in primary antibody overnight at 4°C. The following primary antibodies were used: anti-HTT (1:1000; MAB5492, Millipore), anti-Ubiquitin (1:1000; sc-8017, Santa Cruz Biotechnology) (Ochaba et al., 2016), anti-p62 (1:1000;

BML-PW9860, Enzo) (Wong et al., 2015), and anti-GAPDH (1:2500; 1D4, Novus Biologicals) (Zhang et al., 2018). Insoluble fibrils were labeled with anti-HTT (1:1000; VB3130, Viva Biosciences) (Ochaba et al., 2016). Western blot and AGE data were quantified by measuring mean pixel intensity using Scion Image processing software. Detergent-soluble fraction lysates were normalized to house-keeping protein loading control (GAPDH) prior to statistical analysis. Detergent-insoluble and oligomeric protein were quantified as relative protein abundance as before (Morozko et al., 2018).

qPCR and Nanostring: RNA was extracted and purified from frozen striatal tissue using a RNeasy Plus Universal Mini Kit (73404, Qiagen). qPCR was performed as before (Morozko et al., 2018) with reverse transcription using the SuperScript 3 First-strand synthesis system (Invitrogen) and the following primers for cDNA amplification: R6/2 transgene (F: CCGCTCAGGTTCTGCTTTTA, R: TGGAGGGACTTGAGGGACTC), *Rplp0* (F: GCTTCGTGTTCACCAAGGAGGA, R: GTCCTAGACCAGTGTTCTGAGC). For nCounter© analysis, total RNA was diluted to 20 ng/µl and probed using a mouse nCounter© PanCancer Immune Profiling Panel (NS_Mm_CancerImm_C3400, Nanostring Technologies) profiling ~700 immunology-related mouse genes. Counts for target genes were normalized to the best fitting house-keeping genes as determined by nSolver software. The WGCNA package was used to evaluate the quality of reads, as well, as identify and remove appropriate outliers, based on standard deviation within normalized expression values. PCA plots were generated using plot3D. Negative binomial linear regression analysis was performed using EdgeR, DESeq, and Limma packages to generate FDR and log fold change values. Top significant genes are

displayed as a volcano plot constructed using GLimma, ggplot2, and EnhancedVolcano (FDR<0.10, LogFC>1).

RNA-sequencing and analysis

For mRNA-seq, RNA from the same striatal samples used for Nanostring was analyzed, and as such was previously extracted using the RNeasy Plus Universal Mini Kit (73404, Qiagen). Total RNA was monitored for quality control using the Agilent Bioanalyzer Nano RNA chip (Agilent) and Nanodrop absorbance ratios for 260/280nm and 260/230nm. Library construction was performed according to the Illumina TruSeq mRNA stranded protocol. The input quantity for total RNA was 700ng and mRNA was enriched using oligo dT magnetic beads. The enriched mRNA was chemically fragmented for 3 minutes. First strand synthesis used random primers and reverse transcriptase to make cDNA. After second strand synthesis the ds cDNA was cleaned using AMPure XP beads (Beckman Coulter) and the cDNA was end repaired and then the 3' ends were adenylated. Illumina barcoded adapters were ligated on the ends and the adapter ligated fragments were enriched by nine cycles of PCR. The resulting libraries were validated by qPCR and sized by Agilent Bioanalyzer DNA high sensitivity chip (Agilent). The concentrations for the libraries were normalized and then multiplexed together. The concentration used for clustering the flowcell was 200pM. The multiplexed libraries were sequenced on 1 lane using PE 100 cycles chemistry for the HiSeq 4000 (Illumina). The version of HiSeq control software was HCS 3.3.76 with real time analysis software, RTA 2.7.6.

Read alignment and expression quantification: Pair-end RNA-seq reads were first filtered for ribosomal RNA using SortMeRNA v.2.1b followed by trimmomatic v.0.35 to correct for

overrepresented sequences via quality trimming and adapter removal. Paired-end reads were then aligned using STAR v.2.5.1b (Dobin et al., 2013) with the options (--outFilterMismatchNmax 10 --outFilterMismatchNoverReadLmax 1 --outFilterMultimapNmax 10). Rsubread was used to generate feature counts. Gene expression was measured using Limma, edgeR, and org.Mm.eg.db packages with expression values normalized into RPKM. Differential expression analysis: Libraries with uniquely mapping percentages higher than 80% were considered to be of good quality and kept for downstream analysis. Transcripts with expression RPKM >=1 in at least three samples, were collected for subsequent analysis. Differential expression analysis was performed by using Limma, edgeR, and org.Mm.eg.dbt (Robinson et al., 2010). Differentially expressed genes (DEGs) were selected by using false discovery rate (FDR)≤0.05. Top significant genes are displayed as a volcano plot constructed using GLimma, ggplot2, and EnhancedVolcano (FDR≤ 0.05, LogFC >1). PCA plots were generated using plot3D. Gene enrichment pathway analysis was performed using Ingenuity Pathway Analysis (IPA, Qiagen) of DEGs detected at FDR≤0.10, and predicted upstream regulators are reported with activation z-scores and p-values.

Data analysis and statistics

Statistical analysis was performed with Prism Graph Pad (v.8.0.1). To assess linear relationships, the two-tailed Pearson correlation test was used. To compare one variable, the two-tailed unpaired Student's t-test was used. To compare two variables, two-way ANOVA with Tukey's post-hoc test was used. To compare two variables over multiple timepoints (Rotarod, grip strength), the MIXED procedure of the Statistical Analysis Systems software (SAS Institute Inc.) and subsequent post-hoc contrasts were used to

examine interactions as before (Elmore et al., 2015; Elmore et al., 2018). All bar graphs are represented as means ± standard error of the mean (SEM) with individual sample values overlain. Significance is expressed as follows: * $p<0.05$, ** $p<0.01$, *** $p<0.001$, **** $p<0.0001$

Data availability

Gene expression data is deposited in GEO (ascension number GSE136158), and all RPKM values can be viewed and searched through at http://rnaseq.mind.uci.edu/green/R62_PLX/gene_search.php. All other data is available upon reasonable request.

Results

CSF1Ri via PLX3397 depletes microglia in R6/2 mice

To evaluate the dependency of microglia on CSF1R signaling in R6/2 mice – a rapidly progressing mouse model expressing an expanded repeat exon 1 transgene (Mangiarini et al., 1996) – the CSF1R/c-Kit inhibitor PLX3397 (275 mg/kg) or vehicle was provided in chow to R6/2 mice and nontransgenic littermates for 7 days to generate four experimental groups: NT + vehicle (**Control**), NT + PLX3397 (**7d PLX3397**), R6/2 + vehicle (**R6/2**), and R6/2 + PLX3397 (**R6/2 + 7d PLX3397**). IHC with the myeloid marker IBA1 revealed a significant increase in striatal R6/2 microglial densities at 7 weeks of age ($p<0.001$) that was not seen in the diseased somatosensory cortex at this timepoint (Fig. 1.1). Importantly, 7 days of PLX3397 delivered at 6 weeks significantly depleted striatal and cortical microglia from R6/2 ($p<0.0001$, $p<0.0001$) and nontransgenic mice ($p<0.001$, $p<0.001$) to comparable densities of surviving cells ($p>0.05$), suggesting that microglial

mHTT expression does not appear to alter their dependence on CSF1R signaling for survival.

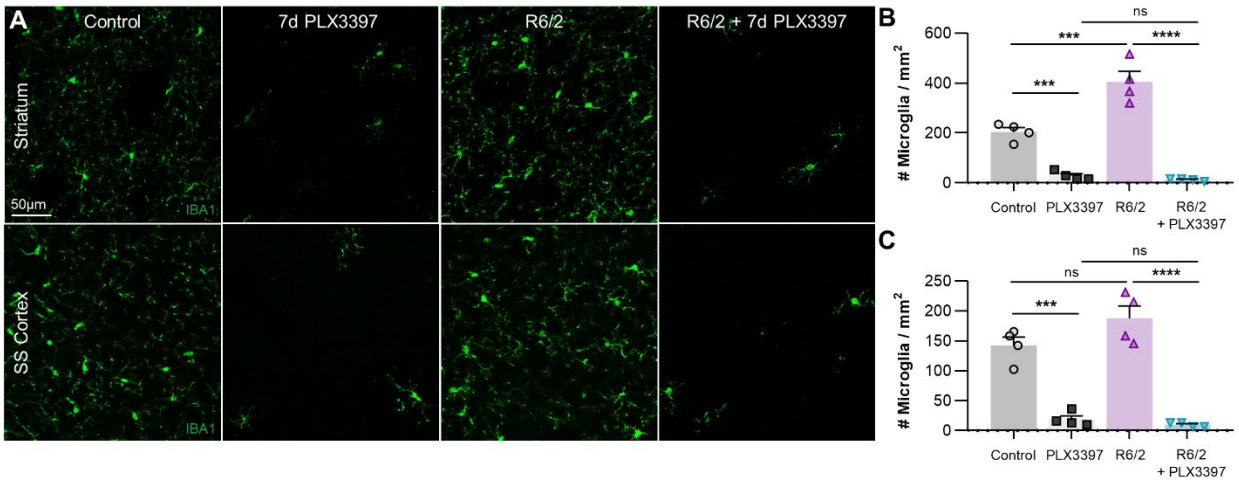

Figure 1.1. 7 days of 275mg/kg PLX3397 significantly reduces elevated IBA1⁺ microglia numbers in 6-week-old R6/2 mice. A. Representative 20X images of striatal/cortical IBA1⁺ microglia from 6-week-old R6/2 or nontransgenic mice treated with vehicle or 275mg/kg PLX3397 for 7 days. **B-C.** Quantification of microglia revealed significantly increased densities in the R6/2 striatum at 7 weeks ($p<0.001$) and confirm significant and comparable depletion with 7d 275 mg/kg PLX3397 compared to vehicle-treated controls in R6/2 ($p<0.0001$, $p<0.0001$) and NT ($p<0.001$, $p<0.001$) striatum/somatosensory cortex (two-way ANOVA with Tukey's post-hoc test; n=4/group). Statistical significance is denoted by * $p<0.05$, ** $p<0.01$, *** $p<0.001$, **** $p<0.0001$. Error bars indicate SEM.

CSF1Ri via PLX3397 ameliorates grip strength and novel object recognition deficits in R6/2 mice

Having demonstrated that microglia could be eliminated in R6/2 mice, we next set out to investigate the roles these cells play in disease progression. Following baseline behavioral measurements, 6 week-old R6/2 mice and NT littermates were placed on diet containing 275 mg/kg PLX3397 or vehicle (n=6/group) until sacrifice at 11 weeks (Fig. 1.2A). CAG repeats were confirmed at a range of 126-130 repeats in R6/2 mice. While treatment had no effect on body weight, which displayed the stereotypical plateauing in R6/2 mice at ~7 weeks (Fig. 1.2B), we found that over the duration of CSF1Ri, HD-related grip strength deficits were prevented up to week 11, with significant improvement

remaining even at that time point (Fig. 1.2C). While inhibitor treatment could potentially affect muscle macrophages in a way that reduces skeletal muscle mHTT inclusions (Moffitt et al., 2009) or transcriptional alterations (Strand et al., 2005), PLX3397 has not been reported to reduce peripheral macrophage numbers (Elmore et al., 2014; Mok et al., 2014; Szalay et al., 2016). Cognitively, treatment prevented R6/2 deficits in novel object recognition at 11 weeks (Fig. 1.2D) while having no effect on controls, consistent with previous measures of cognition following CSF1Ri in healthy mice (Elmore et al., 2014). No groups differed statistically in average velocity or distance traveled by open field analysis (data not shown) indicating that these differences are due to effects on cognition. We did not observe any effect of treatment on HD-related Rotarod performance deficits (Fig. 1.2E). Finally, to verify cognitive and motor improvements with CSF1Ri in this model, these behavioral tasks were replicated in a second cohort of n=10/group (Fig. 1.2F-I), producing similar results. The failure to achieve statistical significance in NOR with this second cohort may be attributed to the rapid progression of the model, as many R6/2 mice were largely immobile/lethargic at week 11 just prior to sacrifice, increasing the number of animals excluded during novel object training and consequently decreasing statistical power. Nonetheless, the similar cognitive and grip strength effects observed between cohorts suggests that PLX3397 may have therapeutic potential in HD, particularly in the case of grip strength.

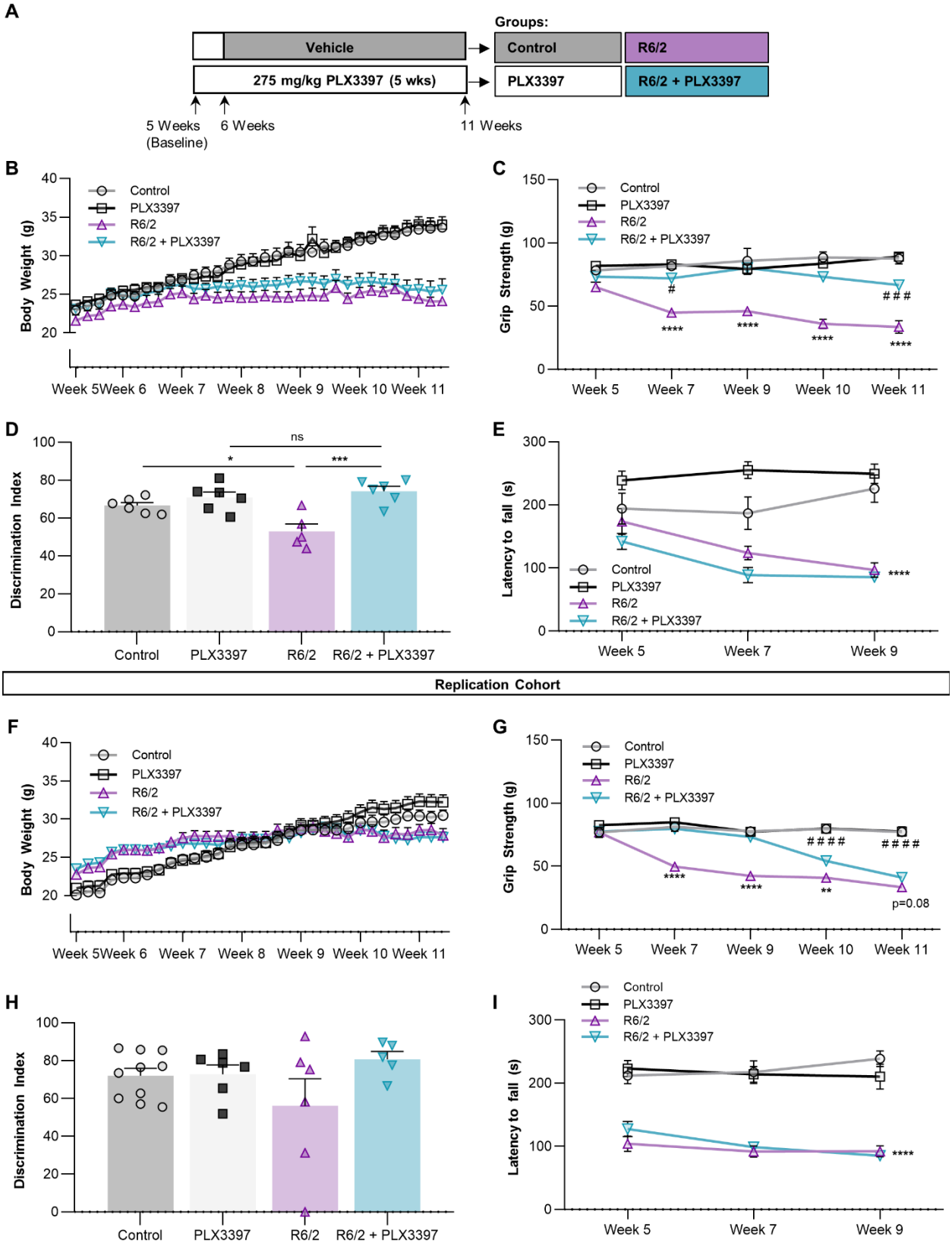

Figure 1.2. PLX3397 (CSF1Ri) ameliorates grip strength and object memory deficits in R6/2 mice. Following baseline

measurements, 6-week-old nontransgenic or R6/2 mice were treated with vehicle (Control, R6/2) or 275 mg/kg PLX3397 (PLX3397, R6/2+PLX3397) for 5 weeks to attain microglial depletion through colony-stimulating factor 1 receptor inhibition (CSF1Ri). **A.** Experimental design (n=5-6/group). **B.** Body weight from baseline to end of experiment displayed stereotypical R6/2 plateauing (n=5-6/group). **C.** R6/2+PLX3397 forelimb grip strength deficits were significantly reduced compared to R6/2 at every timepoint tested ($p<0.0001$; MIXED procedure with post-hoc contrasts; n=5-6/group). **D.** Performance in novel object recognition (NOR) test by R6/2+PLX3397 mice at week 11 was significantly better than R6/2 mice ($p<0.001$) and not different from PLX3397 controls (two-way ANOVA with Tukey's post-hoc test; n=5-6/group). **E.** Latency to fall from an accelerating Rotarod was not altered with treatment and displayed the stereotypical R6/2 genotype effect ($p<0.0001$; MIXED procedure; n=6/group). **F-I.** Replication cohort for validation of behavioral outcomes utilizing the same statistical analyses. (n=8-10/group, except for NOR where n=5-10/group due to exclusion criteria from day 1 acquisition period). Statistical significance is denoted by * $p<0.05$, ** $p<0.01$, *** $p<0.001$, **** $p<0.0001$, ns = not significant. For grip strength, * indicates R6/2 vs. R6/2+PLX3397 and # indicates PLX3397 vs. R6/2+PLX3397. Error bars indicate SEM.

R6/2 microglia display regional differences but are ubiquitously depleted with CSF1Ri

To assess the microglial response to disease, IHC with the myeloid marker IBA1 was performed on coronal brain sections from each group. Microglial number, cell body area, and IBA1 intensity were measured in the disease-relevant striatum as well as in multiple cortical regions (motor, somatosensory, and piriform cortex) (Fig. 1.3A). R6/2 mice displayed elevated microglial densities in the striatum ($p=0.01$) and motor cortex ($p=0.05$), in addition to a trending increase in the somatosensory cortex ($p=0.06$; Fig. 1.3B, C). Microglial cell body area (Fig. 1.3D) and IBA1 intensity (Fig. 1.3E) were significantly increased only in the motor ($p<0.01$, $p<0.01$) and somatosensory cortices ($p<0.05$, $p<0.05$). Striatal microglia, although at greater densities, did not appear activated morphologically or by $IBA1^+$ intensity, and were negative for the activation marker IB4 (data not shown). Together, this suggests that "classical" microglial activation is not an overt feature of the R6/2 brain. Consistent with the data from 7 days of treatment, CSF1Ri

significantly depleted microglial numbers in all tissue regions and in both genotypes as expected (Fig. 1.3C).

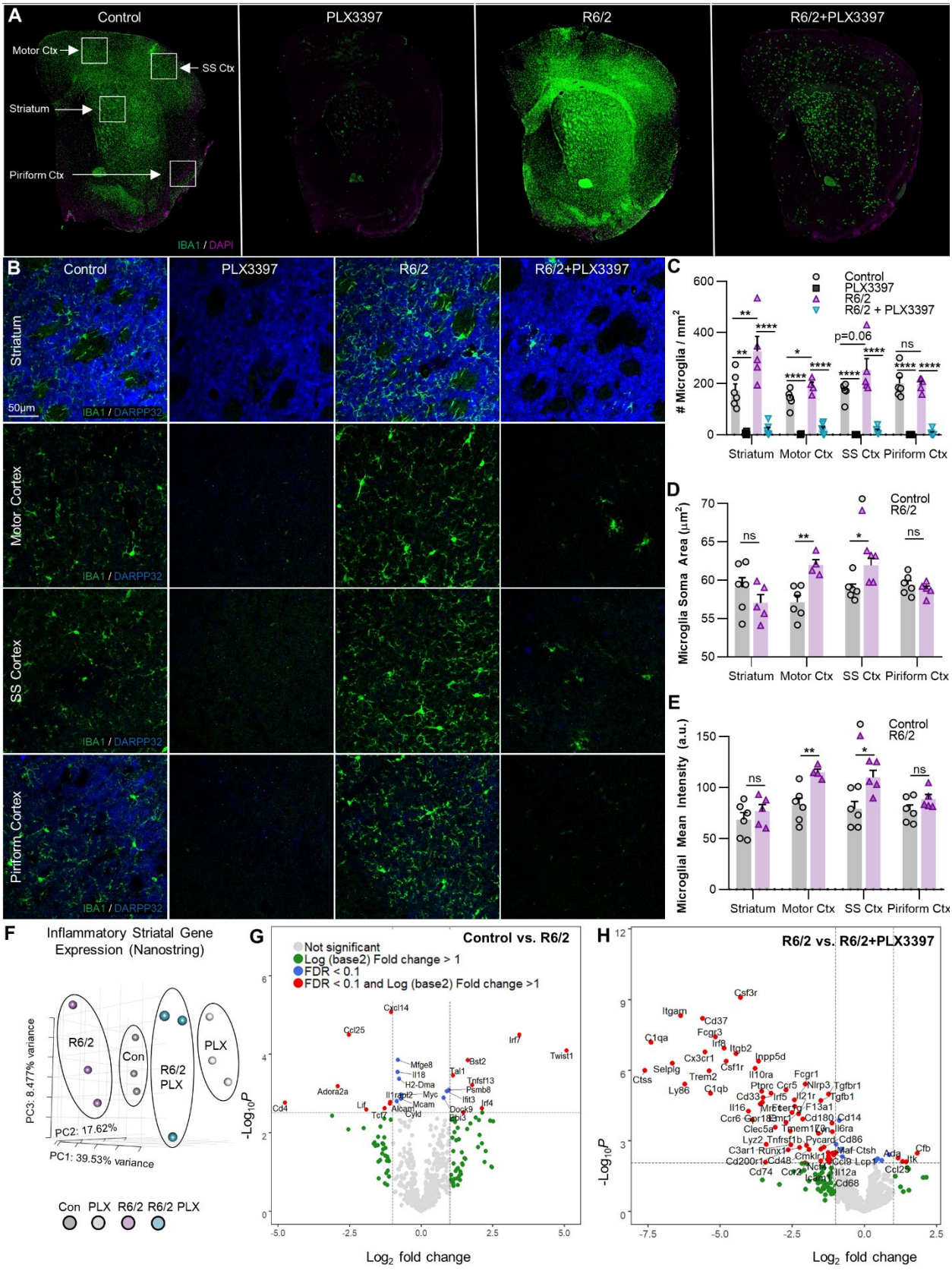

Figure 1.3. CSF1Ri depletes striatal and cortical R6/2 microglia, which are increased in number but do not appear

"classically" activated. A. Representative IBA1$^+$ whole-brain and **B.** 20X striatal and motor, somatosensory (SS), and piriform cortex images from nontransgenic and R6/2 mice treated with vehicle or PLX3397 confirmed R6/2 microgliosis and microglial depletion (n=5-6/group). **C.** Quantification of IBA1$^+$ microglia revealed significant increases in the R6/2 striatum ($p<0.01$) and motor cortex ($p<0.05$), with a trending increase in the SS cortex ($p=0.06$) but no change in the piriform cortex compared to control. PLX3397 significantly depleted microglia in both genotypes and in all regions (two-way ANOVAs with Tukey's post-hoc test; n=4-6/group). **D.** Microglia increased in size with disease in the motor ($p<0.01$) and SS ($p<0.05$) cortices but remained ramified and did not adopt an amoeboid morphology (two-tailed unpaired t-tests; n=4-6/group). **E.** IBA1$^+$ intensity mirrored changes in cell size, with significant increases in motor ($p<0.01$) and SS ($p<0.05$) cortices in R6/2 mice compared to control (two-tailed unpaired t-tests; n=4-6/group). **F.** Striatal inflammatory gene expression assessed with a NanoString immune panel revealed non-overlapping clustering of samples in each group by principal component analysis (PCA; n=3/group). **G-H.** Volcano plots of differentially expressed genes (DEGs) in R6/2 vs. control striatum (**G**) indicated a lack of inflammatory transcription at a false-discovery rate (FDR) of < 0.1, but (**H**) confirmed loss of the microglial gene signature with PLX3397 in R6/2 striatum (n=3/group). Statistical significance is denoted by * $p<0.05$, ** $p<0.01$, *** $p<0.001$, **** $p<0.0001$, ns = not significant. Error bars indicate SEM.

R6/2 striatal mRNA expression reveals dysregulated interferon signaling and significant gene enrichment overlap with human HD caudate that is partially mitigated with CSF1Ri

A NanoString inflammatory panel (NS_Mm_CancerImm_C3400) was used to assess endpoint DEGs in striatal tissue from 3 mice per group. PCA of normalized gene counts revealed separate clustering of control and R6/2 tissue both prior to and following CSF1Ri (Fig. 1.3F). However, even at FDR < 0.1, few inflammation-related DEGs were found in R6/2 striatal tissue (Fig. 1.3G). In addition to a marked decrease in striatal adenosine A2a receptor (*Adora2a*), canonically downregulated in HD (Blum et al., 2018), we noted altered T-cell and interferon signaling (↑ *Twist1, Ebi3, Tal1, Ccl19, Irf7, Irf4, Bst2, Ifit3, Psmb8;* ↓ *CD4, Alcam, Tcf7, Mcam, Ccl25, Il18*), similar to recent reports of peripheral T-cell suppression in R6/2 mice (Lee et al., 2018). Surprisingly, we found no evidence of disease-related inflammation in terms of cytokine transcript expression (*Il6, Il1β, Ifnγ, Tnfα*) at the 11-week timepoint using this panel (Fig. 1.3H). DEGs in CSF1Ri-treated R6/2 mice largely reflected microglial depletion, in addition to partial reversals in T-cell

transcript levels (*Tal1, Ccl25)*. As before (Najafi et al., 2018), CSF1Ri treatment in nontransgenic mice induced the expected loss of microglial gene signature from the brain transcriptome (data not shown).

To broaden our scope of gene expression analysis, we performed RNA-seq on the same striatal extracts used for NanoString. All RPKM values can be searched and visualized at http://rnaseq.mind.uci.edu/green/R62_PLX/gene_search.php. We again observed distinct clustering of genotypes, but this time divergent effects of CSF1Ri on the R6/2 transcriptome were detected (Fig. 1.4A). At week 11, striatal R6/2 transcription was considerably suppressed relative to controls (Fig. 1.4B) as has been described previously (Hodges et al., 2006; Luthi-Carter et al., 2003; Runne et al., 2008; Vashishtha et al., 2013). Among the downregulated genes were *GAD1* and *GAD2*, which encode the enzymes that catalyze GABA synthesis (2017), as well as the MSN voltage-gated sodium channel β4 subunit *Scn4b* (Miyazaki et al., 2014; Oyama et al., 2006), and the astrocyte glutamate transporter *Slc7a11*, all indicative of dysregulated excitatory/inhibitory balance. Microglial elimination was followed by telltale loss of microglial gene expression in control (not shown) and R6/2 mice (Fig. 1.4C). Among other genes, CSF1Ri prevented the disease-associated suppression of *Isl1*, a gene involved in motor neuron development (Liang et al., 2011) the conditional deletion of which results in striatal cholinergic interneuron loss (Elshatory and Gan, 2008), as well as *Cacna2d2*, mutations in which decrease Ca^{2+} channel subunit expression and drive epileptic seizures (Barclay et al., 2001; Pippucci et al., 2013). Importantly, this differential expression occurred in the absence of detectable changes in endogenous wild-type *HTT* transcript levels across

groups. RNAseq DEGs were validated by and mirrored in the prior results from the more sensitive NanoString assay covering a subset of immune genes.

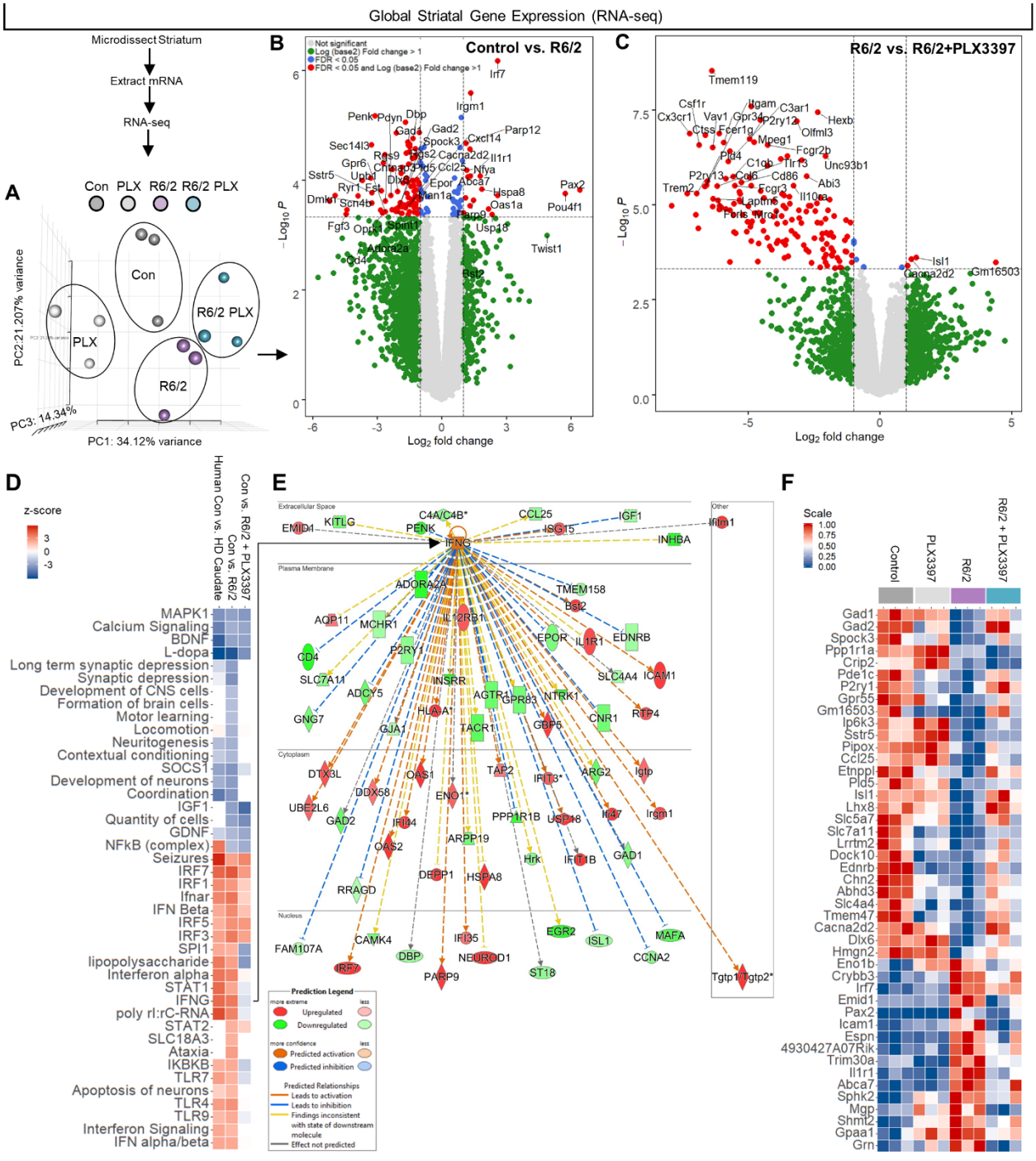

Figure 1.4. RNA-seq and pathway analysis confirms lack of inflammatory transcriptional polarization in R6/2 striatum, except for a dysregulated interferon signature resembling the human HD caudate that is partially resolved following CSF1Ri. A. PCA of striatal gene expression as determined by mRNA-seq confirmed similar non-overlapping clustering of control and R6/2 samples but

a divergent effect of PLX3397 (n=3/group). **B-C.** Volcano plots of control vs. R6/2 DEGs (**B**) confirmed an absence of inflammatory transcript upregulation in the R6/2 striatum and (**C**) a loss of microglial gene expression with PLX3397 (FDR≤0.05; n=3/group). **D.** Pathway analysis (IPA) of 860 control vs. R6/2 DEGs and 1380 control vs. R6/2+PLX3397 DEGs (FDR≤0.1; n=3/group) revealed a distinct interferon signature and suppressed neuronal development and neuritogenesis pathways in the R6/2 striatum that closely resembled the human HD caudate, and which were partially resolved following PLX3397. Top significant predicted upstream regulators included HTT, IFNγ, L-DOPA, IRF7, and TRIM24, with associated activation z-scores of 2.151 (p<8.31E-22), 3.727 (p<1.01E-15), -5.654 (p<1.19E-20), 4.589 (p<7.47E-13), and -3.970 (p<3.58E-12) respectively. **E.** IPA predicted IFNγ as the major cytokine upstream regulator in the R6/2 striatum, signaling which, along with IFNα, is no longer enriched in R6/2+PLX3397 striatum. **F.** A heatmap of control vs. R6/2 DEGs (FDR<0.1) that were reversed with treatment by unadjusted p-value (p<0.05) to indicate potential mediators of beneficial PLX3397 effects (n=3/group). All RPKM values can be searched and visualized at http://rnaseq.mind.uci.edu/green/R62_PLX/gene_search.php.

A growing number of non-viral diseases are characterized by the presence of a similar IFN transcriptional signature (Mostafavi et al., 2016) evident within the microglial transcriptome itself as upregulated interferon signaling gene sets in cells isolated from both an AD-like model of neurodegeneration as well as aging humans (Galatro et al., 2017; Mathys et al., 2017). We compared the activation z-scores of significantly overrepresented pathways in human control vs. HD caudate (z-score overall = 41.23; gene expression data taken from (Hodges et al., 2006)) to those in control vs. R6/2 striatal tissue and found concordance between the mouse model and the human disease (Fig. 1.4D). A dysregulated IFN signature was found in both the murine and human manifestation of disease (Fig. 1.4D), facets of which were ameliorated with CSF1Ri-mediated microglial elimination as indicated by a resolution of IFNα and IFNγ, but not IFNβ, gene enrichment in control vs. R6/2 + PLX3397 samples. This was accompanied by a concurrent loss of IFN-involved toll-like receptor signaling (*Tlr4, 7, 9*) as well as downstream IFN effector pathways (*Stat1*). Pathway enrichment predicted HTT as the most significant upstream regulator of R6/2 DEGs (z-score: 2.151, p<8.31E-22), in addition to IFNγ (z-score: 3.727, p<1.01E-15), L-dopa (z-score: -5.654, p<1.19E-20), the

type I IFN regulator IRF7 (z-score: 4.589, p<7.47E-13), and TRIM24 (z-score: -3.970, p<3.58E-12). Thus, pathway analysis of the R6/2 vs control brain predicted IFNγ as the primary cytokine regulator of disease DEGs (Fig. 1.4E), a potent stimulator of microglial activation (Monteiro et al., 2017). Interestingly, *Usp18* was markedly increased in HD, which inhibits microglial activation by specifically blocking IFN-induced transcription (Goldmann et al., 2015), suggesting the mobilization of relevant compensatory mechanisms in the R6/2 striatum.

Microglial elimination normalized several additional overrepresented human/murine HD pathways, i.e. impaired neuronal development, neuritogenesis, contextual conditioning, and coordination. This occurred in the absence of an extensive inflammatory transcriptional signature. Indeed, the pro-inflammatory NFκβ pathway was upregulated in the human HD caudate, but not R6/2, where inflammatory transcripts such as *Il6* and *Il1b* were in fact below detection limits, indicating that this model likely does not fully recapitulate the neuroinflammation observed in end-stage human HD (Crotti and Glass, 2015; Rodrigues et al., 2016; Yang et al., 2017). Accordingly, FDR and unadjusted p-values (FDR<0.1 for Control vs. R6/2 plus p<0.05 for R6/2 vs. R6/2 + PLX3397) in addition to hierarchical clustering were used to identify genes that were changed in R6/2 mice and subsequently prevented with treatment in order to identify potential non-immune targets of CSF1Ri-mediated microglial elimination (Fig. 1.4F).

CSF1Ri and consequent microglial depletion reduces mHTT accumulation and disease-related protein clearance pathway dysregulation

To investigate whether sustained CSF1R inhibition altered the accumulation of mHTT, we first examined intranuclear mHTT inclusion bodies (EM48) in the same regions

assessed for microgliosis (Fig. 1.5A). Nuclear inclusion bodies were rarely seen in microglia, consistent with previous studies finding that they are predominantly neuronal (Jansen et al., 2017). Instead, when we found EM48^{+} staining in microglia it was localized to cytoplasmic CD68^{+} lysosomal granules (Fig. 1.5B; arrows). Following CSF1Ri the total number of EM48-labeled inclusion bodies was modestly reduced in the striatum (~25%; $p<0.05$), consistent with the results from a recent study suppressing microglial Galectin-3 in HD models (Siew et al., 2019), while EM48 intensity was significantly reduced in the somatosensory cortex ($p<0.05$) (Fig. 1.5C-E). We also confirmed previous reports of colocalization of the autophagic protein p62 with EM48^{+} inclusion bodies in R6/2 mice (Kurosawa et al., 2015) (Fig. 1.5F). Finally, although PLX3397 is more selective for CSF1R, it can also inhibit c-Kit and, at higher concentrations, Flt3 receptor tyrosine kinases (IC50 of 0.013, 0.027 and 0.16 μM respectively (Tap et al., 2015)). Staining for c-Kit and Flt3 revealed no colocalization with neurons or microglia (Fig. 1.6, 1.7), and no significant differences were detected in their transcript levels (*Kit*, *Flt3*) by RNAseq across groups, supporting the notion that the effects seen here are due specifically to the inhibition of microglial CSF1R and subsequent microglial depletion.

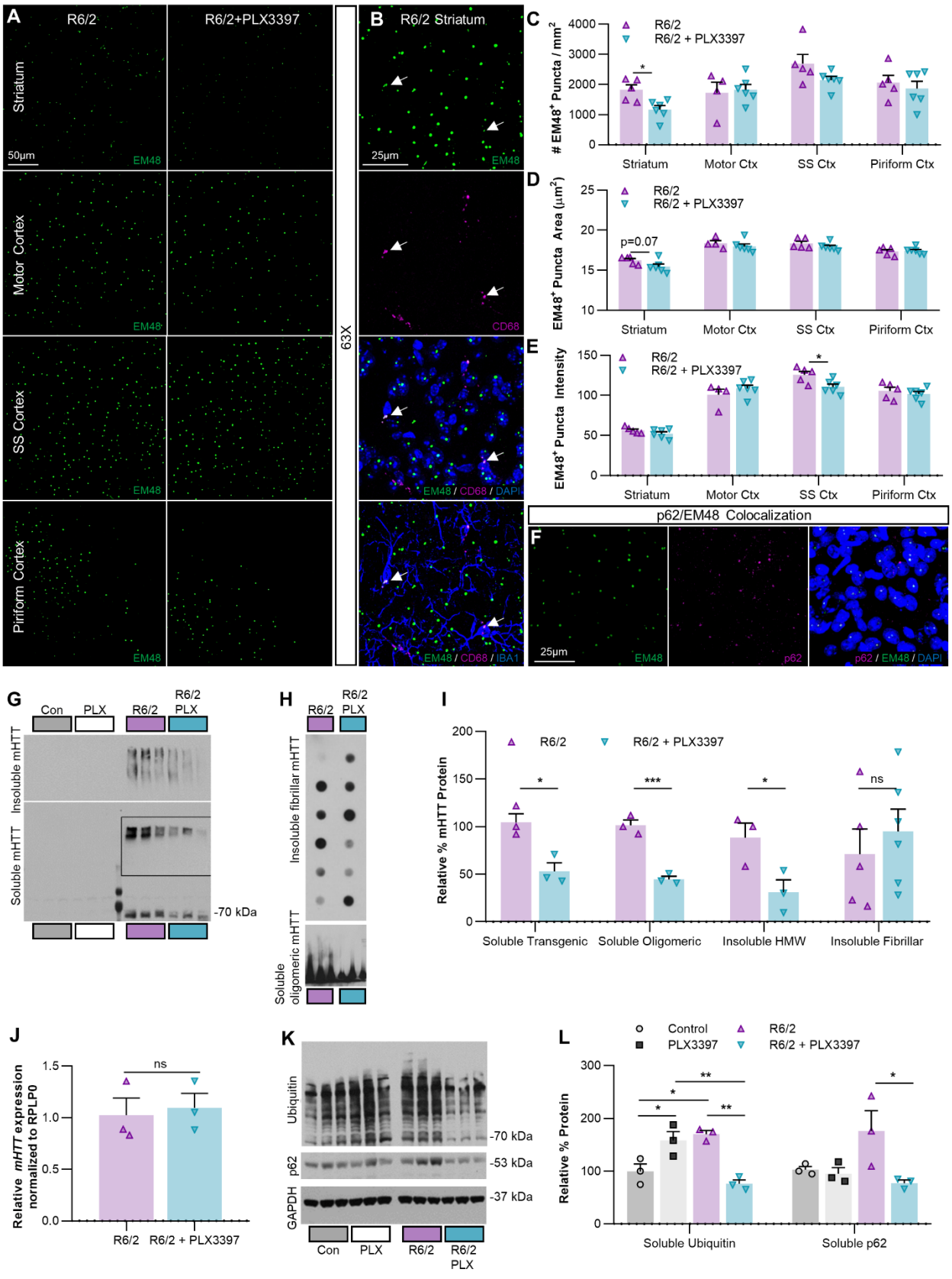

Figure 1.5. CSF1Ri-mediated microglial depletion reduces striatal R6/2 mHTT accumulation and protein clearance system

dysregulation. A. Representative 20X images of R6/2 and R6/2+PLX3397 striatal and cortical EM48^{+} nuclear mHTT inclusions in 11-week-old R6/2 mice (n=4-6/group). **B.** Representative 63X images of microglial EM48+ mHTT. When it occurs, it is non-nuclear and colocalizes with CD68^{+} lysozomes. **C-E.** Quantification of R6/2 EM48^{+} nuclear puncta, which are (C) significantly reduced in number in the striatum with PLX3397 ($p<0.05$), where they (D) also display a trending decrease in area ($p=0.07$). Treatment also (E) significantly reduced mean EM48^{+} intensity ($p<0.05$) in the SS cortex (two-tailed unpaired t-tests; n=4-6/group). **F.** Representative 63X images of p62^{+}/EM48^{+} nuclear colocalization in R6/2 striatum. **G-H.** Western blots of striatal homogenates separated into detergent-soluble and insoluble fractions and probed for mHTT protein species (n=3-6/group). **I.** Quantification of immunoblotted mHTT species revealed that R6/2+PLX3397 mice had significantly reduced soluble transgenic ($p<0.05$), soluble oligomeric ($p<0.001$), and insoluble high molecular weight (HMW) mHTT ($p<0.05$) in the striatum compared to R6/2 (two-tailed unpaired t-tests; n=3-6/group). **J**. qPCR of striatal R6/2 RNA indicates that PLX3397 did not change mHTT expression (two-tailed unpaired t-test; n=3/group). **K**. Western blots of striatal homogenates immunoblotted for soluble ubiquitinated proteins, p62, and the housekeeping protein GAPDH (n=3/group). **L.** The accumulation of ubiquitinated species was significantly increased in R6/2 striatum compared to control ($p<0.05$) and this was prevented with PLX3397 ($p<0.01$); interestingly, PLX3397 also significantly increased ubiquitination in control mice ($p<0.05$). PLX3397 also induced a significant reduction in R6/2 striatal p62 levels ($p<0.05$) (two-way ANOVAs with Tukey's post-hoc test; n=3/group). Statistical significance is denoted by * $p<0.05$, ** $p<0.01$, ***$p<0.001$, ns = not significant. Error bars indicate SEM.

In addition to nuclear inclusions, mHTT fragments build up in multiple detergent-soluble and -insoluble biochemical species of increasing complexity that can be resolved by fractionation (Ochaba et al., 2018). To further assess mHTT flux accompanying the observed changes in inclusion body number following CSF1Ri, we immunoblotted for detergent-soluble and insoluble mHTT in striatal homogenates from R6/2 mice as described (Ochaba et al., 2016) (Fig. 1.5G-I). CSF1Ri and microglial depletion significantly reduced both monomeric ($p<0.05$) and oligomeric ($p<0.001$) mHTT in the detergent-soluble fraction, consisting of largely cytoplasmic proteins (O'Rourke et al., 2013). In the detergent-insoluble fraction, containing high molecular weight (HMW) mHTT multimers, insoluble fibrils, and nuclear proteins, we found that CSF1R reduced HMW ($p<0.05$) but not fibrillar mHTT species. While microglia do express *mHTT*, the paucity of nuclear inclusions in these cells (Jansen et al., 2017) compared to the more abundant

neurons – potentially due to the former's greater proteosomal and autophagic capacity (Yang et al., 2017) – suggests that elimination of microglia reduces neuronal mHTT accumulation. To confirm that mHTT changes did not stem from transcriptional suppression or "gene knockdown" via microglial elimination, we performed qPCR of the mutant transgene in the striatum and found that CSF1Ri did not alter *mHTT* expression (Fig. 1.5J), thus suggesting that changes in protein level were independent of transcript abundance.

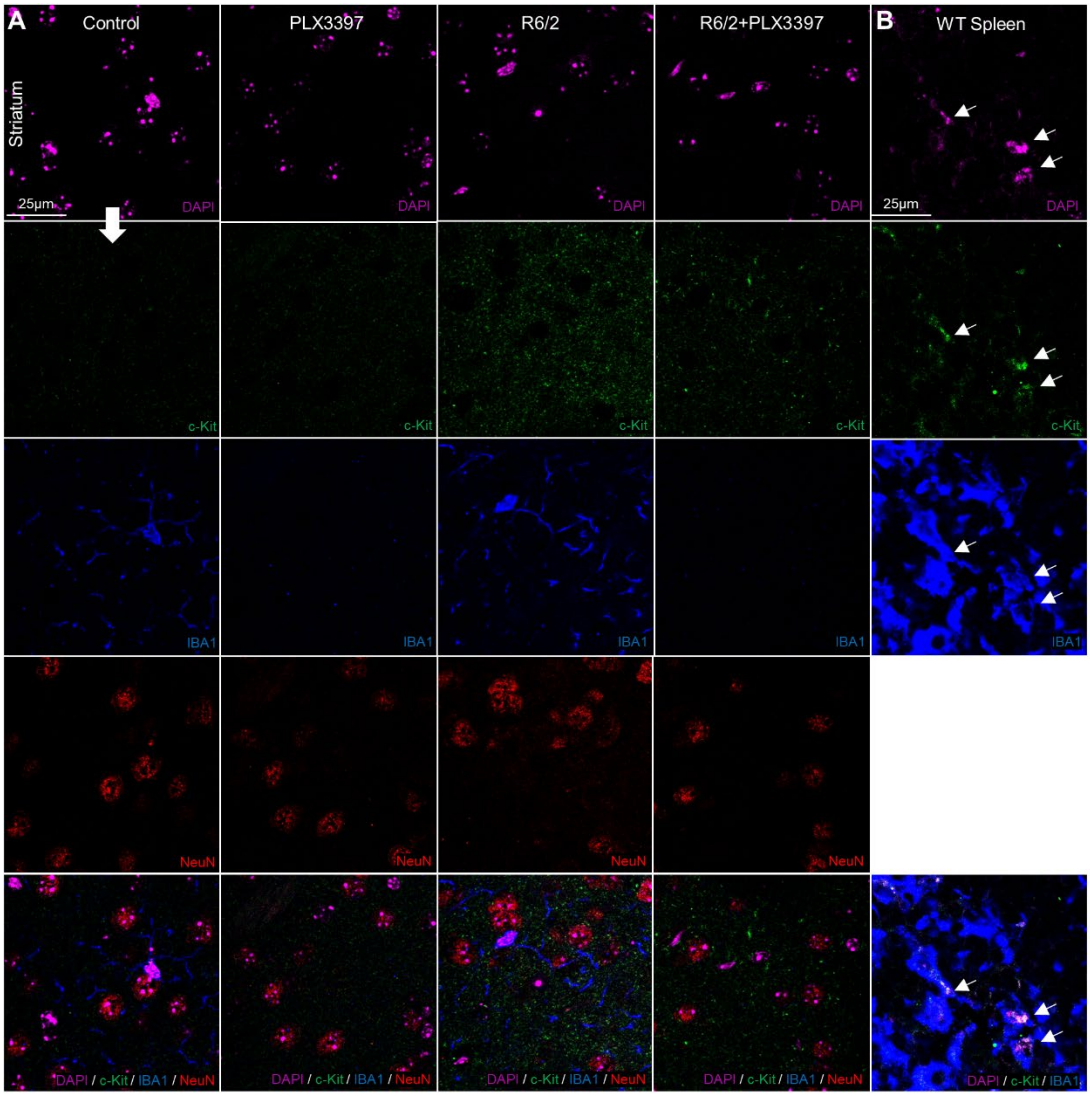

Figure 1.6. c-Kit is not expressed by neurons or microglia in R6/2 or nontransgenic brains. A. Representative 63X images

confirming absence of neuronal or microglial c-Kit expression in vehicle- or PLX3397-treated R6/2 or nontransgenic striatum at 11 weeks. **B.** Representative 63X image of c-Kit^{+}IBA1^{+} cells in adult wild-type spleen.

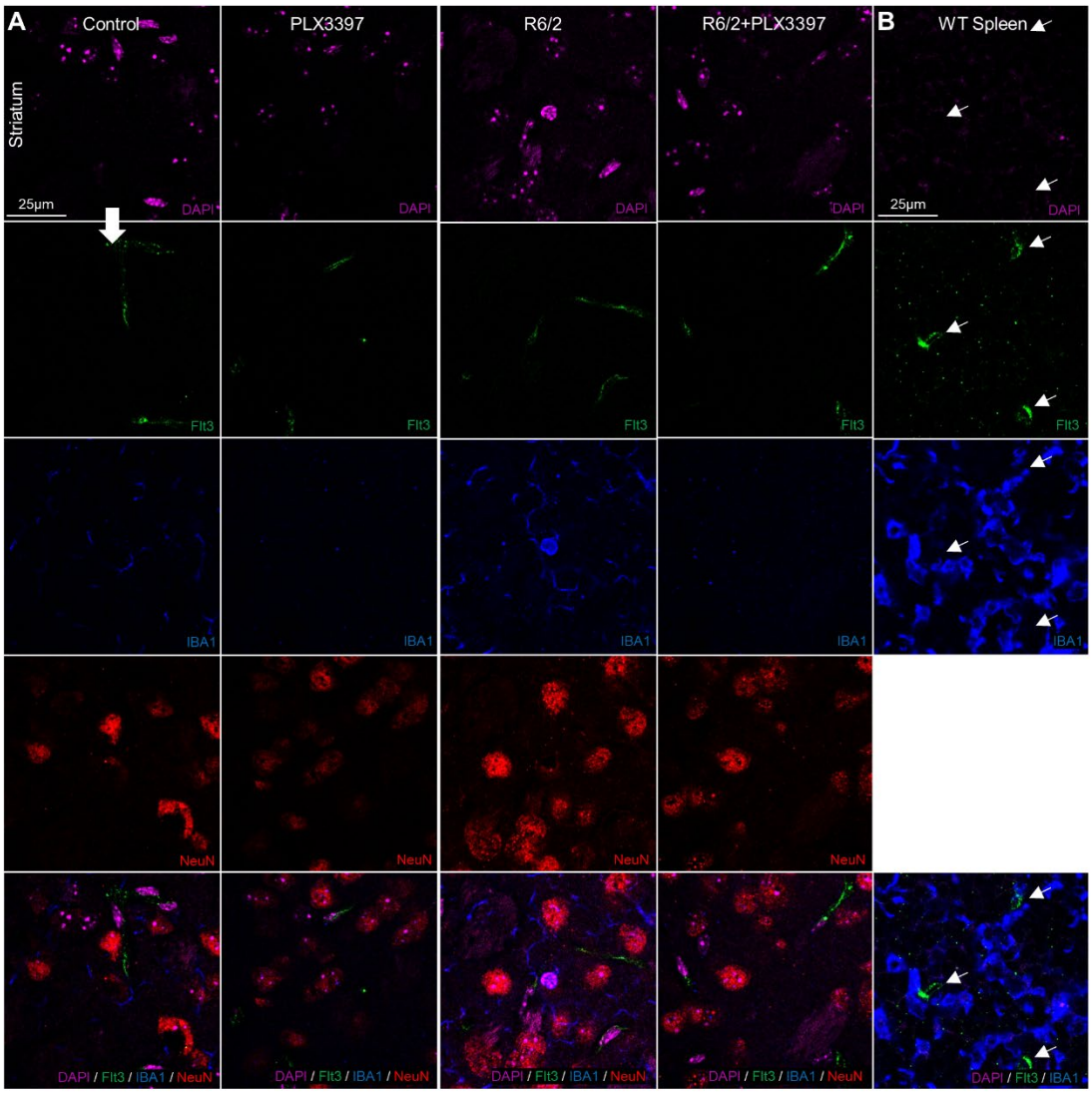

Figure 1.7. Flt3 is not expressed by neurons or microglia in R6/2 or nontransgenic brains. A. Representative 63X images confirming absence of neuronal or microglial Flt3 expression in vehicle- or PLX3397-treated R6/2 or nontransgenic striatum at 11 weeks. **B.** Representative 63X images of Flt3^{+} cells in adult wild-type spleen.

Ubiquitin- and autophagy-based protein clearance systems are highly impaired in HD, as evidenced by a striking build-up of ubiquitinated species in patient brain and mouse models (Bennett et al., 2007; Ochaba et al., 2016) and an upregulation of the autophagy marker p62 (Lee et al., 2012). Immunoblotting for ubiquitinated proteins in the detergent-

soluble striatal fraction confirmed significantly greater ubiquitination in R6/2 mice ($p<0.05$), but also, surprisingly, that CSF1Ri completely prevented this phenotype (Fig. 1.5K, L). Striatal p62 was significantly reduced in CSF1Ri-treated R6/2 mice ($p<0.05$), although levels were not statistically higher in these compared to controls (Fig. 1.5L). Together, these data suggest that microglial depletion via CSF1Ri slows the accumulation of multiple species of mHTT in the R6/2 striatum by at least partially reversing dysfunctional protein clearance systems. Interestingly, the removal of microglia from control mice enhanced ubiquitination ($p<0.05$), suggesting a potential role for these myeloid cells in homeostatic non-microglial protein clearance.

Microglial depletion with CSF1Ri prevents R6/2 striatal atrophy

Despite minimal neuronal loss even in late stages of the disease (Dodds et al., 2014), R6/2 mice display marked striatal atrophy (Hansson et al., 1999; Li et al., 2005) similar to humans. *mHTT* expression in R6/2 microglia effectively "primes" the cell by increasing expression of the myeloid transcription factor Pu.1 (Crotti et al., 2014), a positive regulator of microglial phagocytosis (Smith et al., 2013). We hypothesized that enhanced phagocytic capability of mHTT-containing microglia could mediate remodeling of striatal neurites and/or ECM in HD. We performed double-blinded stereology of the anterior caudoputamen, representing the dorsal striatum, using 6 coronal sections collected at 240μm intervals from CSF1Ri- and vehicle-treated control and R6/2 mice (Fig. 1.8A). Surprisingly, we found that microglial elimination via CSF1Ri completely prevented the decrease in striatal volume observed in R6/2 mice (Fig. 1.8B) independent of changes in neuronal density (Fig. 1.8C, D). In fact, we found significantly greater $NeuN^+$ cell density in the HD striatum ($p<0.05$) that did not change with treatment.

To better understand the structural relationship between the neural components of the diseased striatum, we next examined neuropil by staining for the Type II microtubule-associated proteins MAP2 and tau, localized to neuronal dendrites and axons, respectively (Zhang and Dong, 2012). Both proteins stabilize microtubules critical for autophagosome transport (Kast and Dominguez, 2017) especially in neurons where distal autophagosomes travel long distances to fuse with soma-localized lysosomes (La Spada and Taylor, 2010). Furthermore, faulty splicing in HD increases total tau and the juvenile form of MAP2 (Fernandez-Nogales et al., 2016), which retracts from the dendrites towards the neuronal cell body in HD patients (Cabrera and Lucas, 2017), together promoting dendritic and striatal atrophy. We found significant elevations in the integrated densities of MAP2 ($p<0.0001$) and tau ($p<0.0001$) fluorescent signal in the R6/2 striatum (Fig 1.8E-H), alterations which were either partially (MAP2) or entirely (tau) normalized with CSF1Ri.

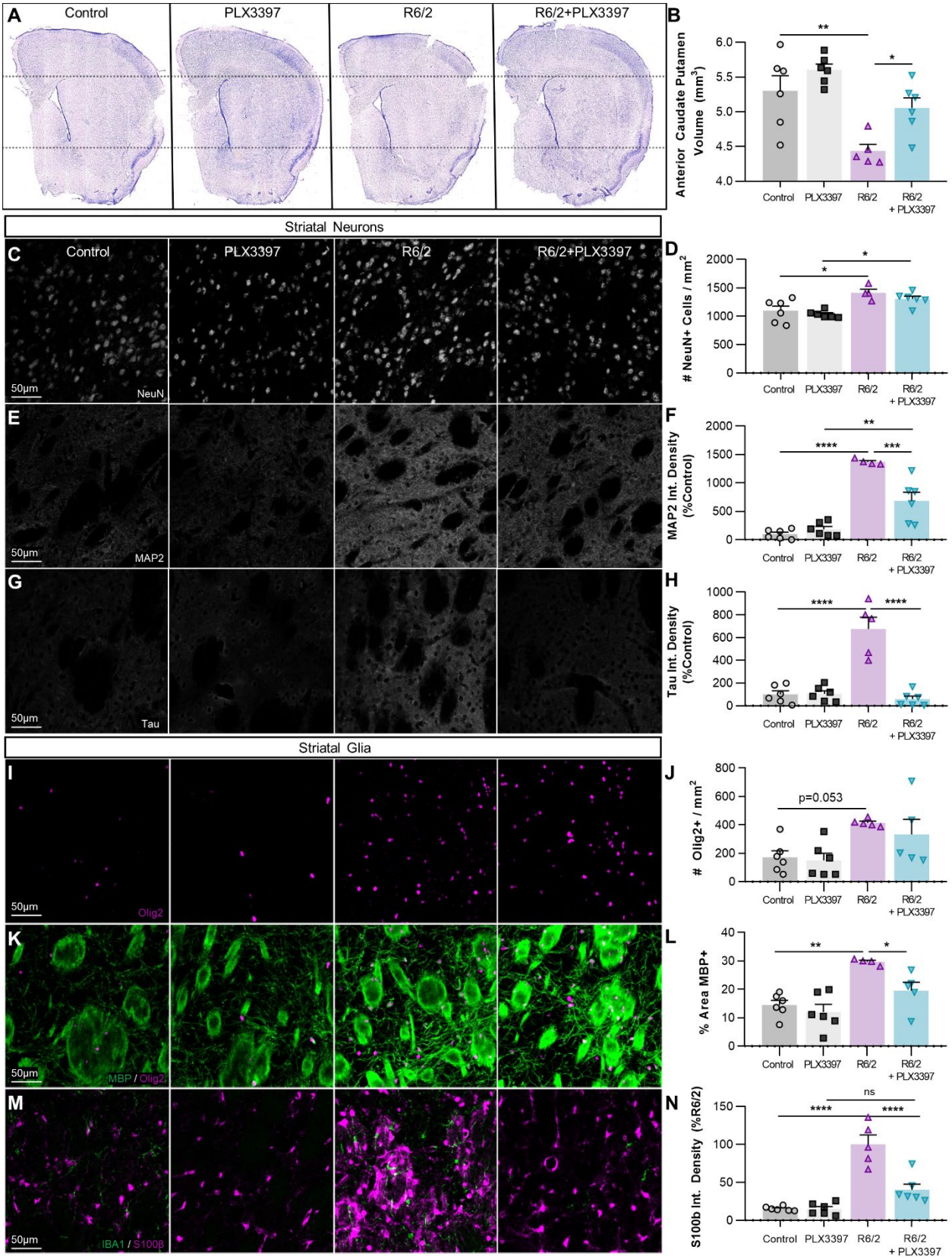

Figure 1.8. PLX3397 prevents R6/2 striatal volume loss, neurite abnormalities, and astrogliosis. **A.** Representative images of

cresyl-violet stained coronal sections used for stereological assessment of striatal volume (n=5-6/group, 6 sections/mouse separated by 240μm intervals, spanning the anterior caudoputamen). **B.** Quantification of stereological analysis reveals a significant reduction in R6/2 striatal volume vs. control ($p<0.01$) that is prevented with PLX3397 ($p<0.01$) (two-way ANOVA with Tukey's post hoc test; n=5-6/group). **C-H.** Investigation of striatal neurons revealed increased $NeuN^+$ density (20X **C**, **D**) in R6/2 and R6/2+PLX3397 mice compared to respective controls ($p<0.05$) (two-way ANOVA with Tukey's post-hoc test; n=4-6/group). Integrated $MAP2^+$ (20X **E, F**) and tau^+ (20X **G, H**) signal density, staining for microtubule-associated proteins localized to the dendrites and axons respectively, were significantly increased in R6/2 striatum vs. control ($p<0.0001$, $p<0.0001$) and this was significantly prevented with PLX3397 ($p<0.001$, $p<0.0001$) (two-way ANOVAs with Tukey's post-hoc test; n=4-6/group). **I-N.** Analysis of striatal glia revealed a significant R6/2 genotype effect ($p<0.01$) on $Olig2^+$ number (20X **I**, **J**) coincident with a significant increase in R6/2 myelinated (MBP^+, 20X **K**, **L**) white matter area coverage ($p<0.01$) that is normalized with PLX3397 ($p<0.05$) (two-way ANOVAs with Tukey's post-hoc test; n=4-6/group). Quantification of integrated $S100\beta^+$ signal density (20X **M, N**) revealed extensive astrogliosis in the R6/2 striatum ($p<0.0001$) that was prevented with PLX3397 ($p<0.0001$) (two-way ANOVA with Tukey's post-hoc test; n=5-6/group). Significance is denoted by * $p<0.05$, ** $p<0.01$, *** $p<0.001$, **** $p<0.0001$. Errors bars indicate SEM.

Staining for MBP revealed increased striatal white matter density with disease ($p<0.01$), concordant with a significant effect of the HD genotype on $Olig2^+$ oligodendrocyte lineage cell number ($p<0.01$; Fig. 1.8I-L) which are reported to be uniquely proliferative in the R6/2 striatum (McCollum et al., 2013). While oligodendrocyte lineage numbers were not attenuated, CSF1Ri returned white matter densities to control levels in R6/2 mice. Furthermore, analysis of striatal astrocytes revealed marked disease-related astrogliosis as measured by integrated S100β signal density ($p<0.0001$; Fig. 1.8M-N). This was prevented with CSF1Ri and microglial depletion, in line with the increasingly reported role of microglia in directing astrocyte reactivity (Gibson et al., 2019; Liddelow et al., 2017; Rothhammer et al., 2018; Yun et al., 2018). Although seemingly in juxtaposition to one another, the enhanced white matter and neuropil density coincident with striatal volume loss in R6/2 mice may stem from impaired neurite outgrowth (Mehta et al., 2018) or disrupted synaptic connections (2017; Ferrante et al., 1991) in HD, consistent with the downregulated neuronal and synaptic development pathways seen in this study.

However, ECM degradation could also contribute to volume loss, and so we aimed next to extend our structural findings beyond neuronal cell bodies and processes to the extracellular milieu.

CSF1Ri reduces global ECM proteoglycan deposition in the R6/2 brain

Cell-matrix adhesion is in the brain is mediated largely by the transmembrane receptor CD44, which binds the primary component of parenchymal ECM, the glycosaminoglycan (GAG; polysaccharides consisting of a repeating disaccharide unit) hyaluronan, as well as other matrix constituents such as glycoproteins and proteoglycans (Dzwonek and Wilczynski, 2015). CD44 immunoreactivity was robustly enhanced in the R6/2 striatum ($p<0.01$) and this was prevented with treatment (Fig. 1.9A, B). CD44 expression in the adult brain is primarily confined to astrocytes and activated microglia (Matsumoto et al., 2012), and while we did not observe colocalization of CD44 with the latter, microglia have been shown to regulate astrocytic expression of the receptor (Liddelow et al., 2017).

CD44 is a one of a family of mostly secreted molecules termed chondroitin sulfate proteoglycans (CSPGs) that are involved in neural development and glial scar formation, due largely in part to their role as negative guidance cues in axon growth (Ohtake et al., 2016) as well as their ability to form specialized ECM structures critical to plasticity (Tewari et al., 2018; Yutsudo and Kitagawa, 2015). CSPGs consist of a core protein covalently bound to one or more sulfated GAG sidechains, structurally related to the unsulfated GAG hyaluronan coexisting in the ECM, and are primarily produced by reactive astrocytes (Silver and Miller, 2004; Yu et al., 2012).

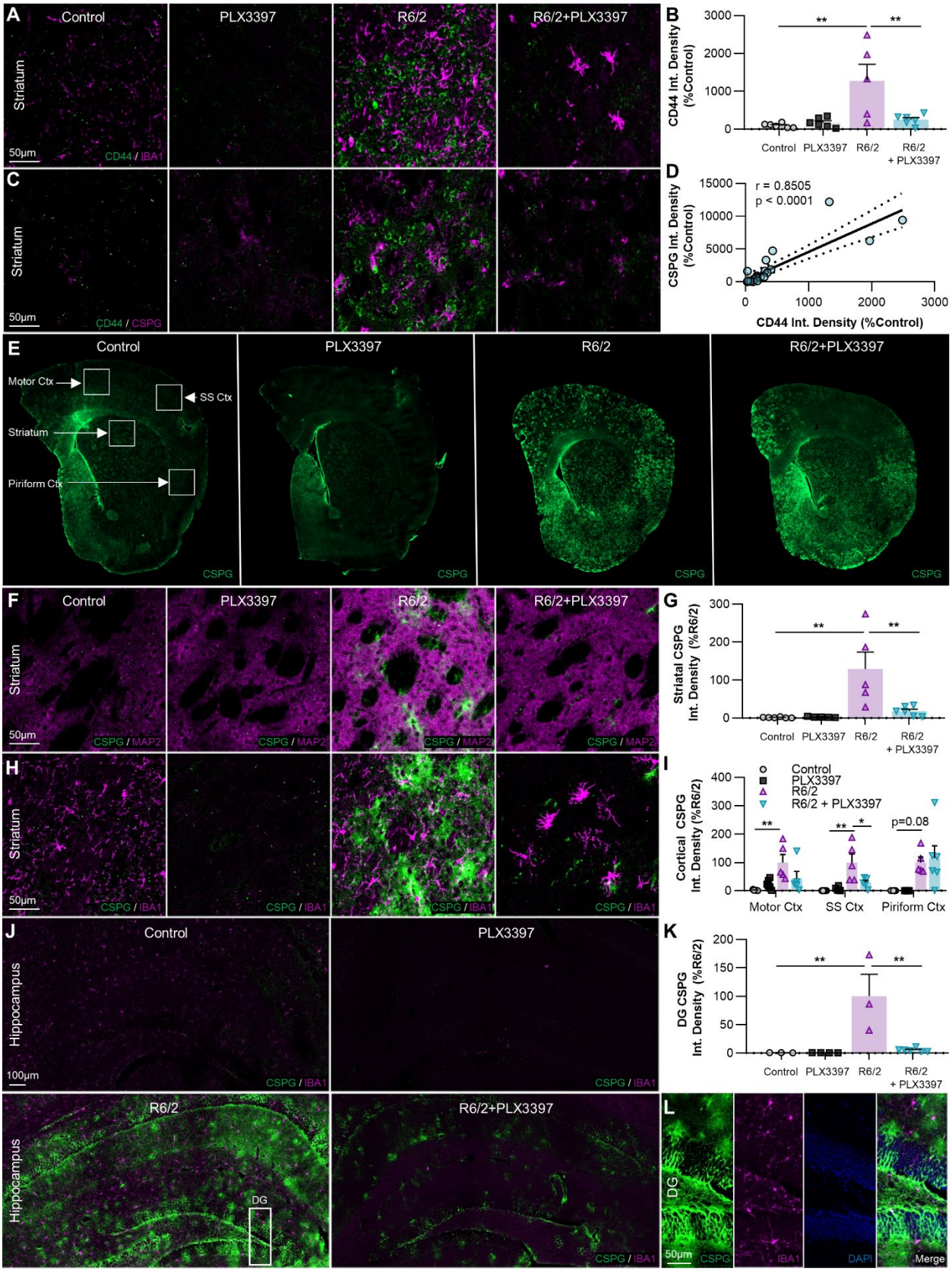

Figure 1.9. Extracellular chondroitin sulfate proteoglycans (CSPGs) accumulate in the R6/2 striatum, cortex, and

hippocampus, but are reduced with PLX3397. A-D. Non-microglial expression of the cell-ECM receptor CSPG8/CD44 (20X with IBA1$^+$ **A**, same images with pan-CSPG$^+$ **C**) is significantly increased in R6/2 striatum (**B**) compared to control and R6/2+PLX3397 ($p<0.01$, $p<0.01$) (two-way ANOVA with Tukey's post-hoc test; n=5-6/group), and correlated with CSPG accumulation (**D**) across all samples ($p<0.0001$, $r=0.8505$) (Pearson correlation test; n=23). **E-K.** Representative whole-brain (**E**), 20X striatal (with MAP2$^+$ **F,** same images with IBA1$^+$ **H**), and 20X hippocampal stitched (**J**) images of CSPG$^+$ accumulation, quantified in the striatum (**G**), cortex (**I**) and dentate gyrus (DG) of the hippocampus (**K**) as integrated signal density (n=5-6/group, except DG where n=3-6/group). Significant increases compared to control were found in R6/2 striatum ($p<0.01$), motor cortex ($p<0.01$), SS cortex ($p<0.01$), and DG ($p<0.01$), along with a trending increase in the piriform cortex ($p=0.08$) (two-way ANOVAs with Tukey's post-hoc test). Interestingly, disease-related accumulation was significantly reduced with PLX3397 in the striatum ($p<0.01$), SS cortex ($p<0.05$), and DG ($p<0.01$) (two-way ANOVAs with Tukey's post-hoc test; n=5-6/group, except DG where n=3-6/group). **L.** Inlet of DG from R6/2 hippocampus (**J**) showing CSPG+ staining in all layers. Statistical significance is denoted by * $p<0.05$, ** $p<0.01$. Error bars indicate SEM.

We therefore wondered whether other members of the CSPG family followed a similar expression pattern. Using the CS-56 antibody targeting CSPG-GAG sidechains, we performed a pan-CSPG stain and found that global CSPG signal varied directly with CD44 expression, regardless of experimental group (Pearson correlation coefficient $r = 0.8505$, $p<0.0001$; Fig. 1.9C, D). Furthermore, we observed a striking and ubiquitous accumulation of extracellular CSPG throughout the R6/2 brain, which we quantified in the striatum, cortex, and dentate gyrus (DG) of the hippocampus (Fig. 1.9E-K). There was a significant ($p<0.01$; striatum, motor cortex, SS cortex, DG) or trending increase ($p=0.08$; piriform cortex) in CSPG signal in every region examined. In appearance, the diffuse patches of elevated CS-56 staining often resembled "DAndelion Clock-like Structure" (DACS), extracellular CSPG lattices reported to form around neurons at the end of the developmental critical period (Hayashi et al., 2007) as well as following kainic acid (KA)-induced seizure (Yutsudo and Kitagawa, 2015), and sometimes localized to MAP2-negative striatal fiber tracts (Fig. 1.9F, R6/2). The depletion of microglia with CSF1Ri significantly reduced CSPG accumulation to control levels in the striatum ($p<0.01$), somatosensory cortex ($p<0.05$), and DG ($p<0.01$), supporting the idea that microglia can

directly or indirectly (i.e. through regulation of astrocyte reactivity) mediate the aberrant deposition of CSPG proteoglycans into the extracellular space.

CSF1Ri-driven microglial elimination ubiquitously increases the density of ECM perineuronal nets, which are degraded in the R6/2 brain

Depending on side chain sulfation pattern, CSPGs can also be preferentially incorporated into conventional perineuronal nets (PNNs) (Fawcett et al., 2019) where they form a reticular dendrosomatic structure around largely parvalbumin (PV)-expressing interneurons (Miyata et al., 2012; Yutsudo and Kitagawa, 2015) thought to “lock” synapses in place during development. PV interneurons are reduced in number by ~75% in the anterior caudate of HD patients (Reiner et al., 2013). Furthermore, it is now known that PNN degradation impairs the inhibitory firing of GABAergic interneurons, thus contributing to tumor-associated seizures (Tewari et al., 2018) akin to those observed in R6/2 mice. Therefore, to investigate disease-associated changes in another relevant CSPG-based ECM structure, PNNs, we used the canonical lectin marker *Wisteria floribunda agglutinin* (WFA) to examine the same striatal and cortical regions where we observed increased CS-56 immunolabeling in the R6/2 brain (Fig. 1.10A). Of the regions examined, PNNs were always most abundant in the somatosensory cortex, where, along with the motor cortex, they were significantly decreased in R6/2 mice ($p<0.01$ and 0.001, respectively; Fig. 1.10D, E), with trends to reduction seen in regions of lower PNN density and intensity (striatum, piriform cortex; Fig. 1.10B, C, E). Importantly, PV-expressing interneurons in the HD striatum displayed a significant reduction ($p<0.01$) in mean WFA^+ co-staining intensity (Fig. 1.10F, G) suggesting degradation of encapsulating PNNs.

IBA1$^+$ microglial processes were frequently observed proximal to and in contact with the surface of PNNs in both control and R6/2 brains (Fig. 1.10F). Indeed, it has been postulated that microglia mediate the degradation of PNNs in certain disease states, likely through enhanced production of extracellular proteases (Franklin et al., 2008; Sandvig et al., 2018). Microglial elimination with CSF1Ri prevented the disease-associated PNN loss observed in the somatosensory and motor cortices ($p<0.001$ and 0.05, respectively), regions where microglia had adopted a more activated phenotype in R6/2 mice as measured by cell size and IBA1$^+$ intensity. Remarkably, the depletion of microglia from naïve nontransgenic mice significantly and dramatically elevated PNN densities in every brain region examined.

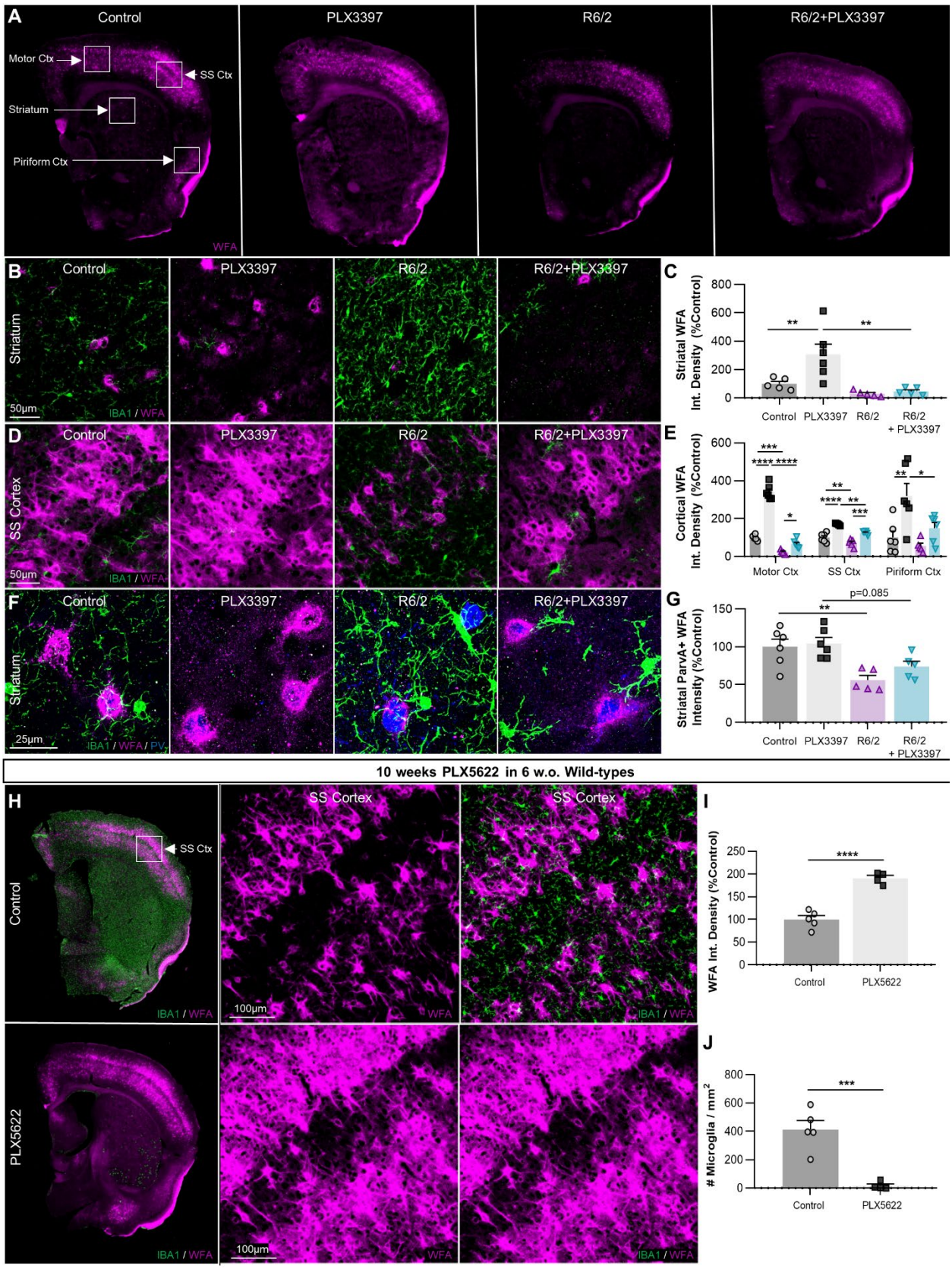

Figure 1.10 The density of CSPG-containing perineuronal nets (PNNs) is reduced in R6/2 mice and this is prevented with

microglial depletion, which also ubiquitously enhances PNN formation in healthy controls. A. Representative whole-brain images of *Wisteria floribunda agglutinin* (WFA) lectin staining of PNNs (n=5-6/group). **B-E.** 20X striatal and cortical images of WFA^+ PNN staining (with IBA1+ **B** and **D**) quantified as integrated density (**C**, **E)** revealed significant reductions in the motor ($p<0.001$) and SS ($p<0.01$) cortices, which were restored by microglial depletion with PLX3397 ($p<0.05$, $p<0.001$) (two-way ANOVAs with Tukey's post-hoc test; n=5-6/group). Surprisingly, PLX3397 in healthy nontransgenic controls significantly increased WFA^+ PNN density in every region examined: striatum ($p<0.01$), motor cortex ($p<0.0001$), SS cortex ($p<0.0001$), and piriform cortex ($p<0.01$) (two-way ANOVAs with Tukey's post-hoc test; n=5-6/group). Quantification of mean WFA^+ intensity colocalizing with striatal parvalbumin-expressing GABAergic interneurons (63X **F**, **G**) revealed significant ($p<0.01$) and trending ($p=0.085$) reductions in R6/2 and R6/2+PLX3397 mice respectively, indicating loss of interneuron-associated PNN integrity (two-way ANOVA with Tukey's post-hoc test; n=5-6/group). **H.** Representative whole-brain and 20X cortical images of WFA^+ PNN staining in wild-type mice treated for 10 weeks (from 6 weeks) with 1200mg/kg PLX5622 (n=4-5/group). Analysis of PNN density as integrated WFA^+ signal in the SS cortex (**I**) revealed a significant elevation with PLX5622 ($p<0.0001$) that occurred alongside the CSF1Ri-induced loss of microglia (**J**) ($p<0.001$) (two-tailed unpaired t-tests; n=4-5/group). Statistical significance is denoted by * $p<0.05$, ** $p<0.01$, *** $p<0.001$, **** $p<0.0001$. Error bars indicate SEM.

Finally, to confirm that the robust enhancement of PNNs in wild-type mice are due solely to the loss of microglia, we performed IHC on previously generated brain tissue from 6 week-old congenic C57BL/6J mixed-sex mice treated for 10 weeks with the highly selective CSF1R inhibitor PLX5622 (Spangenberg et al., 2019) at 1200mg/kg (Fig. 1.10H). WFA^+ PNNs in the somatosensory cortex were significantly enhanced with PLX5622 treatment compared to vehicle ($p<0.0001$; Fig. 1.10I) and this was accompanied by the depletion of $IBA1^+$ microglia ($p<0.001$; Fig. 1.10J). Unlike CSPGs secreted by glia, PNNs and their proteoglycan constituents are synthesized by neurons (Miyata et al., 2005). Taken together, this indicates that microglia tightly regulate basal PNN formation through sustained levels of homeostatic degradation, a function that can be pathologically altered in the context of brain injury or disease.

Discussion

The contribution of microglia to Huntington's disease pathogenesis has been a topic of recent investigation. Although neuroinflammation is characteristic of HD (Crotti and Glass,

2015), treatment of R6/2 mice with the tetracycline derivative minocycline, an inhibitor of inflammatory microglial activation (Kobayashi et al., 2013), has produced mixed results (Chen et al., 2000; Smith et al., 2003). Furthermore, mHTT-expressing microglia generate exacerbated responses to inflammatory stimuli and consequently greater neuronal damage *in vivo (Crotti et al., 2014)*, but depletion of mHTT from myeloid cells does not significantly rescue disease phenotype in the BACHD mouse model (Petkau et al., 2019). To further clarify microglial function in disease, we used the targeted and sustained inhibition of CSF1R to pharmacologically deplete microglia from the R6/2 brain and assessed the behavioral, transcriptional, and pathological consequences.

Microgliosis is a hallmark of the HD brain, both in patients (Sapp et al., 2001; Tai et al., 2007) and in cell (Kraft et al., 2012) and mouse models (Siew et al., 2019; Simmons et al., 2007). Further, inflammatory cytokines have been detected in plasma, myeloid cells and CSF from HD subjects (Chang et al., 2015; Miller et al., 2016; Rodrigues et al., 2016). Accordingly, we observed elevated densities of cortical and striatal microglia, which displayed several morphological features of immune reactivity (larger soma, higher IBA1 intensity) in the motor and somatosensory cortices specifically. Beyond this, however, R6/2 microglia did not appear overtly activated *in vivo*, at least to the extent seen in other neurodegenerative disease models (Liberatore et al., 1999; Spangenberg et al., 2016): their processes remained ramified and thin, they did not adopt an amoeboid morphology, and the striatal transcriptome did not reflect broad pro-inflammatory polarization. However, microglia exist within a spectrum of functional states, and their dynamic developmental (Lehrman et al., 2018) and homeostatic (Bennett et al., 2018) roles could also be affected by proteinopathy.

In this study, we began CSF1R-mediated microglial depletion at week 6, after microglial development but before overt R6/2 symptomology, attaining successful microglial elimination in all brain regions examined. We reported beneficial effects of treatment on both grip strength and novel object recognition deficits in R6/2 mice. Of clinical relevance, it is possible that peripheral actions of PLX3397 may contribute to delayed grip strength deficits, e.g. by altering CSF1R signaling in skeletal muscle macrophages. Polyglutamine inclusions accumulate in skeletal muscle from HD models (R6/2, HdhQ150) and patients, which display myopathic structural abnormalities (Ciammola et al., 2006; Moffitt et al., 2009; Zielonka et al., 2014). Furthermore, similar downregulations of macrophage-related transcripts we observed in the striatum here have also been reported in R6/2 skeletal muscle (*Igf1*, *Ccl25*, *H2-DMa*) (Strand et al., 2005) and peripheral HD monocyte/macrophages show dysregulated transcriptional polarization as well as impaired migration to stimuli (Crotti and Glass, 2015). Although PLX3397 has modest to no effects on homeostatic peripheral tissue macrophage numbers (Mok et al., 2014) including at doses virtually equivalent to that used in this study (Szalay et al., 2016), disruption of CSF1R signaling may alter the functional phenotype of skeletal muscle macrophages in a manner that slows disease-related muscle weakness. Future studies should investigate the effects of more translationally amenable doses of PLX3397 that do not cross the BBB on R6/2 grip strength and muscle tissue changes. Additionally, the effects seen here should be validated in longer-lived models of HD (e.g. BACHD (Gray et al., 2008b) or zQ175 mice (Menalled et al., 2012)), where greater behavioral readout and postsymptomatic treatment opportunities are feasible than with the more aggressive R6/2 model.

Transcript analysis of the R6/2 striatum revealed a robust upregulation of IFN pathway signaling that closely resembled the affected human caudate. This is suggestive of the existence of an “interferon signature” in HD, increasingly reported in other diseases (Mathys et al., 2017; Mostafavi et al., 2016), aspects of which were partially resolved upon microglial elimination here. Of note, microglia were recently reported to accelerate neurodegeneration in a model of prion disease via reactive upregulation of type I interferon (Nazmi et al., 2019). Consistent with a secondary rather than initiating role in HD, microglial depletion with CSF1Ri reduced the striatal accumulation of several pathologic mHTT species in R6/2 mice, even though microglia rarely contain nuclear mHTT inclusions themselves (Jansen et al., 2017).

While investigating the cellular integrity of the HD striatum, we found markedly increased expression of the cell-matrix adhesion receptor CD44, the expression of which by microglia and astrocytes is associated with ALS progression (Matsumoto et al., 2012). While we did not observe microglial colocalization, its upregulation in astrocytes is microglia-dependent (Liddelow et al., 2017), consistent with the observed astrogliosis that is abrogated alongside striatal CD44 expression with microglial elimination. CD44 (CSPG8) belongs to a family of mostly secreted proteoglycans that are fundamental components of glial scars (Anderson et al., 2016) and the brain ECM (Tewari et al., 2018; Yutsudo and Kitagawa, 2015), and staining for CSPG with CS-56 revealed a strong correlation with CD44. Indeed, HD mice displayed a remarkable accumulation of CSPG in the cerebral cortex, striatum, and hippocampus, consistent with reports of astrocytic CSPG expression in human HD striatum (DeWitt et al., 1994). Interestingly, kainic acid-

induced seizures (Yutsudo and Kitagawa, 2015) which directly enhance glutamate signaling (Iadarola et al., 2015), are followed by similar CS-56^{+} deposition.

CSPGs generally exert inhibitory effects on axon growth (Fidler et al., 1999; Fisher et al., 2011; Ohtake et al., 2016; Pearson et al., 2018; Properzi et al., 2005). Consistent with this, transcriptomic pathway analysis confirmed impairments in striatal neuritogenesis and neuronal development, which were restored alongside CSPG levels following microglial depletion. Importantly, the same human striatal samples displayed elevated astrocyte and CSPG mRNA with disease (Hodges et al., 2006). It is possible that the loss of microglia represses astrocyte activation and CSPG secretion (Liddelow et al., 2017; Silver and Miller, 2004; Yu et al., 2012), thereby permitting neuropil and axonal outgrowth in the striatum and restored striatal volume. Consistent with this, astrocyte reactivity and CSPG production is stimulated by TGFβ (Ohtake et al., 2016; Yu et al., 2012), which is primarily produced by microglia (Zhang et al., 2014) and disease astrocytes (Endo et al., 2015), and was significantly reduced in R6/2 striatum following CSF1Ri (*Tgfb1*, LogFC = -2.0535, FDR<0.01) alongside astrogliosis. Additionally, the depletion of mHTT from astrocytes alone (Wood et al., 2018), but not microglia (Petkau et al., 2019), reduces mHTT accumulation and striatal volume loss in the BACHD mouse model. Furthermore, bilateral intra-striatal AAV-RNAi delivery of HTT-suppressing miRNA targeted to neurons and astrocytes (AAV1), but not neurons alone (AAV2-HBKO), rescued motor deficits in the YAC128 mouse model of HD, suggesting that astrocyte mHTT directly alters reactivity in a manner detrimental to disease (Stanek et al., 2019). In light of the current study, these reports suggest that astrocytes directly contribute to neurodegeneration, while microglia promote secondary damage through modulation of astrocyte reactivity and/or

other pathways, thereby accelerating pathogenesis. The loss of the homeostatic microglial gene *P2ry12* (Bennett et al., 2018) from the R6/2 striatum in our dataset (FDR<0.1, LogFC = -0.7083 vs. control) further suggests microglial dysfunction in the context of HD.

CSPGs are also core structural elements of conventional perineuronal nets, reticular structures that form along the soma and proximal dendrites of primarily GABAergic PV interneurons soon after synaptic pruning is completed by microglia (Paolicelli et al., 2011), stabilizing the neuronal circuitry and inhibiting plasticity (Fawcett et al., 2019; Wang and Fawcett, 2012). CSPGs contained in PNNs are labeled by the plant lectin WFA in a manner distinct from CS-56 (Hayashi et al., 2007; Pantazopoulos et al., 2015; Yutsudo and Kitagawa, 2015), potentially due to differences in CSPG sidechain sulfation status (Sorg et al., 2016) or epitope availability. PNNs are autonomously constructed by neurons (Fowke et al., 2017; Geissler et al., 2013; Miyata et al., 2005), and in stark contrast to CS-56 staining, we found a loss of WFA^+ PNN density with disease in motor and somatosensory cortices. R6/2 PV striatal interneurons also displayed a reduction in WFA^+ intensity and an apparent loss of PNN structural integrity, which has before been shown to contribute to tumor-associated seizures (Tewari et al., 2018) due to impaired GABAergic inhibitory firing as PNNs are thought to enhance GABAergic electrical transmission akin to a myelin sheath. As such, their loss may further contribute to the excitatory/inhibitory imbalance observed in the R6/2 brain. Surprisingly, the depletion of microglia from healthy, nontransgenic mice produced a dramatic and ubiquitous accumulation of PNNs, which we verified in brain tissue from adult wild-type mice treated

with the selective CSF1R inhibitor PLX5622, underscoring a yet unstudied role of microglia as homeostatic regulators of perineuronal net formation in the healthy brain.

In conclusion, we show that sustained CSF1R inhibition in the R6/2 mouse model of HD, which exhibited elevated microglial numbers but not broad inflammation at the transcriptional or morphological level, mitigated grip strength and object memory deficits. Microglial depletion was accompanied by a reduction in striatal mHTT accumulation and partial or full reversals of dysregulated interferon signaling, neuritogenesis, and neuronal development pathways. Furthermore, we report a massive accumulation of extracellular CSPG with disease, which is associated with striatal volume loss, astrogliosis, and neuropil alterations in the R6/2 brain, and microglial depletion with CSF1Ri partially or completely prevented each of these phenotypes. Finally, we show that a related but distinct CSPG-containing structure, the perineuronal net, is disrupted in a region-specific manner with disease, and that the elimination of microglial not only ameliorates this, but greatly enhances PNN density in the naïve adult brain.

CHAPTER TWO

Dyshomeostatic microglia and the ECM in Alzheimer's disease

Introduction

Alzheimer's disease (AD) is a progressive neurodegenerative disorder characterized pathologically by the accumulation of extracellular amyloid-β (Aβ) plaques and intraneuronal neurofibrillary tangles (NFTs) composed of hyperphosphorylated tau. The appearance and spread of these pathological substrates is fundamentally linked to a cascade of events that results in the synaptic dysfunction and neuronal loss characteristic of the disease, manifesting behaviorally as progressive impairments in memory and cognition (Selkoe and Hardy, 2016). Research spanning the past decade has identified numerous genes that confer increased risk of disease development (Karch et al., 2012; Van Cauwenberghe et al., 2016), and the majority of these risk genes are highly or solely expressed in myeloid cells (e.g. *Trem2*, *Cd33*, *Spi1*, *Abi3*, *Plcg2*, *Apoe*) thereby implicating microglia in AD etiology (Sierksma et al.; Sims et al., 2017). In addition, genes expressed in other CNS cell types (e.g. neurons and astrocytes) have microglia-specific enhancers with risk polymorphisms that selectively affect myeloid expression (i.e. *Bin1*) (Nott et al., 2019).

Brain myeloid cells consist primarily of microglia, the resident parenchymal macrophages, and border macrophages along CNS interfaces (e.g. meningeal, perivascular, and choroid plexus macrophages) (Kierdorf and Prinz, 2017; Li and Barres, 2018). As part of the glial activation characterized by Alois Alzheimer in his initial report (Stelzmann et al., 1995), the microglial response to amyloid plaques and/or tau pathology is increasingly thought to cause or contribute heavily to disease-related neurodegeneration (Krasemann

et al., 2017; Shi et al., 2019b; Spangenberg et al., 2019; Spangenberg et al., 2016). Thus, elucidating the cellular mechanisms by which microglia drive disease progression in the AD brain – and how this may be linked to downstream cognitive and behavioral phenotypes – is critical to understanding the disease, and in a similar vein, to the development of therapeutics that counteract these effects.

Microglia adopt a multitude of functions in the healthy and diseased CNS, and aside from immunological roles, evidence indicates that these cells interact with and modulate neuronal and synaptic elements, with direct effects on learning and memory (Elmore et al., 2014; Elmore et al., 2018; Rice et al., 2015; Tremblay et al., 2011; Wang et al., 2020; Werneburg et al., 2020). The extracellular matrix (ECM), specifically the condensed ECM structure known as the perineuronal net (PNN), is an essential component of the synapse involved in the regulation of plasticity that, along with astrocytes and synaptic terminals, comprise the contemporary “tetrapartite synapse” (Reichelt et al., 2019). PNNs form preferentially around fast-spiking parvalbumin (PV)+ GABAergic interneurons throughout the brain during the closure of the critical period of plasticity, effectively “locking” proximal synapses in place and providing synaptic stability (Fawcett et al., 2019) soon after synaptic pruning is completed by developmental microglia (Paolicelli et al., 2011). Although enhanced plasticity and learning is observed following experimental PNN ablation (Pizzorusso et al., 2002; Rowlands et al., 2018), newly formed memory traces can interfere with the fidelity and recall of previously learned information (Reichelt et al., 2019), as evident by impaired reconsolidation and recall of remote memories following PNN ablation (Shi et al., 2019a; Thompson et al., 2018). Furthermore, the structural modification of PNNs alters synaptic transmission (Blosa et al., 2015), synapse number

(Gottschling et al., 2019), and the ion channel/neurotransmitter receptor composition of synapses (Favuzzi et al., 2017)), and thus may be related to the dysfunctional interneuron activity mediating cognitive impairments in AD (Hijazi et al., 2019; Verret et al., 2012).

The functional capacity of microglia to remodel the ECM is classically demonstrated in acute injuries such as stroke (Patel et al., 2013), in which microglia undergo activation and subsequently release matrix metalloproteinases (e.g. MMP9) or other ECM-degrading proteases that act on PNN components (Wen et al., 2018b), and PNN loss is reported in neurological disorders such as seizure (Rankin-Gee et al., 2015) and prion disease (Franklin et al., 2008). Recent work from our lab identified a role for microglia-mediated PNN loss in Huntington's disease (Crapser et al., 2019). Although PNNs are reported to protect neurons against tau (Brückner et al., 1999; Morawski et al., 2010a) and Aβ pathology (Miyata et al., 2007), the extent to which PNN loss occurs in human and animal models of AD – where microglia are inextricably linked to disease pathogenesis – remains controversial (Baig et al., 2005; Cattaud et al., 2018; Morawski et al., 2012; Morawski et al., 2010b).

Utilizing the aggressive 5xFAD mouse model of disease (Oakley et al., 2006) and corroborated by extensive immunohistochemical (IHC) analysis of human cortical tissue, we report that PNNs are extensively lost in the mouse and human AD brain. We find that PNN deficits occur earlier in 5xFAD brain regions with high pathology, as in the subiculum, where reductions in PV+ interneuron density are observed only after impairments in regional PNN coverage and structural integrity. Activated microglia closely associate with morphologically abnormal nets in the AD brain and staining for PNN components reveals colocalization in both mouse and human microglia. Interestingly, we also find consistent

colocalization of the CSPG aggrecan (ACAN) – critical to PNN structure and function (Rowlands et al., 2018) – with human dense-core plaques, which in turn inversely correlate with total ACAN+ PNNs across unaffected and AD brain samples. Inducing microglial activation via lipopolysaccharide (LPS) injection in wild-type (WT) mice is sufficient to cause overall PNN loss and impairments in the structural integrity of PV+ interneuron-associated PNNs, in addition to reduced PV+ cell densities. We show that chronic depletion of microglia prior to and during plaque development in 5xFAD mice with the selective colony-stimulating factor 1 receptor (CSF1R) inhibitor PLX5622 effectively prevents PNN loss, data substantiated by the similar beneficial effects on PNNs we observe with microglial depletion in aged 3xTg-AD mice. Importantly, this occurs despite the persistence of plaques. Thus, we conclude that disease-altered microglia facilitate plaque-dependent loss of PNNs in the AD mouse model and human brain.

Materials and Methods

Compounds: PLX5622 was provided by Plexxikon Inc. and formulated in AIN-76A standard chow by Research Diets Inc. at 1200ppm.

Mice: All animal experiments were performed according to animal protocols approved by the Institutional Animal Care and Use Committee (IACUC) at the University of California, Irvine, an American Association for Accreditation of Laboratory Animal Care (AAALAC)-accredited institution. We utilized 5xFAD mice in this study, a model of AD harboring five relevant mutations across two human transgenes, amyloid precursor protein (*APP*) and presenilin-1 (*PSEN1*), described in detail elsewhere (Jawhar et al., 2012) and obtained from the Mutant Mouse Resource and Research Centers (MMRRC; 034848-JAX), or 3xTg-AD mice, with three familial AD mutations (in *APP*, *MAPT, PSEN1*) (Oddo et al.,

2003). WT mice (00664) were obtained from the Jackson Laboratory to maintain both lines on a C57BL/6J background. Mice were housed in groups of up to five animals/cage under 12-hr light/dark cycles, with *ad libitum* access to vivarium chow and water. For timecourse experiments, naïve male and female 5xFAD and WT mice were euthanized for investigation at 4, 8, 12, and 18 months (mo). For LPS experiments, 9-month-old male and female WT mice were intraperitoneally (IP) injected with 0.5mg/kg LPS (L4130, Sigma) or saline every other day for a week, followed by euthanasia 24hr after the last dose. To determine the role of microglia in plaque-related PNN disturbances, male and female 5xFAD and WT mice were given AIN-76A chow containing vehicle or 1200ppm PLX5622 from 1.5 months (prior to plaque pathology) to 4 months of age. For post-pathological experiments, male and female 3xTg-AD mice were given vehicle or 1200ppm PLX5622 orally for 1mo starting at 17mo. Assignment of animals to treatment groups was conducted in a random manner and was balanced for sex, and researchers were blinded to genotype and treatment groups during analysis of histological data.

Tissue Collection:

Mouse tissue: At the end of treatment, mice were euthanized via CO2 inhalation and transcardially perfused with ice-cold 1X phosphate buffered saline. For all studies, brains were removed, and hemispheres separated along the midline. Each hemisphere was then either flash frozen and stored at -80°C for subsequent biochemical analysis, or drop-fixed in 4% paraformaldehyde (Thermo Fisher Scientific, Waltham, MA) for 48hrs, cryoprotected in 30% sucrose, and sectioned at 40µm on a Leica SM2000R freezing microtome for immunohistochemical analysis.

Human tissue: For analysis of human brains, postmortem cortical tissue from the middle frontal gyrus (BA9 and 46) of non-demented and AD subjects was obtained from the Alzheimer's Disease Research Center (ADRC), UC Irvine. The protocols for obtaining postmortem brain tissue compiled with all federal and institutional guidelines with special respect for donor identity confidentiality and informed consent. Dementia and AD diagnosis were made by a consensus conference using neuropsychological assessment, neurological examination, and medical records following DSM-IV and National Institute of Neurological and Communicative and Stroke-Alzheimer's Disease and Related Disorders Association criteria, respectively. Neuropathological examination included Braak and Braak staging for plaques and tangles and diagnosis of neuropathological AD using National Institute on Aging-Reagan criteria (Hyman et al., 2012). Neuropathological differences in non-demented (ND) control (cognitive diagnosis: ND; plaque stage: 1.67 +/- 0.24; age: 91 +/- 0.25; MMSE: 27.11 +/- 1.42) and Alzheimer's disease (AD) (cognitive diagnosis: AD; plaque stage: 3.93 +/- 0.07; age: 89.57 +/- 0.88; MMSE: 13.77 +/- 2.13) cases are listed in Table 2.1. Paraformaldehyde-fixed human samples were cryoprotected via 48hr incubation in 30% sucrose + 0.05% sodium azide and samples were cut into serial sections (30µm) using a Leica SM2000R freezing microtome.

Group	PMI (h)	Age (y)	Gender	MMSE	Plaque Stage	Plaque Stage (Frontal)	Tangle Stage
ND- CON	3.61 ± 0.28	91 ± 0.25	6F, 3M	27.11 ± 1.42	1.67 ± 0.24	0.33 ± 0.17	2.78 ± 0.40
AD	4.51 ± 0.39	89.57 ± 0.88	10F, 4M	13.77 ± 2.13	3.93 ± 0.07	3.00 ± 0.00	5.36 ± 0.13

Table 2.1. Neuropathological differences in non-demented control (ND CON) and Alzheimer's disease (AD) cases. Values represent mean ± SEM.

Histology and Confocal Microscopy: Fluorescent immunolabeling followed a standard indirect technique as described previously (Spangenberg et al., 2016). Brain sections were stained with antibodies against IBA1 (1:1000; 019-19741, Wako and ab5076, Abcam), *Wisteria floribunda agglutinin* (WFA) lectin (1:1000, B-1355, Vector Labs), aggrecan 7D4 (1:15, MCA1454G, Bio-Rad), aggrecan (1:200, AB1031, Millipore), CSPG CS-56 (1:200, ab11570, Abcam), and parvalbumin (1:500, MAB1572, Millipore). Thioflavin-S (Thio-S; T1892, Sigma-Aldrich) staining was performed as described before (Spangenberg et al., 2019). Amylo-Glo (TR-300-AG; Biosensis) staining was performed according to the manufacturer's instructions for confirmation of plaques with an additional marker where indicated. IHC was performed the same on human post-mortem cortical tissue, including Tho-S pretreatment, with an additional incubation in Sudan Black B (206470; MP Biomedicals) as a final step to reduce autofluorescence. Antigen retrieval was performed prior to staining 5xFAD tissue with aggrecan (AB1031) and CSPG via 30min incubation in pH 6.0 citric acid buffer at 80°C, after which all IHC steps were performed normally. Immunostained sections were mounted and coverslipped with Fluoromount-G with or without DAPI (0100-20 and 0100-01; SouthernBiotech). High resolution fluorescent images were obtained using a Leica TCS SPE-II confocal microscope and LAS-X software. One 20X field-of-view (FOV) per brain region was captured per mouse, and max projections of 63X Z-stacks were used for representative images when indicated. For whole-brain stitches, automated slide scanning was performed using a ZEISS Axio Scan.Z1 equipped with a Colibri camera and ZEN Axio Scan 2.3 software.

Cell quantities were determined using the spots module in Imaris v9.2, while plaque number and PNN coverage area were determined using the surfaces module. To measure PNN structural integrity, the average value of the mean WFA fluorescence intensity within each PV+ spot (e.g. WFA+ signal colocalizing with PV+ cell body) of a particular sample was compared, adapted and modified from (Tewari and Sontheimer, 2019). To measure the total WFA+ material associated with microglia, the WFA+ intensity sum of each IBA1+ spot was added together for each sample. CSPG immunoreactivity was measured as integrated signal density in ImageJ (NIH) as before (Crapser et al., 2019). For the analysis of human tissue, the number of ACAN+ (aggrecan clone 7D4) PNNs and Thio-S+ dense core plaques were manually quantified and averaged across 4 regionally distinct 20X Z-stack max projections of cortical grey matter per brain sample for n=9 non-demented control and n=12 AD brains to determine statistical differences. All 20X max projection values (rather than patient averages) were utilized for regression and correlation analysis, excluding any replicates in which technical artifacts were observed.

Data analysis and statistics: Statistical analysis was performed with Prism GraphPad (v.8.3.0). To compare two groups, the two-tailed unpaired Student's t-test was used. To compare multiple groups along one or two variables, a one-way or two-way ANOVA, respectively, was performed with Tukey's post-hoc test for multiple comparisons. All bar graphs are represented as mean ± standard error of the mean (SEM) with individual sample values overlain. Nonlinear regression with Akaike's Information Criterion (AICc) was used to determine the statistical model (linear or quadratic) that best explains the data, and Pearson's or Spearman's correlation analysis was performed depending on whether the relationship was linear or nonlinear, respectively (all correlations reported in

this study were nonetheless confirmed significant using both analyses). Statistical significance was accepted at $p \leq 0.05$ and is expressed as follows: *$p \leq 0.05$, **$p < 0.01$, ***$p < 0.001$, ****$p < 0.0001$.

Results

Age- and plaque-dependent PNN loss occurs in 5xFAD mouse brains

5xFAD mice serve as an aggressive mouse model of AD, displaying extensive Aβ plaque deposition and associated gliosis beginning at 3 months of age, particularly in the cortex and the subiculum of the hippocampus (Oakley et al., 2006), in addition to synaptic deficits and neuronal loss at later stages of the disease (Buskila et al., 2013; Jawhar et al., 2012). Microglia from these mice have been extensively characterized, revealing the canonical upregulation of disease-associated microglial markers (e.g. *Cst7, Axl, Trem2, Apoe, Ctss)* and loss of homoestatic markers (*P2ry12, Tmem119)* that reflect disease-related changes in form and function (Griciuc et al., 2019; Keren-Shaul et al., 2017; Spangenberg et al., 2019). As before, we focused our investigation on the subiculum due to its early and aggressive plaque development, which allowed us to study the consequences of high plaque pathology in parallel with analyses of cortical regions, which display relatively lower amyloid burden at the same timepoints and in the same mice. Furthermore, we have previously conducted extensive cellular and transcriptomic characterization of these regions following CSF1R inhibitor or vehicle treatment, providing a growing biological context within which to interpret the findings of the present study. (Spangenberg et al., 2019; Spangenberg et al., 2016). Therefore, to explore the effects of aging and plaque development on PNN integrity, we performed immunohistochemistry (IHC) on 5xFAD and age-matched WT control brain tissue at 4, 8, 12, and 18 months (mo) of age for dense-

core plaques (Thioflavin-S (Thio-S) or Amylo-Glo), microglia (IBA1), and PNNs (WFA; Fig. 2.1A). PNNs were visualized as generally done by immunolabeling with *Wisteria floribunda agglutinin* (WFA) lectin, which binds component chondroitin sulfate proteoglycans (CSPGs) (Wen et al., 2018b). Examination of whole brain images revealed the characteristic presence of PNNs in multiple key regions, including the subiculum (Fig. 2.1B) and visual cortex (Fig. 2.1C).

Plaques were evident in multiple brain regions by 4mo in male and female 5xFAD mice, concomitant with the stereotypical activation and gliosis of plaque- and non-plaque-associated microglia (PAM and NPAM, respectively; Fig. 2.1A-C) (Heneka et al., 2015; Reed-Geaghan et al., 2020). Indeed, 5xFAD mice had significantly higher microglial densities compared to WT at every timepoint in the subiculum, and from 8mo onward in the visual cortex ($p<0.0001$ in each case; Fig. 2.1D,E). Microglia accumulated around and near Thio-S+ plaques, which followed similar patterns of age-dependent aggregation in the two regions. Plaques were abundant in the 5xFAD subiculum at 4mo and significantly increased by 8mo ($p=0.0002$), whereas visual cortex plaques were sparse until 8mo ($p<0.01$ vs 4mo) at which point they were evident across cortical layers, with numbers in both regions remaining stable thereafter (Fig. 2.1F).

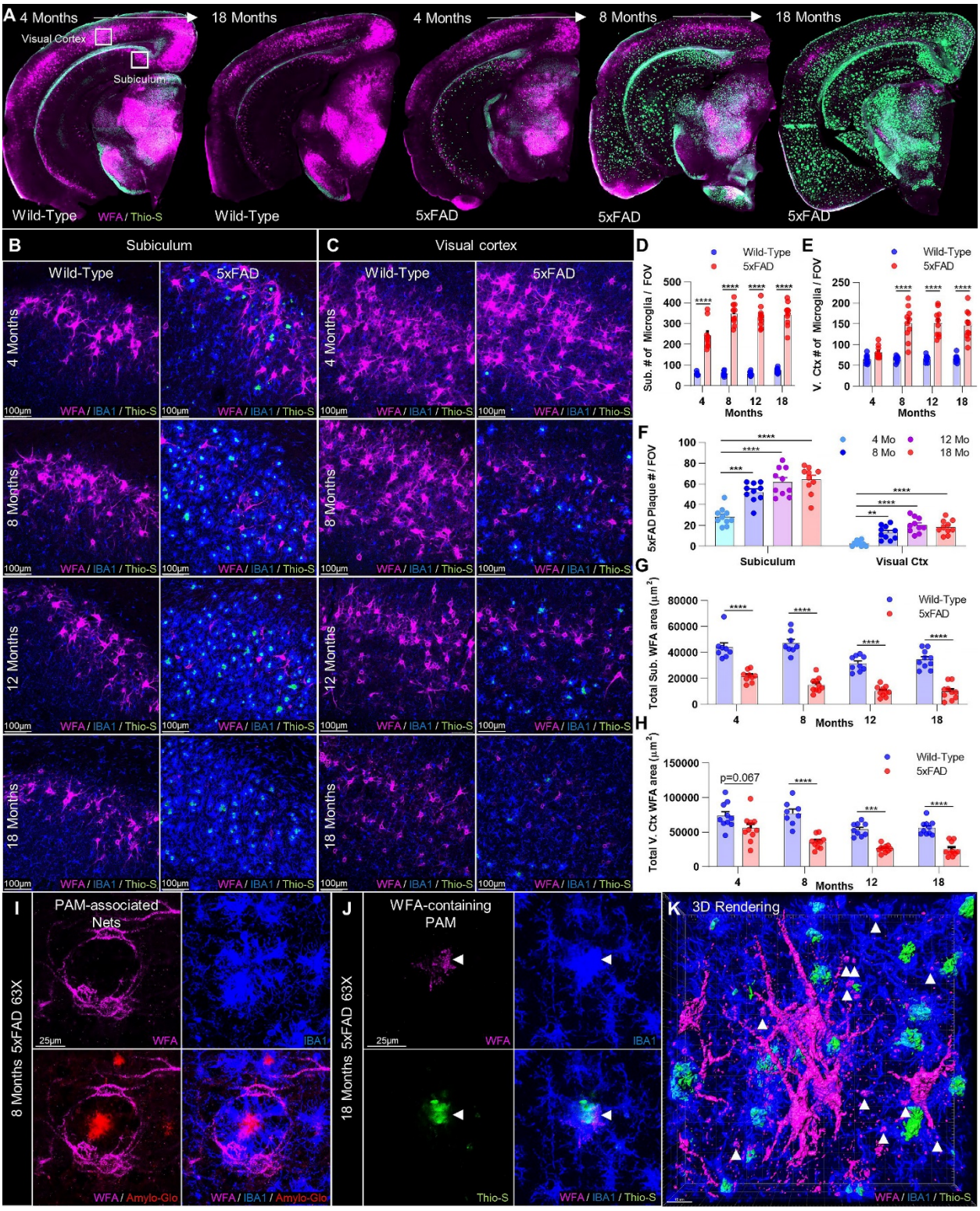

Figure 2.1. Aβ plaques induce local PNN loss that expands with pathology in 5xFAD mice. (A) Representative whole-brain images of WFA+ PNNs and Thio-S+ dense core plaques reveal extensive age- and plaque-related PNN loss in the 5xFAD brain, beginning in high pathology regions (e.g. subiculum) at 4 months (mo) and spreading globally by 18mo. **(B-C)** Representative 20X

subiculum and visual cortex images display Thio-S+ plaque accumulation and IBA1+ microgliosis in spatial association with PNN abnormalities and loss at 4, 8, 12, and 18mo. **(D-E)** Microglial numbers were significantly increased compared to WT at every age in the subiculum and from 8mo on in the visual cortex (all $p<0.0001$; 2-way ANOVAs with Tukey's post-hoc test; n=8-10/group). Age-related increases were also detected in subiculum ($p<0.0001$) and visual cortex ($p<0.0001$) between 4 and 8mo in 5xFAD mice. **(F)** Thio-S+ plaques were substantial in the subiculum but scarce in the visual cortex at 4mo, and increased between 4 and 8mo in both subiculum and cortex ($p<0.001$, $p<0.01$; 1-way ANOVAs with Tukey's post-hoc test; n=10/group), remaining at similar levels thereafter. **(G-H)** Total area coverage of WFA+ PNNs revealed significant decreases in the plaque-laden subiculum ($p<0.0001$) as early as 4mo with disease. Total WFA+ area was significantly diminished at all later timepoints compared to age-matched WT in subiculum (all $p<0.0001$) and visual cortex (8mo $p<0.0001$; 12mo $p<0.001$; 18mo $p<0.0001$). 5xFAD WFA+ area was reduced at 12 ($p<0.01$) and 18mo ($p<0.01$) in the subiculum and at 8 ($p<0.05$), 12 ($p<0.001$) and 18mo ($p<0.0001$) in the visual cortex compared to the same 5xFAD regions at 4mo. WT mice also displayed age-related decreases in WFA+ area between 8 and 12mo in both the subiculum ($p<0.001$) and the visual cortex ($p<0.05$) that did not recover by 18mo (all 2-way ANOVAs with Tukey's post-hoc test; n=8-10/group). **(I)** Representative 63X image displays WFA+ PNNs physically wrapped around an Amylo-Glo+ plaque by intermediary plaque-associated microglia (PAM) at 8mo, commonly seen in the 5xFAD brain. **(J)** Representative 63X image and **(K)** 3D rendering of WFA+ components observable within 5xFAD microglia (arrowheads; primarily in PAM) at 18 months. Statistical significance is denoted by * $p\leq0.05$, ** $p<0.01$, *** $p<0.001$, **** $p<0.0001$, ns = not significant. Error bars indicate SEM.

Notably, we found that WFA+ PNNs were robustly decreased in 5xFAD mice, with the largest effects seen in the areas with the highest plaque number (Fig. 2.1A-C). This negative correlation was modeled best by a linear equation in the subiculum ($Y=-188.8*X+23957$; $r^2=0.2346$; Pearson's $r=-0.4844$, $p<0.01$; Fig. 2.2A), and a nonlinear quadratic equation in the visual cortex ($Y=57400+-2383*X+41.54*X^2$; $r^2=0.4131$; Spearman's $r=-0.6090$, $p<0.0001$; Fig. 2.2B) suggesting potential region-related differences. Total subiculum WFA+ area was reduced at every timepoint compared to age-matched WT mice ($p<0.0001$ in each case; Fig. 2.1B,G), whereas the visual cortex displayed significant losses at 8mo and every timepoint thereafter ($p<0.0001$ or $p<0.001$ in every case; Fig. 2.1C,H). Age-dependent PNN reductions were evident in both genotypes and regions, resulting in even greater PNN loss with disease progression in 5xFAD mice; WFA+ PNNs were significantly reduced by 12mo ($p<0.01$) and 8mo ($p<0.05$)

in the diseased subiculum and visual cortex, respectively, compared to the same 5xFAD regions at 4mo, whereas significant within-genotype decreases in WT subiculum and cortical PNNs were detected later, between 8mo and 12mo ($p<0.001$, $p<0.05$).

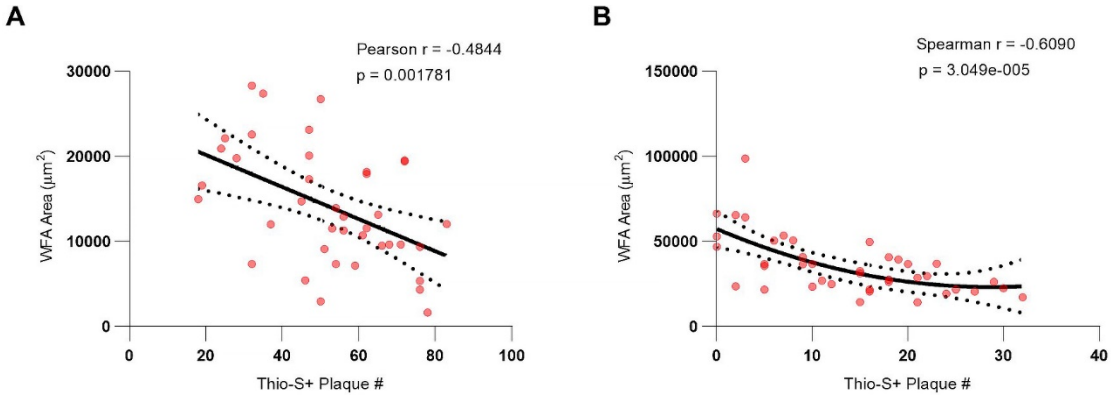

Figure 2.2. 5xFAD PNN abundance varies inversely with plaque load in a region-specific manner. Nonlinear regression and correlational analysis of WFA+ PNN area and Thio-S+ dense core plaque counts across all 5xFAD subiculum **(A)** and visual cortex **(B)** samples (including all timepoints and ages) analyzed in **Fig. 2.1** revealed region-specific inverse relationships between the two variables, which were best modeled by a linear equation in the subiculum ($Y=-188.8*X+23957$; $r^2=0.2346$; Pearson's $r=-0.4844$, $p<0.01$; $n=39$) and a nonlinear second order polynomial (quadratic) equation in the visual cortex ($Y=57400+-2383*X+41.54*X^2$; $r^2=0.4131$; Spearman's $r=-0.6090$, $p<0.0001$; $n=40$).

Analysis of total extracellular CSPG with CS-56 at early stages of PNN loss, which generally labels CSPGs excluded from PNNs e.g. those found in glial scars (Pearson et al., 2018; Yi et al., 2012), revealed significant increases in the subiculum but not visual cortex ($p<0.05$, $p=0.0818$) of 5xFAD mice (Fig. 2.3A-C). These results resemble the observation of CSPG in AD plaques reported almost three decades ago (DeWitt et al., 1993) as well as our previous findings in the context of Huntington's disease, where we observed dense CSPG accumulation in regions of PNN loss (Crapser et al., 2019). Together, this suggests that enhanced ECM CSPG deposition outside of PNNs is an underappreciated feature of neurodegeneration, and may also partially account for the

beneficial effects afforded by treatment with chondroitinase ABC enzyme in AD models (Howell et al., 2015; Végh et al., 2014) which degrades CSPGs not only found in PNNs but also in the general CNS ECM, where 98% of CNS CSPGs are found (Fawcett et al., 2019).

Further examination at higher magnification revealed that 5xFAD PNN-ensheathed neurites and cell bodies were observed physically wrapped around plaques, to which they appeared tethered by intermediary PAM (Fig. 2.1I). Interestingly, intracellular WFA+ material was evident in microglia (Fig. 2.1J, K; arrowheads), consistent with their putative phagocytic clearance. Analysis of total WFA+ intensity associated with IBA1+ microglia in the 18mo 5xFAD subiculum confirmed a significant increase compared to WT ($p<0.001$; Fig. 2.3G-H). Finally, disease-related effects on PNNs were validated at 12mo by staining for aggrecan, a core PNN CSPG (Rowlands et al., 2018), which confirmed the morphological abnormalities as well as the loss of 5xFAD subiculum and cortical PNNs at this timepoint ($p<0.001$, $p<0.05$; Fig. 2.3D-F). This data, together with the overlapping temporal profiles of plaque accumulation, microgliosis, and PNN density reduction, suggest that microglia facilitate the loss of PNNs in the 5xFAD brain.

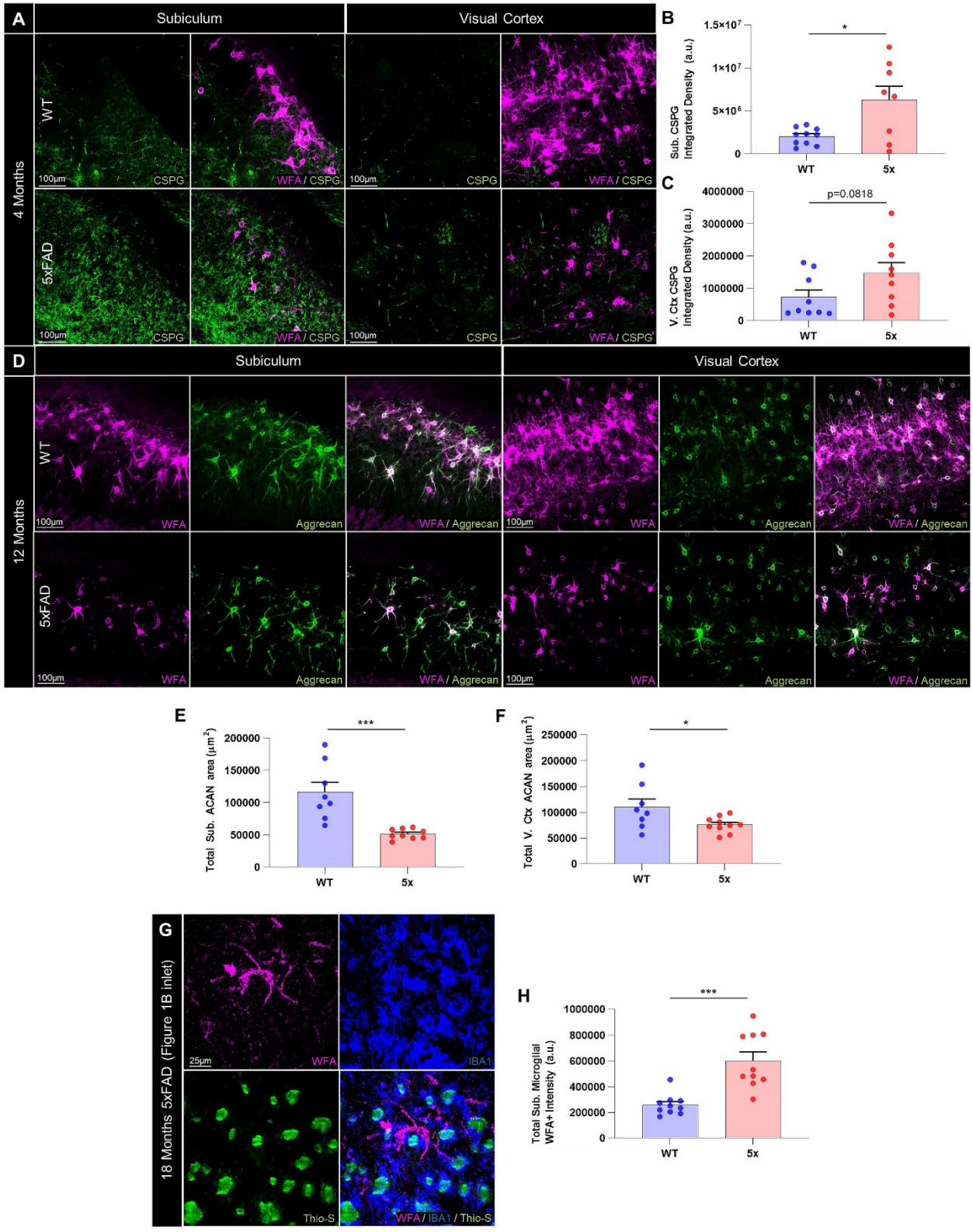

Figure 2.3. ECM CS-56+ CSPGs and ACAN+ PNNs increase and decrease, respectively, in the 5xFAD subiculum, where microglia accumulate elevated levels of PNN material. (A) Representative 20X images of WT and 5xFAD subiculum and visual

cortex at 4 months (mo) stained for CSPG (CS-56) and WFA display enhanced ECM CSPG accumulation with disease. **(B-C)** Quantification of CS-56+ immunoreactivity confirmed a significant increase in the 5xFAD subiculum ($p<0.05$) but not visual cortex ($p=0.0818$) compared to WT (two-tailed unpaired t-test; n=8-10/group). **(D)** Representative 20X images of WT and 5xFAD subiculum and visual cortex stained for aggrecan (ACAN) at 12mo reveal morphologically abnormal and diminished PNNs. **(E-F)** Quantification of ACAN PNN area confirmed significant reductions in PNN area in the 5xFAD subiculum ($p<0.001$) and visual cortex ($p<0.05$), as observed with WFA (two-tailed unpaired t-test; n=8-10/group). **(G)** Representative 63X magnification illustrates the presence of WFA+ microglial inclusions in the 18mo 5xFAD subiculum shown in Fig. 2.1. **(H)** Quantification of total WFA+ signal intensity associated with IBA1+ microglia in the 5xFAD subiculum at 18mo revealed a significant increase compared to WT ($p<0.001$; two-tailed unpaired t-test; n=10/group). * $p\leq0.05$, *** $p<0.001$. Error bars indicate SEM.

Reductions in 5xFAD PV+ interneurons occur only after overt PNN loss

Impaired PV+ interneuron functioning has recently been linked to neuronal network hypersynchrony/hyperexcitability and cognitive deficits in AD (Hijazi et al., 2019; Verret et al., 2012), and PV+ cell loss occurs across multiple AD models (Ali et al., 2019; Saiz-Sanchez et al., 2013; Takahashi et al., 2010; Zallo et al., 2018). Given the protective and physiological benefits PNNs confer upon the neurons they enwrap (Balmer, 2016; Miyata et al., 2007), we set out to investigate the temporal pattern of PV+ interneuron loss reported in the 5xFAD brain (Ali et al., 2019; Flanigan et al., 2014) relative to the onset of overt PNN reductions. To accomplish this, we immunolabeled and quantified PV+ cell density at 4, 8, 12, and 18mo in male and female 5xFAD and WT subiculum (Fig. 2.4A) and at 4mo and 18mo in the cortex (Fig. 2.5A). Interestingly, PV+ cell numbers remained unchanged at 4mo and 8mo in the 5xFAD subiculum ($p=0.085$ at 8mo; Fig. 2.4B), when PNN loss is already extensive, but were significantly reduced at 12mo and 18mo compared to WT ($p<0.0001$, $p<0.01$) and to 5xFAD at 4mo ($p<0.05$, $p<0.05$), indicating that interneurons are included among the general neuronal loss that we and others have reported in the diseased subiculum (Oakley et al., 2006; Spangenberg et al., 2016). Mean

intensity of WFA+ signal colocalizing with subiculum PV+ neurons, a measure of the structural integrity of interneuron-associated PNNs, was significantly reduced at every age compared to WT ($p<0.01$, $p<0.0001$, $p<0.0001$, $p<0.01$ starting at 4mo; Fig. 2.4C), indicating that PV+ PNN component density and/or integrity is diminished prior to PV+ neuronal loss, and remains impaired in surviving cells at later ages. This trajectory of PNN impairment (in overall coverage and in PV+ cell-associated signal) prior to PV+ cell loss is consistent with reports in the hippocampus of the Tg2576 AD model (Cattaud et al., 2018) and with the protective properties of PNNs against AD-relevant neurotoxins (e.g. oxidative stress, Aβ) (Cabungcal et al., 2013; Miyata et al., 2007), which when lost likely render neurons more susceptible to pathology-related death. We were unable to detect any disease-related differences in PV+ cell density in the anterior visual cortex at 4mo or 18mo, although some loss in PV+ neuronal WFA+ intensity was evident (Fig. 2.5A-C).

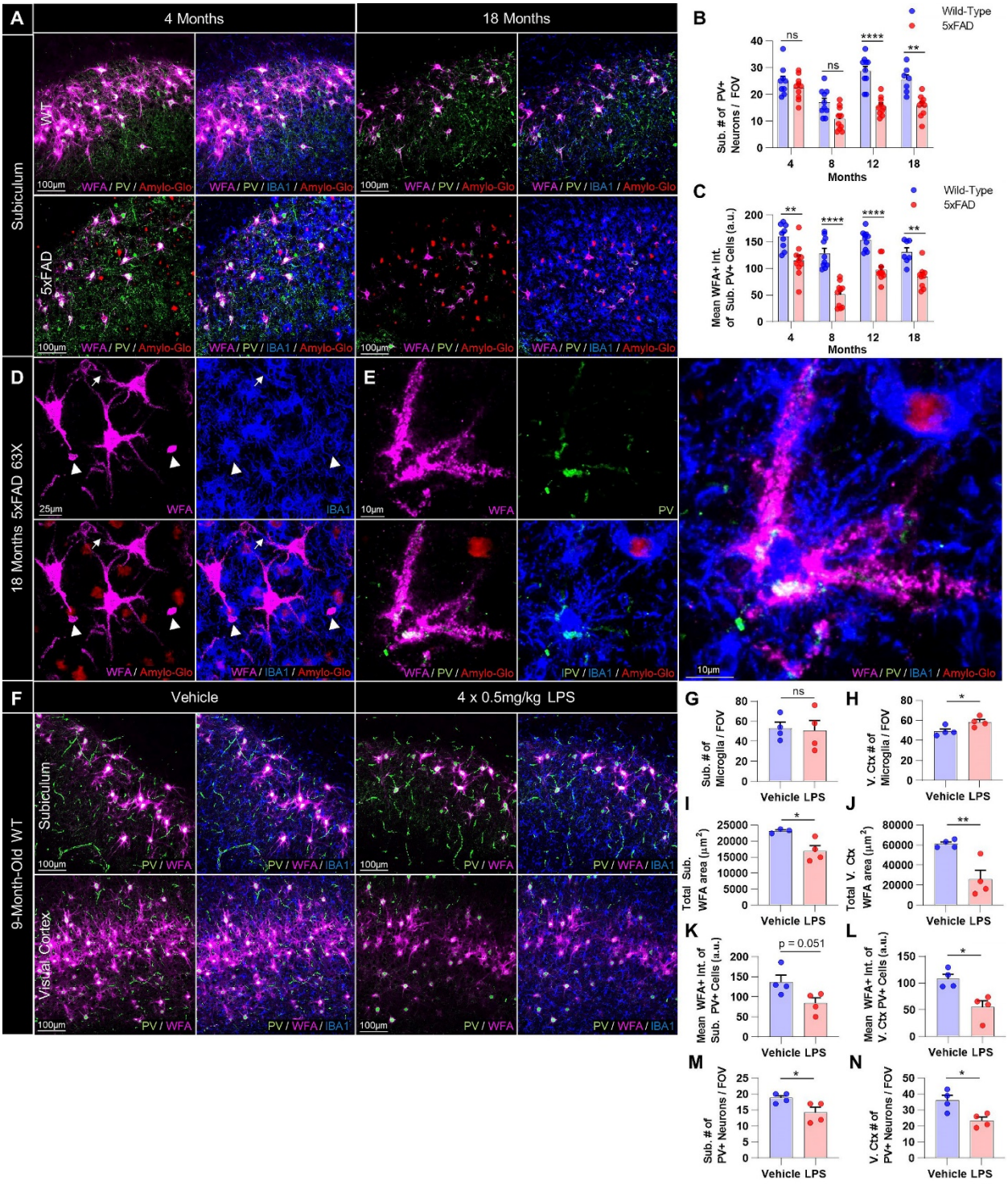

Figure 2.4. PV+ interneurons are decreased following PNN loss in 5xFAD mice and these effects are mirrored by LPS-induced microglial activation. (A) Representative 20X images of WT and 5xFAD subiculum at 4 and 18 months stained for WFA, PV, IBA1, and Amylo-Glo show a loss of PNN-associated PV+ interneurons at later stages of disease. **(B)** Quantification of PV+ interneurons in 5xFAD subiculum revealed significant reductions in cell density at 12 ($p<0.0001$), and 18mo ($p<0.01$) compared to age-matched controls, and significant within-genotype decreases between 4 and 18mo in 5xFAD mice ($p<0.05$; 2-way ANOVA with Tukey's post-

hoc test; n=7-10 WT and 9-10 5xFAD/timepoint). **(C)** Mean intensity of WFA+ signal colocalizing with PV+ cell soma, a measure of structural PNN integrity, was significantly reduced in existing PV+ cells at every timepoint examined in 5xFAD subiculum (4mo $p<0.01$; 8mo $p<0.0001$; 12mo $p<0.0001$; 18mo $p<0.01$; 2-way ANOVA with Tukey's post-hoc test; n=7-10 WT and 9-10 5xFAD/timepoint). **(D)** Representative 63X images of 18mo 5xFAD subiculum display the condensed, debris-like WFA+ puncta (arrowheads; also see Fig. 2.6) that accumulate around microglia as PNN degradation progresses in late stages of disease, particularly abundant in the hippocampus but also evident in other regions (e.g. cortex). Notably, microglial process coverage of PNN-enwrapped neurites is extensive in regions of lower WFA+ intensity (arrows). **(E)** Representative 63X image of morphologically dystrophic PV+ interneuron and associated PNN in spatial relation to activated microglia in 18mo 5xFAD CA1 shows direct contact. **(F)** Representative 20X images of adult 9mo WT subiculum and visual cortex from mice given IP injections of saline or LPS every other day for 7 days (4 doses) demonstrating microglia-mediated neuroinflammation and consequent loss of PNNs and PV+ cell density. **(G-H)** Microglia were increased in number in the visual cortex ($p<0.05$; two-tailed unpaired t-test; n=4/group) and displayed morphological hallmarks of activation in both subiculum and cortex. **(I-J)** LPS induced significant decreases in WFA+ coverage in the subiculum ($p<0.05$) and visual cortex of adult WT mice ($p<0.01$; two-tailed unpaired t-test; n=3-4/group), **(K-L)** diminished WFA+ signal intensity of subiculum and visual cortex PV+ neurons ($p=0.051$, $p<0.05$; two-tailed unpaired t-test; n=4/group), and **(M-N)** reduced PV+ cell densities in both regions ($p<0.05$, $p<0.05$; two-tailed unpaired t-test; n=4/group). Statistical significance is denoted by * $p\leq0.05$, ** $p<0.01$, *** $p<0.001$, **** $p<0.0001$, ns = not significant. Error bars indicate SEM.

Interestingly, small debris-like WFA+ puncta, phenotypically distinct from PNNs, were abundant throughout the 5xFAD brain by 18mo, particularly in the hippocampus (e.g. subiculum, CA1) where they associated with PAM (Fig. 2.4D; arrowheads) and NPAM (Fig. 2.6A; arrowheads). Gross morphological deficits in PNNs and PV+ neurons were apparent proximal to activated (e.g. amoeboid) microglia, often suggestive in appearance of microglial-mediated disruption and/or engulfment of PV+ soma and encapsulating PNN (Fig. 2.4E). To determine whether microglial activation in an established model of neuroinflammation was sufficient to induce PNN degradation, adult male and female WT mice were I.P. injected at 9mo with 0.5mg/kg LPS every other day for 7d (4 doses total) and their brains immunolabeled for PV, WFA, and IBA1 (Fig. 2.4F)(Elmore et al., 2014). LPS induced phenotypic activation of subiculum and cortical microglia (e.g. process

retraction and enlargement), and while IBA1+ numbers were significantly elevated only in the latter ($p<0.05$; Fig. 2.4G, H), WFA+ area was significantly reduced in both regions ($p<0.05$, $p<0.01$; Fig. 2.4I, J) with reductions in mean WFA+ intensity of PV+ neurons ($p=0.051$, $p<0.05$; Fig. 2.4K, L) and PV+ cell densities ($p<0.05$, $p<0.05$; Fig. 2.4M, N) resembling that seen in 5xFAD mice. Together, these data suggest that microglial activation or dyshomeostasis (induced by plaques or LPS) can result in PNN breakdown, potentially leaving interneurons and other PNN-associated subtypes susceptible to changes in synaptic connectivity (Reichelt et al., 2019), excitability (Balmer, 2016), firing rate (Tewari et al., 2018), and damage (Miyata et al., 2007).

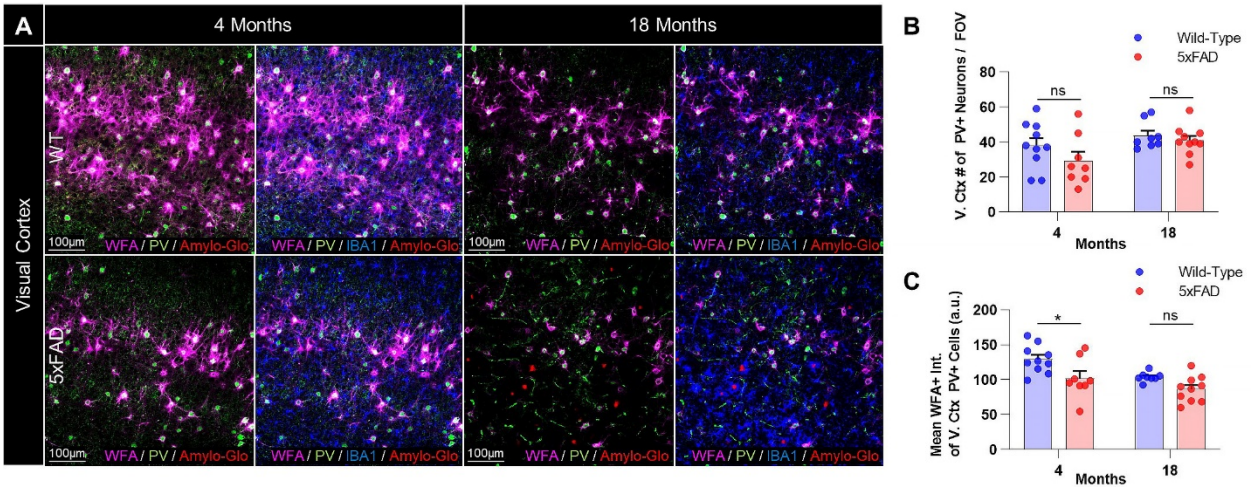

Figure 2.5. 5xFAD visual cortex PV+ interneurons are unchanged between 4 and 18 months. (A) Representative 20X images of WT and 5xFAD visual cortex at 4 and 18mo stained for WFA, PV, IBA1, and Amylo-Glo show no changes in PV+ interneuron cell density with disease. **(B)** Quantification of PV+ interneurons in 5xFAD visual cortex did not suggest any significant differences between 5xFAD and WT at 4 or 18mo, or in 5xFAD tissue between 4 and 18mo (all $p>0.10$; 2-way ANOVA with Tukey's post-hoc test; n=8-10/group). **(C)** Mean intensity of WFA+ signal colocalizing with PV+ cell soma was significantly reduced in visual cortex PV+ cells at 4mo ($p<0.05$) but not 18mo due to age-related loss in WT PV+ cells over the same time period ($p=0.0531$; 2-way ANOVA with Tukey's post-hoc test; n=8-10/timepoint). * $p\leq0.05$, ns = not significant. Error bars indicate SEM.

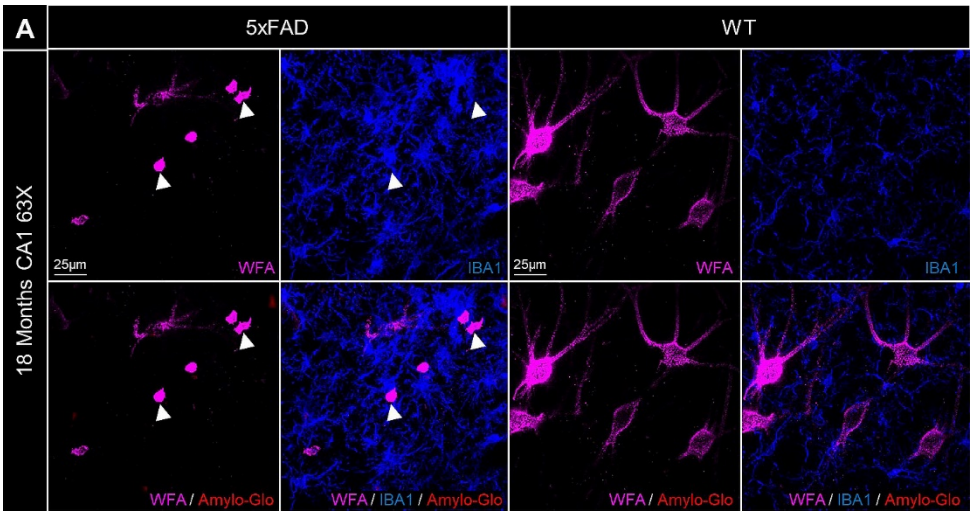

Figure 2.6. Abnormal WFA+ debris accumulates in the 5xFAD brain during disease progression and associates with microglia. (A) Representative 63X images displaying the aberrant accumulation of, and IBA1+ microglial association with, dense WFA+ debris puncta (arrowheads) in the 5xFAD brain at later stages of disease, particularly abundant in the 18mo hippocampus (here shown in CA1; 63X), where morphologically normal PNNs are instead observable in WT brains, as shown on the right.

PNNs are reduced in human AD brains and are inversely related to plaque burden

The vulnerability of PNNs to AD pathology in humans is unclear, with some groups reporting no changes (Lendvai et al., 2013; Morawski et al., 2012; Morawski et al., 2010b) and others reporting disease-associated reductions (Baig et al., 2005; Kobayashi et al., 1989); such ambiguity may be due in part to differences in quantitative technique, disease stage/pathology progression, or regional variability. As prolonged post-mortem delay (PMD) between death and tissue collection/fixation has been shown to reduce reactivity for WFA lectin in mice, but not for the major PNN component aggrecan (using pan-aggrecan clone 7D4 (Virgintino et al., 2009)), it has been suggested that early lectin binding site loss due to PMD may lead to discrepancies upon autopsy (Morawski et al., 2012). A recent report furthermore found clone 7D4 to be uniquely efficacious in staining PNNs in banked post-mortem human middle frontal gyrus and hippocampal brain tissue,

even among other aggrecan antibodies and where WFA had failed (Rogers et al., 2018). Therefore, we immunolabeled post-mortem cortical tissue from clinically and neuropathologically diagnosed AD and non-demented control brains for ACAN+ PNNs (aggrecan 7D4), dense-core plaques (Thio-S), and microglia (IBA1+) (Fig. 2.7A-D). As in the animal studies, we included only dense-core plaques in our analysis, meaning plaques composed of a central amyloid core surrounded by a fibrillar “halo” (Kumar-Singh et al., 2002; Wisniewski et al., 1989), due to the unique association and response of microglia to dense-core rather than diffuse plaques (Mandrekar-Colucci and Landreth, 2010; Serrano-Pozo et al., 2013; Spangenberg et al., 2019; Yin et al., 2017). Neuropathological scoring of post-mortem samples can be found in Table 2.1.

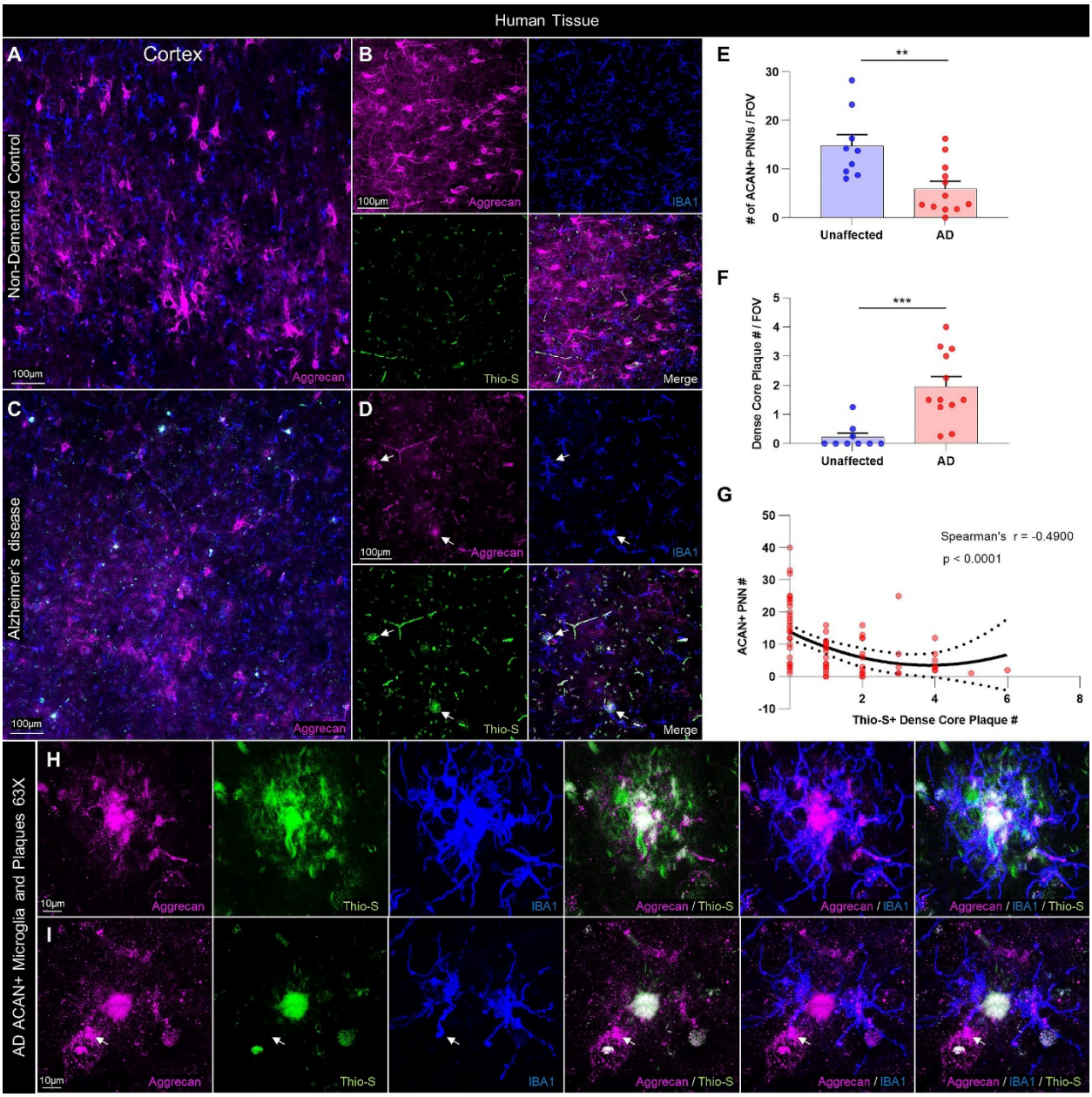

Figure 2.7. PNNs are reduced in the human AD cortex and correlate negatively with dense-core plaque load. (A-B) Representative stitched and 20X images of grey matter (GM) aggrecan (ACAN)+ PNNs immunolabeled in post-mortem cortical tissue from the middle frontal gyrus (BA9 and BA46) of non-demented control or **(C-D)** clinically diagnosed AD patients reveals substantial PNN loss in the diseased brain, where Thio-S+ dense core plaques (arrows) and immediately proximal IBA1+ PAMs accumulate. **(E)** Quantification of ACAN+ PNN number in sections from n=9 non-demented control and n=12 AD brains revealed a significant loss with disease ($p<0.01$; two-tailed unpaired t-test; n=9-12/group) in parallel with **(F)** a significant increase in Thio-S+ dense core plaques in AD compared to non-demented control brains ($p<0.001$; two-tailed unpaired t-test; n=9-12/group). **(G)** Nonlinear regression and correlational analysis of human PNN and dense core plaque counts across all sample replicates from AD and non-demented control brains identified a nonlinear ($Y=13.91+-5.414*X+0.7059*X^2$; $r^2=0.2094$) and highly significant inverse relationship between PNNs and

plaque count in human prefrontal cortex GM (Spearman's r=-0.49, p<0.0001; n=80). **(H-I)** Representative 63X images of AD patient cortical GM displays colocalization of ACAN+ signal (clone 7D4) within Thio-S+ plaques and IBA1+ microglia, suggesting the presence of PNN material. As in 5xFAD mice, PAM processes were seen in contact with proximal PNNs, occasionally with morphology resembling phagocytic cups (arrow). Statistical significance is denoted by * p≤0.05, ** p<0.01, *** p<0.001, **** p<0.0001, ns = not significant. Error bars indicate SEM.

We found that AD patient brains exhibited significantly fewer PNNs (p<0.01; Fig. 2.7E) and more Thio-S+ dense core plaques (p<0.001; Fig. 2.7F) compared to non-demented control brains, such that a highly significant negative correlation between ACAN+ PNNs and Thio-S+ plaques was observed across unaffected and diseased tissue samples (Spearman's r=-0.49, p<0.0001; Fig. 2.7G). Interestingly, these data were best described by a nonlinear quadratic model ($Y=13.91+-5.414*X+0.7059*X^2$; $r^2=0.2094$), as paralleled by the distribution of WFA+ PNN area vs. Thio-S+ plaque number in the murine cortex but not subiculum (Fig. 2.2B, A), providing additional cross-species corroboration on the brain-region dependent relationship between PNNs and plaques. PAM were readily evident around dense-core plaques (Fig. 2.7D, arrows), and closer examination revealed the ubiquitous presence of aggrecan within both the plaque core and surrounding microglia (Fig. 2.7H), the processes of which could be seen in close spatial association with nearby intact PNNs (Fig. 2.7I).

Microglia facilitate plaque-dependent loss of PNNs

Given the relationships between plaques, microglia, and PNNs, the physical associations between NPAMs/PAMs and PNNs, and the observation that LPS also induces microglial activation and PNN degradation, we set out to directly test the involvement of microglia-mediated PNN loss in two AD mouse models. Microglia express and are critically dependent upon signaling through the myeloid CSF1/IL-34 receptor CSF1R for survival (Elmore et al., 2014). In recent years, we have developed microglial depletion paradigms

based on oral delivery of CSF1R inhibitors in chow at concentrations that cross the blood-brain barrier, inducing scalable microglial death and sustained depletion from the brain (Elmore et al., 2014; Najafi et al., 2018), including in mouse models of AD (Dagher et al., 2015; Spangenberg et al., 2019; Spangenberg et al., 2016). Thus, to elucidate the role of microglia in plaque-induced PNN degradation, we treated WT and 5xFAD mice with the selective CSF1R inhibitor PLX5622 (1200ppm in chow) or vehicle from 1.5 – 4 months of age, encompassing the period in which plaques begin to form and cause PNN loss. Brain sections collected from 4mo mice at the end of the experiment were stained with Thio-S, IBA1, and WFA, and the relationships between plaques, microglia, and PNNs were explored (Fig. 2.8A, B).

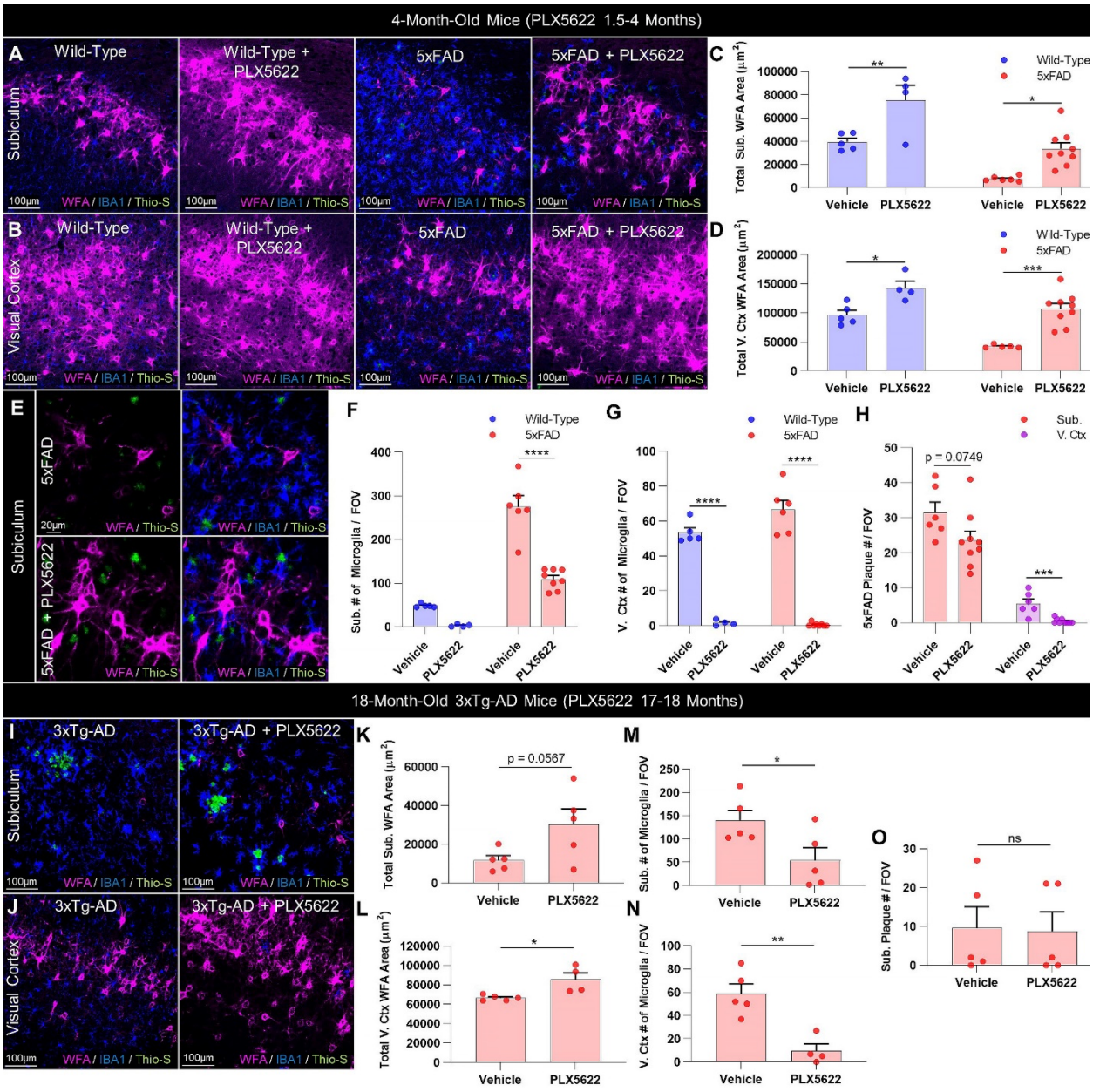

Figure 2.8. Microglia mediate plaque-driven PNN loss in AD. (A-B) Representative 20X images of subiculum and visual cortex in 4mo 5xFAD and WT mice treated prior to and during plaque development (1.5-4mo) with sustained delivery of CSF1R inhibitor PLX5622 (1200ppm in chow) demonstrate complete prevention of WFA+ PNN loss with microglial depletion in 5xFAD subiculum and cortex, even despite the persistence of Thio-S+ plaques in the former. **(C-D)** Quantification of WFA+ area in vehicle-treated mice revealed a significant decrease in 4mo 5xFAD subiculum ($p<0.01$) and visual cortex in this cohort ($p<0.01$), both of which were prevented with PLX5622 treatment (Subiculum: 5xFAD vs. 5xFAD+PLX5622, $p<0.05$; WT vs. 5xFAD+PLX5622, $p=0.884$. Visual cortex: 5xFAD vs. 5xFAD+PLX5622, $p<0.001$; WT vs 5xFAD+PLX5622, $p=0.827$; all 2-way ANOVAs with Tukey's post-hoc test; n=4-5 WT and 5-9 5xFAD/group). **(E)** Representative scaled 20X images and **(F)** quantification of IBA1+ microglia in vehicle- and PLX5622-treated 5xFAD subiculum confirm significant microglial depletion with treatment in diseased mice ($p<0.0001$) with predominantly PAM

remaining, whereas microglia were elevated in vehicle-treated 5xFAD subiculum compared to control ($p<0.0001$; 2-way ANOVA with Tukey's post-hoc test; n=4-5 WT and 6-8 5xFAD/group). **(G)** Visual cortex microglia were significantly elevated at 4mo in vehicle-treated 5xFAD compared to WT ($p<0.05$) but were virtually absent following PLX5622 ($p<0.0001$; 2-way ANOVA with Tukey's post-hoc test; n=4-5 WT and 6-8 5xFAD/group). **(H)** PLX5622 significantly reduced Thio-S+ plaque numbers in the visual cortex ($p<0.001$) but not subiculum ($p=0.0749$; two-tailed unpaired t-tests; n=6-9/group), together suggesting that microglial depletion can prevent PNN loss even without significant changes in plaque load. **(I-J)** Representative 20X images of aged 18mo 3xTg-AD subiculum and visual cortex following 1mo treatment with PLX5622 (1200ppm in chow) display beneficial effects of post-pathological IBA1+ microglial depletion on WFA+ PNNs independent of Thio-S+ plaque burden. **(K-L)** Quantification of WFA+ area reveals significant increases in subiculum and visual cortex PNNs ($p=0.0567$, $p<0.05$) following 1-month PLX5622, which **(M-N)** significantly reduced microglia in the respective regions ($p<0.05$, $p<0.01$) but **(O)** had no effect on plaque number (subiculum $p=0.917$; two-tailed unpaired t-tests; n=4-5/group). No plaques were detected in any 3xTg-AD visual cortex images examined regardless of treatment. Statistical significance is denoted by * $p\leq0.05$, ** $p<0.01$, *** $p<0.001$, **** $p<0.0001$, ns = not significant. Error bars indicate SEM.

Significant reductions in PNN area were evident in vehicle-treated 5xFAD subiculum compared to vehicle-treated WT at 4 months ($p<0.01$), as previously observed. However, PLX5622 completely prevented the loss of 5xFAD PNNs ($p<0.05$), which were consequently no different from vehicle-treated WT levels ($p=0.884$; Fig. 2.8C). In this cohort, we detected a significant reduction in 5xFAD visual cortex WFA+ coverage at 4mo compared to vehicle-treated WT ($p<0.01$), which was also prevented in 5xFAD+PLX5622 tissue ($p<0.001$) where PNN abundance was indistinguishable from WT controls ($p=0.827$; Fig. 2.8D). Importantly, the preservation of PNNs in the 5xFAD brain with PLX5622 coincided with extensive microglial depletion in both the subiculum ($p<0.0001$) and visual cortex ($p<0.0001$) compared to respective vehicle-treated 5xFAD regions (Fig. 2.8F, G). However, only Thio-S+ plaques in the visual cortex ($p<0.001$) were significantly reduced with treatment (Fig. 2.8H), consistent with prior data (Spangenberg et al., 2019). A small population of mostly PAM remained in the subiculum, a region of high pathology, at 4mo following sustained CSF1R inhibition, but the reduction in overall microglial densities with PLX5622 fully preserved subiculum PNNs despite partial contact with

surviving PAM (Fig. 2.8E). Significant microgliosis occurred alongside disease-related PNN loss in vehicle-treated 5xFAD subiculum ($p<0.0001$) and cortex ($p<0.05$) compared to vehicle-treated WT (Fig. 2.8F, G). PLX5622 treatment in WT mice also enhanced basal PNN levels in subiculum ($p<0.01$) and cortex ($p<0.05$) compared to vehicle treatment (Fig. 2.8C, D), consistent with our prior reports of homeostatic PNN regulation by microglia in the healthy adult brain (Crapser et al., 2019).

To expand upon this data and to determine if microglial-mediated PNN loss could be ameliorated in late stages of disease, we treated 17mo 3xTg-AD mice, an AD line that develops clinically-relevant neurofibrillary tangles of hyperphosphorylated tau in addition to Aβ plaques (Oddo et al., 2004), for 1mo with PLX5622 (1200ppm in chow). PLX5622 treatment in 3xTg-AD mice induced extensive IBA1+ microglial depletion (subiculum $p<0.05$; visual cortex $p<0.01$) but no changes in Thio-S+ plaques (subiculum $p=0.917$; visual cortex had no detectable plaques). Nonetheless treatment was accompanied by significant WFA+ PNN upregulation (subiculum $p=0.0567$; visual cortex $p<0.05$; Fig. 2.8I-O). Together, this data collectively suggests that the deleterious effects of AD-associated plaques on PNNs are mediated by microglia, the pre- or post-pathological depletion of which mitigates perineuronal net loss even in the absence of significant changes in plaque load.

Discussion

In conclusion, our data show that microglia are critical homeostatic regulators of PNNs in the healthy adult brain, and that their phenotypic changes in response to plaques mediates extensive PNN loss in AD. We observed PNN components within microglia in both mice and humans, suggesting that microglia directly phagocytose these ECM

structures or debris resulting from their degradation, as well as within human dense core plaques. The inversely correlative relationship between plaques and PNNs in the human cortex suggests that degraded PNN components may accumulate in plaques following PNN loss as AD progresses. As PNNs are implicated in neuronal health and function, protecting cells against neurotoxins such as $A\beta_{1-42}$ (Miyata et al., 2007) and oxidative stress (Cabungcal et al., 2013) in addition to modulating neuronal activity (Balmer, 2016; Tewari et al., 2018), the microglial-mediated loss of these structures in disease likely plays an important role in AD pathogenesis.

For instance, synaptic loss is a key feature of AD pathogenesis mediated, at least in part, by microglia (Hong et al., 2016; Spangenberg et al., 2016). This may be due in part to the degradation of the PNNs in which synapses are embedded, as the genetic ablation of one or more PNN structural components and consequent loss of neuronal PNN integrity can induce in the loss of synapses (Geissler et al., 2013; Gottschling et al., 2019) and impaired synaptic colocalization/expression of neurotransmitter receptor subunits (Favuzzi et al., 2017), potentially manifesting as deficits in synaptic plasticity (e.g. LTP) (Brakebusch et al., 2002; Bukalo et al., 2001; Evers et al., 2002). We previously reported that neuronal and synaptic genes (e.g. *Dlk2*, *Kcnq3*, *Nrg3*, *Scn1b*) and related functional pathways (e.g. synaptic vesicles, glutamate receptors, neuronal membranes) were extensively and uniquely downregulated in the 7mo 5xFAD hippocampus compared to WT hippocampus and other 5xFAD brain regions (Spangenberg et al., 2019), respectively, in addition to a loss of subiculum neurons and dendritic spines in 10-month-old 5xFAD mice (Spangenberg et al., 2016). We now know that these transcriptional and cellular alterations indicative of impaired plasticity occur alongside contemporaneous

PNN loss in the subiculum, and as microglial depletion was able to prevent or rescue the regional deficits in neuronal form and function in both prior studies, we are inclined to speculate that microglial-mediated PNN loss underlies at least aspects of impaired neuronal plasticity in 5xFAD mice.

Of further relevance to AD, the enzymatic degradation of auditory cortex PNNs with chondroitinase ABC (chABC) disrupts consolidation of auditory fear learning (Banerjee et al., 2017), which is restored upon PNN recovery, whereas PNN digestion in the amygdala or visual cortex disrupts the recall of contextual fear memories (Gogolla et al., 2009) and remote visual fear memories (Thompson et al., 2018), respectively. Similarly, PNN formation in the hippocampus is required for the consolidation and reconsolidation of recent and remote fear memories (Shi et al., 2019a). In light of such data, PNNs have been proposed as the molecular substrate underpinning long-term memory storage, by serving as a scaffold that retains synapse position and strength (Tsien, 2013). Although contrasting effects of PNN ablation on certain (specifically object recognition) memory tasks and measures of plasticity suggest this is not the case for all types of memory (Favuzzi et al., 2017; Fawcett et al., 2019; Romberg et al., 2013), but such differences may also be at least partly attributable to the PNN ablation method utilized (e.g. enzymatic digestion or genetic deletion of PNN components) which can produce differential effects on the same measures of plasticity (Bukalo et al., 2001). On the other hand, enhanced plasticity and learning can impair the storage and recall of remote memories due to interference from new memory traces (Reichelt et al., 2019), and so the enhancement of these factors following PNN loss would still be consistent with the consequently impaired reconsolidation and recall of remote, long-term memories reported by others (Shi et al.,

2019a; Thompson et al., 2018). Supporting this, a recent study found that while PNN digestion enhanced learning rate, it ultimately impaired memory retention, due in part to the extensive synaptic remodeling induced by PNN loss (Carulli et al., 2020).

It is interesting to note that we identified here and elsewhere (Crapser et al., 2019) a homeostatic role for microglia in the maintenance of PNNs, such that basal PNN levels in the healthy adult brain are elevated following microglial depletion. Recent work in mice shows that microglial clearance of ECM in response to neuronal IL-33 promotes synaptic remodeling and plasticity (Nguyen et al., 2020). Importantly, inhibiting this pathway results in reduced microglial phagocytosis and engulfment of ECM components (e.g. aggrecan) and conversely enhanced deposition of ECM at synapses (Nguyen et al., 2020), and therefore the consequences of this loss of microglial function resemble the enhanced accumulation of ECM-composed PNNs that we have shown occurs in healthy adult mice following the pharmacological depletion of microglia (Crapser et al., 2019). Microglial depletion also enhances performance in certain memory tasks (Elmore et al., 2014; Rice et al., 2015; Spangenberg et al., 2019) and prevents the forgetting of remote memories and, in association, the dissociation of memory engram cells in healthy adult mice (Wang et al., 2020). While further research is necessary to unweave the complexities and mechanisms of PNN modulation by microglia and specifically how this relates to changes in synapses and memory, the occurrence of microglia-mediated PNN loss, which we first reported in the Huntington's disease brain even in the absence of overt microglial activation (Crapser et al., 2019), and now extended to the AD brain, suggests that ECM remodeling by glia is a common feature of neurodegenerative disorders. Identifying

therapeutic avenues that inhibit microglial-mediated PNN loss without requiring their cellular ablation will be critical going forward.

DISSERTATION CONCLUDING REMARKS

Microglia exert top-down influence on all major components of the modernly conceptualized tetrapartite synapse (Dityatev and Schachner, 2003; Dityatev et al., 2010), namely pre- and post-synaptic compartments (Schafer et al., 2012; Tremblay et al., 2010), glia (Hagemeyer et al., 2017; Liddelow et al., 2017), and, as evidenced within this thesis and by recent work from other groups, the extracellular matrix (ECM) (Crapser et al., 2019; Crapser et al., 2020; Liu et al., 2021; Nguyen et al., 2020). Previous studies have postulated that microglia may drive PNN loss in certain disease contexts due to their ability to secrete matrix-degrading enzymes (e.g. matrix metalloproteinases; MMPs) and/or their molecular activators or inhibitors (Belichenko et al., 1997; Bitanihirwe and Woo, 2014; Franklin et al., 2008; Gray et al., 2008a). Indeed, the experiments in this thesis show that CSF1R inhibitor-based microglial depletion prevents disease-associated PNN reductions in models of Huntington's (Crapser et al., 2019) and Alzheimer's diseases (AD) (Crapser et al., 2020). PNN components were evident in microglia in both AD mice as well as human brain tissue, where they were also colocalized with canonical dense-core plaques (Crapser et al., 2020). That we observed similar effects on PNN abundance in the relative absence of microglia across these models is striking, both due to their differential etiologies – intracellular vs. extracellular protein accumulation in the R6/2 HD (Mangiarini et al., 1996) and 5xFAD model of AD (Oakley et al., 2006), respectively – and the variable microglial phenotypes we observed, which resembled "classical activation" in 5xFAD but not R6/2 brains, where they instead were associated with an interferon signature.

In a similar vein, we have extended these findings to CSF1R$^{+/-}$ mice, a neurodegenerative model of adult-onset leukoencephalopathy with axonal spheroids and pigmented glia (ALSP) (Biundo et al., 2021; Chitu et al., 2015), where early disease stage microglia that displayed homeostatic marker loss, but not pro-inflammatory gene upregulation, induced decreases in PNNs and presynaptic puncta (Arreola et al., in revision). In the same study, we confirmed these changes with inducible microglia-specific *Csf1r* haploinsufficiency (*CX3CR1*$^{+/CreERT2}$*:Csf1r*$^{+/fl}$ mice) and their normalization following CSF1R inhibitor-based depletion, validating the microglial origin of ALSP PNN and synaptic deficits. Therefore, it appears that microglia drive PNN loss in disease, as has been suggested based on temporal analysis of microglial activation and their accumulation of net material in prion disease (Belichenko et al., 1999; Borner et al., 2011; Franklin et al., 2008) and following infection with human or simian immunodeficiency virus (HIV or SIV), which preferentially infects microglia and causes PNN degradation (Belichenko et al., 1997; Bozzelli et al., 2020; Medina-Flores et al., 2004).

The loss of protective PNNs leaves PV+ and other enwrapped neurons susceptible to injury (Cabungcal et al., 2013; Miyata et al., 2007; Reichelt et al., 2019), and accordingly we found that PNN reductions preceded decreases in PV+ neurons in AD (Crapser et al., 2020), where PV+ cells are particularly relevant to disease (Ali et al., 2019; Hijazi et al., 2019; Iaccarino et al., 2016; Verret et al., 2012). Indeed, PNN loss is associated with neuronal death and/or degeneration in a number of disease contexts (Belichenko et al., 1999; Cattaud et al., 2018; Gray et al., 2008a; Guentchev et al., 1998; Hobohm et al., 2005; Reichelt et al., 2021; Tewari et al., 2018). It should be noted that several studies failed to detect differences in PNN abundance in clinical AD (Brückner et al., 1999;

Lendvai et al., 2013; Morawski et al., 2010a; Morawski et al., 2012), and this may be partly attributable to the brain region under investigation or the method of PNN labeling used. While changes with non-diseased aging are less clear (Brewton et al., 2016; Cattaud et al., 2018; Crapser et al., 2020; Hilbig et al., 2002; Mafi et al., 2020; Ueno et al., 2019), we and others have found age-related reductions in PNN density in older animals (Brewton et al., 2016; Cattaud et al., 2018; Crapser et al., 2020; Hilbig et al., 2002), and discrepancies across studies may depend on the inclusion of both sexes and the brain region(s), mouse strain, and/or model organism being studied.

Even more striking, however, is the observation that PNN abundance is dramatically upregulated throughout the healthy adult brain following microglial depletion (Crapser et al., 2019; Crapser et al., 2020; Liu et al., 2021). While neurons and glia may both express components that contribute to PNNs (Fawcett et al., 2019), neurons can express the core components of nets themselves and are capable of forming PNNs *in vitro* in the absence of glia (Miyata et al., 2005). For instance, neurons produce aggrecan (Lander et al., 1998), the inducible neuron-specific removal of which results in PNN ablation (Rowlands et al., 2018), as well as hyaluronan (Fowke et al., 2017), which is continuously secreted and serves as a backbone by tethering associated CSPGs into PNNs with the aid of link proteins (Carulli et al., 2010; Jäger et al., 2013; Kwok et al., 2010)). Therefore, our findings suggest that microglia basally regulate PNN density in the homeostatic brain, whether via direct or indirect enzymatic degradation and/or phagocytosis, such that their absence allows PNN components to accumulate. PNN enhancements induced by microglial depletion are also associated with increased excitatory and inhibitory synaptic connections to excitatory cortical neurons, as well as augmented neural activity in both

cortical excitatory neurons and PV+ interneurons as assessed by *in vivo* calcium imaging (Liu et al., 2021). Importantly, no overt changes in astrocytes were found in this study, as reported previously following pharmacological depletion with either CSF1R inhibitor utilized (Crapser et al., 2019; Elmore et al., 2014; Spangenberg et al., 2019). Synaptic connectivity and neural activity are both normalized following microglial repopulation (Liu et al., 2021), and this is consistent with the normalization of PNN densities we observe under similar conditions of inhibitor cessation following microglial elimination (Hohsfield et al., 2021). Loss of PNNs with disease then likely reflect a toxic gain-of-function in microglia of this newly identified homeostatic role, whereby augmented or complementary PNN-degradative processes are activated, either via enhanced or alternative secretion of ECM-cleaving proteases or their modulators, and/or increased phagocytosis.

Suggesting a direct role for microglia in the regulation of perisynaptic matrix-controlled synaptic plasticity, a recent study by Nguyen et al. determined that, in response to neuronal IL-33, microglia in the adult brain phagocytose and clear perisynaptic ECM components to promote dendritic spine formation, synaptic plasticity, and fear memory precision (Nguyen et al., 2020). Importantly, they found that inhibition of this pathway decreased microglial engulfment of aggrecan and consequently enhanced aggrecan puncta density and deposition at the synapse, in addition to increasing total intact brevican while reducing levels of proteolyzed brevican. Thus, as in our work, loss of microglial function results in enhanced ECM deposition in the homeostatic brain. The occurrence of this phenomenon across multiple ECM compartments (i.e. the perisynaptic matrix (Nguyen et al., 2020) and perineuronal nets (Crapser et al., 2019; Crapser et al., 2020)) together suggest a fundamental homeostatic role for microglia in ECM degradation

and remodeling, which may be required for subsequent remodeling of synapses surrounded and stabilized by such ECM. Interestingly, we also found elevated interstitial CSPG deposition in the brain parenchyma of both AD (Crapser et al., 2020) and HD (Crapser et al., 2019) mice, which may at least partially account for some of the beneficial effects of ChABC injections in related disease models that may be acting on the perisynaptic ECM (Howell et al., 2015; Stoyanov et al., 2021; Végh et al., 2014). It should be noted that microglia may also act as a source of CSPGs and other ECM molecules in the interstitial matrix under certain conditions (Jones and Tuszynski, 2002; Lau et al., 2012), but this appears a less prominent role compared to the negative regulatory influence they exert across ECM compartments.

Into the Matrix: Potential mechanisms of microglial ECM regulation

Although microglia are linked to ECM remodeling in disease (i.e. PNN loss (Belichenko et al., 1997; Bitanihirwe and Woo, 2014; Crapser et al., 2019; Crapser et al., 2020; Franklin et al., 2008; Gray et al., 2008a; Hobohm et al., 2005; Reichelt et al., 2021)), and now also in the healthy homeostatic brain (Crapser et al., 2019; Crapser et al., 2020; Liu et al., 2021; Nguyen et al., 2020), the molecular mechanism(s) by which this occurs are unclear. As observed with synapses during developmental pruning (Paolicelli et al., 2011; Schafer et al., 2012), microglia may directly engulf and phagocytose ECM components. Indeed, aggrecan colocalizes with lysosomal CD68 in microglia, a marker of phagocytosis, and disrupting IL-33-based ECM engulfment by microglia reduces $CD68^{+}$ lysosome number (Nguyen et al., 2020). Furthermore, proteoglycans and PNN material can accumulate within disease-associated microglia/macrophages (Belichenko et al., 1999; Crapser et al., 2020; Sobel and Ahmed, 2001), and phagocytic genes (e.g. *Itgax,*

Clec7a, Trem2) are upregulated in 5xFAD mice (Spangenberg et al., 2019; Spangenberg et al., 2016), particularly in plaque-associated microglia (Yin et al., 2017), where we observed widespread PNN loss (Crapser et al., 2020). However, it is likely that microglial release of degradative enzymes is also involved in ECM turnover processes, especially as it applies to the remodeling of PNNs, in which CSPGs, tenascins, hyaluronan, and link proteins are more tightly woven together as compared to the diffuse matrix (Deepa et al., 2006).

Several proteases are immediately apparent candidates based on the capability of microglia to produce them and their ability, in turn, to degrade ECM components and core PNN molecules. These proteases primarily include MMPs, ADAMTS, and cathepsins. Microglia may also shape PNNs indirectly via modulators of protease activity, as in tissue inhibitors of metalloproteinases (TIMPs) (Cross and Woodroofe, 1999; Welser-Alves et al., 2011; Yong et al., 2001), or by regulating protease or TIMP expression by other cells. For instance, it has been suggested (Gray et al., 2008a) that glutamate release by activated microglia (Takeuchi et al., 2006) could bind neuronal glutamate receptors and induce neuronal MMP expression (Szklarczyk et al., 2002). While these are important and plausible mechanisms, for the purpose of conciseness this review will focus on the direct action of microglia-sourced protease candidates.

MMPs are expressed at low to undetectable levels under homeostatic conditions in the adult brain and are upregulated in injury and disease; taken together, they have the capacity to degrade the entire gamut of ECM constituents (Yong et al., 2001). Although not exclusively, MMP-2 and MMP-9 are secreted by microglia (Könnecke and Bechmann, 2013; Nakanishi, 2003) and act on a wide range of oftentimes overlapping substrates,

such as link proteins and aggrecan (Yong et al., 2001). Substrate-specificity is also evident in certain cases, as in the digestion of tenascin-C (Siri et al., 1995) and brevican (Nakamura et al., 2000) by MMP-2 but not MMP-9. MMP-2 and/or MMP-9 are upregulated by microglia in disorders where PNN breakdown occurs, such as stroke (Planas et al., 2001; Rosell et al., 2006), multiple sclerosis (Maeda and Sobel, 1996; Milner et al., 2007), and glioma (Hu et al., 2014; Markovic et al., 2005), and pharmacological MMP blockade in glioma ameliorates enhanced MMP-2/9 activity and associated PNN loss (Tewari et al., 2018). While baseline PNNs are largely unchanged in MMP-9$^{-/-}$ mice, developmental monocular deprivation-induced PNN degradation is prevented and ocular dominance (OD) plasticity attenuated (Kelly et al., 2015), findings mirrored in adult mice in the context of light reintroduction-induced plasticity following dark exposure (Murase et al., 2017). Additionally, genetic reduction (e.g. haploinsufficiency) (Wen et al., 2018a) of MMP-9 as well as MMP-2/9 inhibitor treatment (Pirbhoy et al., 2020) restores developmental PNN impairments in *Fmr1* knockout mice, a model of Fragile X Syndrome; interestingly, MMP-2/9 inhibitor treatment also enhances WT PNN formation in the developing auditory cortex (Pirbhoy et al., 2020). Of course, other MMPs may also play a role in brain ECM remodeling, as suggested by microglial *Mmp14* upregulation following treatment with IL-33, which endogenously promotes ECM clearance and dendritic spine formation (Nguyen et al., 2020). Corroborating this, we also independently identified *Mmp14* upregulation in CSF1R+/- mice, a model of leukoencephalopathy and microglial dyshomeostasis, and confirmed its capacity to degrade PNNs via *in vivo* injection of recombinant MMP-14 (Arreola et al., in revision).

In addition to MMPs, microglia can also express ADAMTS-4 (Hamel et al., 2005; Lemarchant et al., 2013; Nguyen et al., 2020), which cleaves aggrecan (Tortorella et al., 1999) and brevican (Nakamura et al., 2000) at sites distinct from MMPs and also, unlike MMPs, degrades CSPGs without affecting laminin (Cua et al., 2013). Furthermore, the effects of MMP-2 and ADAMTS-4 are additive in degrading brevican (Nakamura et al., 2000), which may offer one plausible explanation for the ability of exogenous ADAMTS-4 to degrade PNNs in amyotrophic lateral sclerosis model $SOD1^{G93A}$ mice, where PNN breakdown had already occurred, but not WT mice (Fang et al., 2010; Lemarchant et al., 2016). Microglial cathepsins also represent prime candidates in brain ECM turnover. Canonically localized to and functioning within the endolysosomal pathway to degrade proteins in bulk, several secreted cathepsins exist, including cathepsins S (CTSS) and B (CTSB) (Nakanishi, 2003, 2020). CTSB is secreted by microglia following LPS activation (Ryan et al., 1995) as is CTSS, which is also upregulated by brain lesion injury (Petanceska et al., 1996) and in bulk tissue of 5xFAD mice where we have reported PNN deficits (hippocampus, cortex) (Crapser et al., 2020; Spangenberg et al., 2019); it should be noted in the latter case that we did not observe significant upregulation of any *Mmp* genes in any regions examined (Spangenberg et al., 2019). We find that *Ctss* expression in the brain most closely follows the kinetics of microglial elimination and repopulation (Najafi et al., 2018), which increases (Crapser et al., 2019; Crapser et al., 2020; Liu et al., 2021) and normalizes (Hohsfield et al., 2021) PNN density respectively, and indeed its transcripts are consistently absent in microglia-depleted brains across our studies (Crapser et al., 2019; Hohsfield et al., 2021; Najafi et al., 2018; Spangenberg et al., 2019). CTSS is functionally stable at the neutral pH of the extracellular space, and in such

conditions can efficiently degrade CSPGs neurocan and phosphacan where CTSB at several-fold greater concentrations could not (Petanceska et al., 1996). Further supporting the plausibility of CTSS-based ECM remodeling in particular, $CTSS^{-/-}$ mice display ameliorated tenascin-R reduction following facial nerve axotomy (Hao et al., 2007), which induces CTSS (but not CTSB) upregulation at the protein and mRNA levels, and incubation of mouse brain sections with CTSS eliminates WFA^{+} PNNs (Pantazopoulos et al., 2020).

These proteases are implicated in remodeling of not only the ECM, but synapses as well (Gottschall and Howell, 2015; Huntley, 2012; Nakanishi, 2020). This may underscore the functional relationship between the two structures – to sculpt synapses, an increasingly salient role of microglia, presumably the matrix in which they are embedded would also have to be restructured. Ongoing research continues to elucidate the bidirectional interactions between ECM and synapses, but the involvement of microglia in this process has just begun to be examined (Nguyen et al., 2020). The thorough monitoring of the CNS parenchyma by microglia (Nimmerjahn et al., 2005) aptly positions these cells to respond rapidly to changes in the synaptic microenvironment. In the healthy brain, they interact with pre- and post-synaptic compartments, perisynaptic astrocytes, and the local extracellular milieu (Schafer et al., 2013; Tremblay et al., 2010; Tremblay et al., 2012; Wake et al., 2009). This has so far been best studied during development when microglia prune excess synapses (Paolicelli et al., 2011; Schafer et al., 2012) to promote the removal of extra-numerous or weak synapses in the refinement of neuronal networks (Frost and Schafer, 2016; Schafer and Stevens, 2015). Accumulating evidence has implicated traditionally immune-associated molecules as critical elements in synaptic

refinement. For example, complement cascade elements (e.g. C1q and C3) localize to synaptic compartments to tag synapses for elimination (Bialas and Stevens, 2013; Linnartz et al., 2012; Stevens et al., 2007) inducing phagocytosis by complement receptor 3 (CR3)-expressing microglia in a neural activity-dependent manner (Schafer et al., 2012). On the other hand, genetic loss of CX3CR1, a receptor primarily expressed by microglia in the brain, is also associated with synaptic pruning deficits, resulting in an excess of dendritic spines, immature synapses, and immature brain circuity in development (Basilico et al., 2019; Hoshiko et al., 2012; Paolicelli et al., 2011) that persists as impaired synaptic transmission and functional brain connectivity in the adult (Zhan et al., 2014).

Microglia can also induce synapse formation, as shown by the addition of developing microglia to cultured hippocampal neurons *in vitro*, which increases dendritic spines and excitatory and inhibitory synapses via microglial IL-10 (Lim et al., 2013). While this process did not require direct microglial contact, a recent study utilizing *in vivo* two-photon imaging of early postnatal (P8-P10) mouse brains observed microglial contact-induced filopodia formation on dendrites, which was reduced following minocycline treatment (Miyamoto et al., 2016). Decreased dendritic spine densities were observed in the same study following microglial depletion (Miyamoto et al., 2016) that resembled the reduced spine formation reported by another group under similar circumstances (Parkhurst et al., 2013). However, caution must be taken regarding the interpretation of this result, as both studies utilized diphtheria toxin-based models of microglial ablation, which are associated with inflammation (e.g. upregulation of TNF-α, IL-1β (Bruttger et al., 2015) or an interferon response (Rubino et al., 2018)) that is not seen with genetic- or inhibitor-based models

due to the manner in which microglial death is achieved (Green et al., 2020). Accordingly, IL-1β attenuates synaptic formation induced by IL-10 (Lim et al., 2013) and postnatal CSF1R inhibitor-based microglial depletion instead results in excess synapses (Milinkeviciute et al., 2019) that are normalized following microglial repopulation (Milinkeviciute et al., 2021). Interestingly, loss of CSPG-5 (neuroglycan C), which normally localizes to the perisynaptic space (Pintér et al., 2020), results in impaired presynaptic maturation as well as synaptic elimination that occurs earlier than normal in cerebellar Purkinje cells (Jüttner et al., 2013), which microglia survey and regulate (Kana et al., 2019; Marín-Teva et al., 2004; Nakayama et al., 2018; Stowell et al., 2018). As early developmental synaptic deficits are observed in other brain regions with CSPG-5 deficiency (Ju¨ttner et al., 2005), together this suggests a role for perisynaptic matrix remodeling during synaptic pruning and maturation.

It is perhaps no coincidence that PNNs begin forming in development soon after synaptic pruning is completed by microglia (Paolicelli et al., 2011; Schafer et al., 2012; Stevens et al., 2007), ~P14 in mouse cortex (finished by P40) and earlier in subcortical regions (Brückner et al., 2000; Carulli et al., 2010), which would place them in ideal positions to guide PNN formation around newly refined synapses e.g. through phagocytosis and/or controlled enzymatic degradation. MMP-2/9 inhibitor treatment enhances basal PNN density in postnatal mice, indicating that protease activity is indeed a limiting factor in their developmental construction (Pirbhoy et al., 2020). Furthermore, formation of adult levels of PNNs around visual cortical neurons by the end of the critical period restricts OD plasticity (Pizzorusso et al., 2002), such that their ablation in the adult restores OD plasticity (Carulli et al., 2010; Lensjø et al., 2017b; Pizzorusso et al., 2002; Rowlands et

al., 2018), and the loss of microglial P2RY12 (Sipe et al., 2016) (but not CX3CR1 (Schecter et al., 2017)) or microglia themselves with CSF1R inhibition (Ma et al., 2020) prevents normal OD plasticity altogether. Therefore, we postulate that the absence of OD plasticity following such microglial loss-of-function may be due to their consequent failure to sculpt PNNs, which may form prematurely in these instances. Interestingly, synaptic elimination in the barrel cortex following developmental whisker trimming – which also specifically reduces barrel cortex PNNs (McRae et al., 2007) – requires CX3CR1 (Gunner et al., 2019), while neither CX3CR1 (Schecter et al., 2017) nor C1q (Welsh et al., 2020) appear necessary for monocular deprivation-induced OD plasticity or related visual cortex synaptic remodeling. Thus, microglial mechanisms of synaptic sculpting are context-dependent, and this may also be the case for the regulation of nearby ECM.

Future studies should investigate to what extent microglia and the microglial proteome are involved in regulating PNN formation during critical period closure, and how this may relate to synaptic pruning. This could be done via developmental or critical period CSF1R inhibition to determine whether PNNs appear earlier and further delineated with a more specific approach (e.g. protease inhibitors) to determine exactly how microglia influence this process. Similar experimental paradigms may be applied to study interactions between microglia, PNNs, and synapses in the homeostatic adult brain and in disease, which could also be extended to include alterations in perisynaptic ECM, so that we may begin to define and better understand the general relationship between microglia and synaptic changes as they relate to the interfacing brain ECM.

References:

(1993). A novel gene containing a trinucleotide repeat that is expanded and unstable on Huntington's disease chromosomes. The Huntington's Disease Collaborative Research Group. Cell *72*, 971-983.
(2017). Developmental alterations in Huntington's disease neural cells and pharmacological rescue in cells and mice. Nature neuroscience *20*, 648-660.
Acharya, M.M., Green, K.N., Allen, B.D., Najafi, A.R., Syage, A., Minasyan, H., Le, M.T., Kawashita, T., Giedzinski, E., Parihar, V.K.*, et al.* (2016). Elimination of microglia improves cognitive function following cranial irradiation. Scientific Reports *6*.
Ali, F., Baringer, S.L., Neal, A., Choi, E.Y., and Kwan, A.C. (2019). Parvalbumin-Positive Neuron Loss and Amyloid-β Deposits in the Frontal Cortex of Alzheimer's Disease-Related Mice. Journal of Alzheimer's Disease *72*, 1323-1339.
Anderson, M.A., Burda, J.E., Ren, Y., Ao, Y., O'Shea, T.M., Kawaguchi, R., Coppola, G., Khakh, B.S., Deming, T.J., and Sofroniew, M.V. (2016). Astrocyte scar formation aids central nervous system axon regeneration. Nature *532*, 195-200.
Asai, H., Ikezu, S., Tsunoda, S., Medalla, M., Luebke, J., Haydar, T., Wolozin, B., Butovsky, O., Kugler, S., and Ikezu, T. (2015). Depletion of microglia and inhibition of exosome synthesis halt tau propagation. Nature neuroscience *18*, 1584-1593.
Baig, S., Wilcock, G.K., and Love, S. (2005). Loss of perineuronal net N-acetylgalactosamine in Alzheimer's disease. Acta Neuropathologica *110*, 393-401.
Balmer, T.S. (2016). Perineuronal Nets Enhance the Excitability of Fast-Spiking Neurons. eneuro *3*, ENEURO.0112-0116.2016.
Banerjee, S.B., Gutzeit, V.A., Baman, J., Aoued, H.S., Doshi, N.K., Liu, R.C., and Ressler, K.J. (2017). Perineuronal Nets in the Adult Sensory Cortex Are Necessary for Fear Learning. Neuron *95*, 169-179.e163.
Barclay, J., Balaguero, N., Mione, M., Ackerman, S.L., Letts, V.A., Brodbeck, J., Canti, C., Meir, A., Page, K.M., Kusumi, K.*, et al.* (2001). Ducky mouse phenotype of epilepsy and ataxia is associated with mutations in the Cacna2d2 gene and decreased calcium channel current in cerebellar Purkinje cells. The Journal of neuroscience : the official journal of the Society for Neuroscience *21*, 6095-6104.
Basilico, B., Pagani, F., Grimaldi, A., Cortese, B., Di Angelantonio, S., Weinhard, L., Gross, C., Limatola, C., Maggi, L., and Ragozzino, D. (2019). Microglia shape presynaptic properties at developing glutamatergic synapses. Glia *67*, 53-67.
Bekku, Y., Saito, M., Moser, M., Fuchigami, M., Maehara, A., Nakayama, M., Kusachi, S., Ninomiya, Y., and Oohashi, T. (2012). Bral2 is indispensable for the proper localization of brevican and the structural integrity of the perineuronal net in the brainstem and cerebellum. Journal of Comparative Neurology *520*, 1721-1736.
Bekku, Y., Vargová, L., Goto, Y., Vorísek, I., Dmytrenko, L., Narasaki, M., Ohtsuka, A., Fässler, R., Ninomiya, Y., Syková, E.*, et al.* (2010). Bral1: Its Role in Diffusion Barrier Formation and Conduction Velocity in the CNS. The Journal of Neuroscience *30*, 3113-3123.
Belichenko, P.V., Miklossy, J., Belser, B., Budka, H., and Celio, M.R. (1999). Early destruction of the extracellular matrix around parvalbumin-immunoreactive interneurons in Creutzfeldt-Jakob disease. Neurobiology of disease *6*, 269-279.
Belichenko, P.V., Miklossy, J., and Celio, M.R. (1997). HIV-I Induced Destruction of Neocortical Extracellular Matrix Components in AIDS Victims. Neurobiology of disease *4*, 301-310.
Bellver-Landete, V., Bretheau, F., Mailhot, B., Vallieres, N., Lessard, M., Janelle, M.E., Vernoux, N., Tremblay, M.E., Fuehrmann, T., Shoichet, M.S.*, et al.* (2019). Microglia are an essential component of the neuroprotective scar that forms after spinal cord injury. Nature communications *10*, 518.
Bennett, E.J., Shaler, T.A., Woodman, B., Ryu, K.Y., Zaitseva, T.S., Becker, C.H., Bates, G.P., Schulman, H., and Kopito, R.R. (2007). Global changes to the ubiquitin system in Huntington's disease. Nature *448*, 704-708.
Bennett, F.C., Bennett, M.L., Yaqoob, F., Mulinyawe, S.B., Grant, G.A., Hayden Gephart, M., Plowey, E.D., and Barres, B.A. (2018). A Combination of Ontogeny and CNS Environment Establishes Microglial Identity. Neuron *98*, 1170-1183.e1178.
Benraiss, A., Wang, S., Herrlinger, S., Li, X., Chandler-Militello, D., Mauceri, J., Burm, H.B., Toner, M., Osipovitch, M., Jim Xu, Q.*, et al.* (2016). Human glia can both induce and rescue aspects of disease phenotype in Huntington disease. Nature communications *7*, 11758.
Bialas, A.R., and Stevens, B. (2013). TGF-β signaling regulates neuronal C1q expression and developmental synaptic refinement. Nature Neuroscience *16*, 1773-1782.

Bikbaev, A., Frischknecht, R., and Heine, M. (2015). Brain extracellular matrix retains connectivity in neuronal networks. Scientific Reports *5*, 14527.
Bitanihirwe, B.K.Y., and Woo, T.-U.W. (2014). Perineuronal nets and schizophrenia: The importance of neuronal coatings. Neuroscience & Biobehavioral Reviews *45*, 85-99.
Biundo, F., Chitu, V., Shlager, G.G.L., Park, E.S., Gulinello, M.E., Saha, K., Ketchum, H.C., Fernandes, C., Gökhan, Ş., Mehler, M.F.*, et al.* (2021). Microglial reduction of colony stimulating factor-1 receptor expression is sufficient to confer adult onset leukodystrophy. Glia *69*, 779-791.
Blosa, M., Sonntag, M., Brückner, G., Jäger, C., Seeger, G., Matthews, R.T., Rübsamen, R., Arendt, T., and Morawski, M. (2013). Unique features of extracellular matrix in the mouse medial nucleus of trapezoid body – Implications for physiological functions. Neuroscience *228*, 215-234.
Blosa, M., Sonntag, M., Jäger, C., Weigel, S., Seeger, J., Frischknecht, R., Seidenbecher, C.I., Matthews, R.T., Arendt, T., Rübsamen, R.*, et al.* (2015). The extracellular matrix molecule brevican is an integral component of the machinery mediating fast synaptic transmission at the calyx of Held. The Journal of Physiology *593*, 4341-4360.
Blum, D., Chern, Y., Domenici, M.R., Buee, L., Lin, C.Y., Rea, W., Ferre, S., and Popoli, P. (2018). The Role of Adenosine Tone and Adenosine Receptors in Huntington's Disease. Journal of caffeine and adenosine research *8*, 43-58.
Boggio, E.M., Ehlert, E.M., Lupori, L., Moloney, E.B., De Winter, F., Vander Kooi, C.W., Baroncelli, L., Mecollari, V., Blits, B., Fawcett, J.W.*, et al.* (2019). Inhibition of Semaphorin3A Promotes Ocular Dominance Plasticity in the Adult Rat Visual Cortex. Mol Neurobiol *56*, 5987-5997.
Borner, R., Bento-Torres, J., Souza, D.R., Sadala, D.B., Trevia, N., Farias, J.A., Lins, N., Passos, A., Quintairos, A., Diniz, J.A.*, et al.* (2011). Early behavioral changes and quantitative analysis of neuropathological features in murine prion disease: stereological analysis in the albino Swiss mice model. Prion *5*, 215-227.
Bozzelli, P.L., Caccavano, A., Avdoshina, V., Mocchetti, I., Wu, J.Y., and Conant, K. (2020). Increased matrix metalloproteinase levels and perineuronal net proteolysis in the HIV-infected brain; relevance to altered neuronal population dynamics. Exp Neurol *323*, 113077.
Bradbury, E.J., and Burnside, E.R. (2019). Moving beyond the glial scar for spinal cord repair. Nature Communications *10*, 3879.
Brakebusch, C., Seidenbecher, C.I., Asztely, F., Rauch, U., Matthies, H., Meyer, H., Krug, M., Böckers, T.M., Zhou, X., Kreutz, M.R.*, et al.* (2002). Brevican-Deficient Mice Display Impaired Hippocampal CA1 Long-Term Potentiation but Show No Obvious Deficits in Learning and Memory. Molecular and Cellular Biology *22*, 7417-7427.
Brewton, D.H., Kokash, J., Jimenez, O., Pena, E.R., and Razak, K.A. (2016). Age-Related Deterioration of Perineuronal Nets in the Primary Auditory Cortex of Mice. Frontiers in aging neuroscience *8*, 270.
Brückner, G., Grosche, J., Schmidt, S., Härtig, W., Margolis, R.U., Delpech, B., Seidenbecher, C.I., Czaniera, R., and Schachner, M. (2000). Postnatal development of perineuronal nets in wild-type mice and in a mutant deficient in tenascin-R. Journal of Comparative Neurology *428*, 616-629.
Brückner, G., Hausen, D., Härtig, W., Drlicek, M., Arendt, T., and Brauer, K. (1999). Cortical areas abundant in extracellular matrix chondroitin sulphate proteoglycans are less affected by cytoskeletal changes in Alzheimer's disease. Neuroscience *92*, 791-805.
Brückner, G., Morawski, M., and Arendt, T. (2008). Aggrecan-based extracellular matrix is an integral part of the human basal ganglia circuit. Neuroscience *151*, 489-504.
Bruttger, J., Karram, K., Wortge, S., Regen, T., Marini, F., Hoppmann, N., Klein, M., Blank, T., Yona, S., Wolf, Y.*, et al.* (2015). Genetic Cell Ablation Reveals Clusters of Local Self-Renewing Microglia in the Mammalian Central Nervous System. Immunity *43*, 92-106.
Bukalo, O., Schachner, M., and Dityatev, A. (2001). Modification of extracellular matrix by enzymatic removal of chondroitin sulfate and by lack of tenascin-R differentially affects several forms of synaptic plasticity in the hippocampus. Neuroscience *104*, 359-369.
Bush, T.G., Puvanachandra, N., Horner, C.H., Polito, A., Ostenfeld, T., Svendsen, C.N., Mucke, L., Johnson, M.H., and Sofroniew, M.V. (1999). Leukocyte Infiltration, Neuronal Degeneration, and Neurite Outgrowth after Ablation of Scar-Forming, Reactive Astrocytes in Adult Transgenic Mice. Neuron *23*, 297-308.
Buskila, Y., Crowe, S.E., and Ellis-Davies, G.C.R. (2013). Synaptic deficits in layer 5 neurons precede overt structural decay in 5xFAD mice. Neuroscience *254*, 152-159.
Cabrera, J.R., and Lucas, J.J. (2017). MAP2 Splicing is Altered in Huntington's Disease. Brain pathology (Zurich, Switzerland) *27*, 181-189.
Cabungcal, J.H., Steullet, P., Morishita, H., Kraftsik, R., Cuenod, M., Hensch, T.K., and Do, K.Q. (2013). Perineuronal nets protect fast-spiking interneurons against oxidative stress. Proceedings of the National Academy of Sciences of the United States of America *110*, 9130-9135.

Cardoso, F.L., Herz, J., Fernandes, A., Rocha, J., Sepodes, B., Brito, M.A., McGavern, D.B., and Brites, D. (2015). Systemic inflammation in early neonatal mice induces transient and lasting neurodegenerative effects. Journal of neuroinflammation *12*, 82.
Carstens, K.E., Phillips, M.L., Pozzo-Miller, L., Weinberg, R.J., and Dudek, S.M. (2016). Perineuronal Nets Suppress Plasticity of Excitatory Synapses on CA2 Pyramidal Neurons. The Journal of Neuroscience *36*, 6312-6320.
Carulli, D., Broersen, R., de Winter, F., Muir, E.M., Mešković, M., de Waal, M., de Vries, S., Boele, H.-J., Canto, C.B., De Zeeuw, C.I.*, et al.* (2020). Cerebellar plasticity and associative memories are controlled by perineuronal nets. Proceedings of the National Academy of Sciences *117*, 6855-6865.
Carulli, D., Pizzorusso, T., Kwok, J.C.F., Putignano, E., Poli, A., Forostyak, S., Andrews, M.R., Deepa, S.S., Glant, T.T., and Fawcett, J.W. (2010). Animals lacking link protein have attenuated perineuronal nets and persistent plasticity. Brain : a journal of neurology *133*, 2331-2347.
Casali, B.T., MacPherson, K.P., Reed-Geaghan, E.G., and Landreth, G.E. (2020). Microglia depletion rapidly and reversibly alters amyloid pathology by modification of plaque compaction and morphologies. Neurobiology of disease *142*, 104956.
Cattaud, V., Bezzina, C., Rey, C.C., Lejards, C., Dahan, L., and Verret, L. (2018). Early disruption of parvalbumin expression and perineuronal nets in the hippocampus of the Tg2576 mouse model of Alzheimer's disease can be rescued by enriched environment. Neurobiology of Aging *72*, 147-158.
Chang, K.H., Wu, Y.R., Chen, Y.C., and Chen, C.M. (2015). Plasma inflammatory biomarkers for Huntington's disease patients and mouse model. Brain, behavior, and immunity *44*, 121-127.
Chen, M., Ona, V.O., Li, M., Ferrante, R.J., Fink, K.B., Zhu, S., Bian, J., Guo, L., Farrell, L.A., Hersch, S.M.*, et al.* (2000). Minocycline inhibits caspase-1 and caspase-3 expression and delays mortality in a transgenic mouse model of Huntington disease. Nature medicine *6*, 797.
Chitu, V., Gokhan, S., Gulinello, M., Branch, C.A., Patil, M., Basu, R., Stoddart, C., Mehler, M.F., and Stanley, E.R. (2015). Phenotypic characterization of a Csf1r haploinsufficient mouse model of adult-onset leukodystrophy with axonal spheroids and pigmented glia (ALSP). Neurobiology of disease *74*, 219-228.
Christensen, A.C., Lensjø, K.K., Lepperød, M.E., Dragly, S.-A., Sutterud, H., Blackstad, J.S., Fyhn, M., and Hafting, T. (2021). Perineuronal nets stabilize the grid cell network. Nature Communications *12*, 253.
Ciammola, A., Sassone, J., Alberti, L., Meola, G., Mancinelli, E., Russo, M.A., Squitieri, F., and Silani, V. (2006). Increased apoptosis, huntingtin inclusions and altered differentiation in muscle cell cultures from Huntington's disease subjects. Cell Death & Differentiation *13*, 2068-2078.
Cingolani, L.A., Thalhammer, A., Yu, L.M., Catalano, M., Ramos, T., Colicos, M.A., and Goda, Y. (2008). Activity-dependent regulation of synaptic AMPA receptor composition and abundance by beta3 integrins. Neuron *58*, 749-762.
Clarke, L.E., Liddelow, S.A., Chakraborty, C., Münch, A.E., Heiman, M., and Barres, B.A. (2018). Normal aging induces A1-like astrocyte reactivity. Proceedings of the National Academy of Sciences *115*, E1896-E1905.
Crapser, J.D., Ochaba, J., Soni, N., Reidling, J.C., Thompson, L.M., and Green, K.N. (2019). Microglial depletion prevents extracellular matrix changes and striatal volume reduction in a model of Huntington's disease. Brain : a journal of neurology *143*, 266-288.
Crapser, J.D., Spangenberg, E.E., Barahona, R.A., Arreola, M.A., Hohsfield, L.A., and Green, K.N. (2020). Microglia facilitate loss of perineuronal nets in the Alzheimer's disease brain. EBioMedicine *58*, 102919.
Cronk, J.C., Filiano, A.J., Louveau, A., Marin, I., Marsh, R., Ji, E., Goldman, D.H., Smirnov, I., Geraci, N., Acton, S.*, et al.* (2018). Peripherally derived macrophages can engraft the brain independent of irradiation and maintain an identity distinct from microglia. The Journal of Experimental Medicine *215*, 1627-1647.
Cross, A.K., and Woodroofe, M.N. (1999). Chemokine modulation of matrix metalloproteinase and TIMP production in adult rat brain microglia and a human microglial cell line in vitro. Glia *28*, 183-189.
Crotti, A., Benner, C., Kerman, B., Gosselin, D., Lagier-Tourenne, C., Zuccato, C., Cattaneo, E., Gage, F., Cleveland, D., and Glass, C. (2014). Mutant Huntingtin promotes autonomous microglia activation via myeloid lineage-determining factors. Nature neuroscience *17*, 513-521.
Crotti, A., and Glass, C.K. (2015). The choreography of neuroinflammation in Huntington's disease. Trends in immunology *36*, 364-373.
Cua, R.C., Lau, L.W., Keough, M.B., Midha, R., Apte, S.S., and Yong, V.W. (2013). Overcoming neurite-inhibitory chondroitin sulfate proteoglycans in the astrocyte matrix. Glia *61*, 972-984.
Dagher, N.N., Najafi, A.R., Kayala, K.M., Elmore, M.R., White, T.E., Medeiros, R., West, B.L., and Green, K.N. (2015). Colony-stimulating factor 1 receptor inhibition prevents microglial plaque association and improves cognition in 3xTg-AD mice. Journal of neuroinflammation *12*, 139.

Dai, X.M., Ryan, G.R., Hapel, A.J., Dominguez, M.G., Russell, R.G., Kapp, S., Sylvestre, V., and Stanley, E.R. (2002). Targeted disruption of the mouse colony-stimulating factor 1 receptor gene results in osteopetrosis, mononuclear phagocyte deficiency, increased primitive progenitor cell frequencies, and reproductive defects. Blood *99*, 111-120.
Davies, S.J., Goucher, D.R., Doller, C., and Silver, J. (1999). Robust regeneration of adult sensory axons in degenerating white matter of the adult rat spinal cord. The Journal of neuroscience : the official journal of the Society for Neuroscience *19*, 5810-5822.
Davies, S.J.A., Fitch, M.T., Memberg, S.P., Hall, A.K., Raisman, G., and Silver, J. (1997). Regeneration of adult axons in white matter tracts of the central nervous system. Nature *390*, 680-683.
de Vivo, L., Landi, S., Panniello, M., Baroncelli, L., Chierzi, S., Mariotti, L., Spolidoro, M., Pizzorusso, T., Maffei, L., and Ratto, G.M. (2013). Extracellular matrix inhibits structural and functional plasticity of dendritic spines in the adult visual cortex. Nature Communications *4*, 1484.
Deepa, S.S., Carulli, D., Galtrey, C., Rhodes, K., Fukuda, J., Mikami, T., Sugahara, K., and Fawcett, J.W. (2006). Composition of Perineuronal Net Extracellular Matrix in Rat Brain: A DIFFERENT DISACCHARIDE COMPOSITION FOR THE NET-ASSOCIATED PROTEOGLYCANS* *The work at Cambridge University was supported by the Wellcome Trust, the UK Medical Research Council, the Christopher Reeve Foundation, and the Henry Smith Charity. The work at Kobe Pharmaceutical University was supported in part by HAITEKU from the Japan Private School Promotion Foundation, Core Research for Evolutional Science and Technology (CREST) of the Japan Science and Technology (JST) Corporation, and grantsin-aid for Scientific Research from the Ministry of Education, Science, Culture, and Sports of Japan (MEXT). The costs of publication of this article were defrayed in part by the payment of page charges. This article must therefore be hereby marked “advertisement” in accordance with 18 U.S.C. Section 1734 solely to indicate this fact. Journal of Biological Chemistry *281*, 17789-17800.
DeWitt, D.A., Richey, P.L., Praprotnik, D., Silver, J., and Perry, G. (1994). Chondroitin sulfate proteoglycans are a common component of neuronal inclusions and astrocytic reaction in neurodegenerative diseases. Brain research *656*, 205-209.
DeWitt, D.A., Silver, J., Canning, D.R., and Perry, G. (1993). Chondroitin Sulfate Proteoglycans Are Associated with the Lesions of Alzheimer's Disease. Experimental Neurology *121*, 149-152.
Dityatev, A., Brückner, G., Dityateva, G., Grosche, J., Kleene, R., and Schachner, M. (2007). Activity-dependent formation and functions of chondroitin sulfate-rich extracellular matrix of perineuronal nets. Developmental Neurobiology *67*, 570-588.
Dityatev, A., and Schachner, M. (2003). Extracellular matrix molecules and synaptic plasticity. Nature Reviews Neuroscience *4*, 456-468.
Dityatev, A., Seidenbecher, C.I., and Schachner, M. (2010). Compartmentalization from the outside: the extracellular matrix and functional microdomains in the brain. Trends Neurosci *33*, 503-512.
Dobin, A., Davis, C.A., Schlesinger, F., Drenkow, J., Zaleski, C., Jha, S., Batut, P., Chaisson, M., and Gingeras, T.R. (2013). STAR: ultrafast universal RNA-seq aligner. Bioinformatics (Oxford, England) *29*, 15-21.
Dodds, L., Chen, J., Berggren, K., and Fox, J. (2014). Characterization of Striatal Neuronal Loss and Atrophy in the R6/2 Mouse Model of Huntington's Disease. PLoS currents *6*.
Duyao, M., Ambrose, C., Myers, R., Novelletto, A., Persichetti, F., Frontali, M., Folstein, S., Ross, C., Franz, M., Abbott, M.*, et al.* (1993). Trinucleotide repeat length instability and age of onset in Huntington's disease. Nature genetics *4*, 387-392.
Dzwonek, J., and Wilczynski, G.M. (2015). CD44: molecular interactions, signaling and functions in the nervous system. Frontiers in cellular neuroscience *9*, 175.
Dzyubenko, E., Manrique-Castano, D., Kleinschnitz, C., Faissner, A., and Hermann, D.M. (2018). Topological remodeling of cortical perineuronal nets in focal cerebral ischemia and mild hypoperfusion. Matrix Biology *74*, 121-132.
Elmore, M.R., Lee, R.J., West, B.L., and Green, K.N. (2015). Characterizing newly repopulated microglia in the adult mouse: impacts on animal behavior, cell morphology, and neuroinflammation. PloS one *10*, e0122912.
Elmore, M.R., Najafi, A.R., Koike, M.A., Dagher, N.N., Spangenberg, E.E., Rice, R.A., Kitazawa, M., Matusow, B., Nguyen, H., West, B.L.*, et al.* (2014). Colony-stimulating factor 1 receptor signaling is necessary for microglia viability, unmasking a microglia progenitor cell in the adult brain. Neuron *82*, 380-397.
Elmore, M.R.P., Hohsfield, L.A., Kramár, E.A., Soreq, L., Lee, R.J., Pham, S.T., Najafi, A.R., Spangenberg, E.E., Wood, M.A., West, B.L.*, et al.* (2018). Replacement of microglia in the aged brain reverses cognitive, synaptic, and neuronal deficits in mice. Aging cell *17*, e12832.

Elshatory, Y., and Gan, L. (2008). The LIM-homeobox gene Islet-1 is required for the development of restricted forebrain cholinergic neurons. The Journal of neuroscience : the official journal of the Society for Neuroscience *28*, 3291-3297.
Endo, F., Komine, O., Fujimori-Tonou, N., Katsuno, M., Jin, S., Watanabe, S., Sobue, G., Dezawa, M., Wyss-Coray, T., and Yamanaka, K. (2015). Astrocyte-derived TGF-beta1 accelerates disease progression in ALS mice by interfering with the neuroprotective functions of microglia and T cells. Cell reports *11*, 592-604.
Erblich, B., Zhu, L., Etgen, A.M., Dobrenis, K., and Pollard, J.W. (2011). Absence of Colony Stimulation Factor-1 Receptor Results in Loss of Microglia, Disrupted Brain Development and Olfactory Deficits. PloS one *6*, e26317.
Evers, M.R., Salmen, B., Bukalo, O., Rollenhagen, A., Bösl, M.R., Morellini, F., Bartsch, U., Dityatev, A., and Schachner, M. (2002). Impairment of L-type Ca²⁺ Channel-Dependent Forms of Hippocampal Synaptic Plasticity in Mice Deficient in the Extracellular Matrix Glycoprotein Tenascin-C. The Journal of Neuroscience *22*, 7177-7194.
Faissner, A., Pyka, M., Geissler, M., Sobik, T., Frischknecht, R., Gundelfinger, E.D., and Seidenbecher, C. (2010). Contributions of astrocytes to synapse formation and maturation — Potential functions of the perisynaptic extracellular matrix. Brain Research Reviews *63*, 26-38.
Fang, L., Teuchert, M., Huber-Abel, F., Schattauer, D., Hendrich, C., Dorst, J., Zettlmeissel, H., Wlaschek, M., Scharffetter-Kochanek, K., Kapfer, T.*, et al.* (2010). MMP-2 and MMP-9 are elevated in spinal cord and skin in a mouse model of ALS. Journal of the neurological sciences *294*, 51-56.
Faulkner, J.R., Herrmann, J.E., Woo, M.J., Tansey, K.E., Doan, N.B., and Sofroniew, M.V. (2004). Reactive Astrocytes Protect Tissue and Preserve Function after Spinal Cord Injury. The Journal of Neuroscience *24*, 2143-2155.
Favuzzi, E., Marques-Smith, A., Deogracias, R., Winterflood, C.M., Sánchez-Aguilera, A., Mantoan, L., Maeso, P., Fernandes, C., Ewers, H., and Rico, B. (2017). Activity-Dependent Gating of Parvalbumin Interneuron Function by the Perineuronal Net Protein Brevican. Neuron *95*, 639-655.e610.
Fawcett, J.W., Oohashi, T., and Pizzorusso, T. (2019). The roles of perineuronal nets and the perinodal extracellular matrix in neuronal function. Nature Reviews Neuroscience *20*, 451-465.
Feng, X., Jopson, T.D., Paladini, M.S., Liu, S., West, B.L., Gupta, N., and Rosi, S. (2016). Colony-stimulating factor 1 receptor blockade prevents fractionated whole-brain irradiation-induced memory deficits. Journal of neuroinflammation *13*, 215.
Fernandez-Nogales, M., Santos-Galindo, M., Hernandez, I.H., Cabrera, J.R., and Lucas, J.J. (2016). Faulty splicing and cytoskeleton abnormalities in Huntington's disease. Brain pathology (Zurich, Switzerland) *26*, 772-778.
Ferrante, R., Kowall, N., and Richardson, E. (1991). Proliferative and degenerative changes in striatal spiny neurons in Huntington's disease: a combined study using the section-Golgi method and calbindin D28k immunocytochemistry. The Journal of Neuroscience *11*, 3877-3887.
Fidler, P.S., Schuette, K., Asher, R.A., Dobbertin, A., Thornton, S.R., Calle-Patino, Y., Muir, E., Levine, J.M., Geller, H.M., Rogers, J.H.*, et al.* (1999). Comparing astrocytic cell lines that are inhibitory or permissive for axon growth: the major axon-inhibitory proteoglycan is NG2. The Journal of neuroscience : the official journal of the Society for Neuroscience *19*, 8778-8788.
Fisher, D., Xing, B., Dill, J., Li, H., Hoang, H.H., Zhao, Z., Yang, X.-L., Bachoo, R., Cannon, S., Longo, F.M.*, et al.* (2011). Leukocyte Common Antigen-Related Phosphatase Is a Functional Receptor for Chondroitin Sulfate Proteoglycan Axon Growth Inhibitors. The Journal of Neuroscience *31*, 14051-14066.
Flanigan, T.J., Xue, Y., Kishan Rao, S., Dhanushkodi, A., and McDonald, M.P. (2014). Abnormal vibrissa-related behavior and loss of barrel field inhibitory neurons in 5xFAD transgenics. Genes, brain, and behavior *13*, 488-500.
Fowke, T.M., Karunasinghe, R.N., Bai, J.-Z., Jordan, S., Gunn, A.J., and Dean, J.M. (2017). Hyaluronan synthesis by developing cortical neurons in vitro. Scientific Reports *7*, 44135.
Franklin, S.L., Love, S., Greene, J.R., and Betmouni, S. (2008). Loss of Perineuronal Net in ME7 Prion Disease. Journal of neuropathology and experimental neurology *67*, 189-199.
Frischknecht, R., Heine, M., Perrais, D., Seidenbecher, C.I., Choquet, D., and Gundelfinger, E.D. (2009). Brain extracellular matrix affects AMPA receptor lateral mobility and short-term synaptic plasticity. Nat Neurosci *12*, 897-904.
Frischknecht, R., and Seidenbecher, C.I. (2012). Brevican: A key proteoglycan in the perisynaptic extracellular matrix of the brain. The International Journal of Biochemistry & Cell Biology *44*, 1051-1054.
Frost, J.L., and Schafer, D.P. (2016). Microglia: Architects of the Developing Nervous System. Trends Cell Biol *26*, 587-597.

Galatro, T.F., Holtman, I.R., Lerario, A.M., Vainchtein, I.D., Brouwer, N., Sola, P.R., Veras, M.M., Pereira, T.F., Leite, R.E.P., Möller, T.*, et al.* (2017). Transcriptomic analysis of purified human cortical microglia reveals age-associated changes. Nature neuroscience *20*, 1162.
Galindo, L.T., Mundim, M., Pinto, A.S., Chiarantin, G.M.D., Almeida, M.E.S., Lamers, M.L., Horwitz, A.R., Santos, M.F., and Porcionatto, M. (2018). Chondroitin Sulfate Impairs Neural Stem Cell Migration Through ROCK Activation. Mol Neurobiol *55*, 3185-3195.
Gautier, E.L., Shay, T., Miller, J., Greter, M., Jakubzick, C., Ivanov, S., Helft, J., Chow, A., Elpek, K.G., Gordonov, S.*, et al.* (2012). Gene-expression profiles and transcriptional regulatory pathways that underlie the identity and diversity of mouse tissue macrophages. Nature Immunology *13*, 1118.
Geissler, M., Gottschling, C., Aguado, A., Rauch, U., Wetzel, C.H., Hatt, H., and Faissner, A. (2013). Primary Hippocampal Neurons, Which Lack Four Crucial Extracellular Matrix Molecules, Display Abnormalities of Synaptic Structure and Function and Severe Deficits in Perineuronal Net Formation. The Journal of Neuroscience *33*, 7742-7755.
Gibson, E.M., Nagaraja, S., Ocampo, A., Tam, L.T., Wood, L.S., Pallegar, P.N., Greene, J.J., Geraghty, A.C., Goldstein, A.K., Ni, L.*, et al.* (2019). Methotrexate Chemotherapy Induces Persistent Tri-glial Dysregulation that Underlies Chemotherapy-Related Cognitive Impairment. Cell *176*, 43-55.e13.
Ginhoux, F., Greter, M., Leboeuf, M., Nandi, S., See, P., Gokhan, S., Mehler, M.F., Conway, S.J., Ng, L.G., Stanley, E.R.*, et al.* (2010). Fate mapping analysis reveals that adult microglia derive from primitive macrophages. Science (New York, NY) *330*, 841-845.
Ginhoux, F., and Guilliams, M. (2016). Tissue-Resident Macrophage Ontogeny and Homeostasis. Immunity *44*, 439-449.
Gogolla, N., Caroni, P., Lüthi, A., and Herry, C. (2009). Perineuronal Nets Protect Fear Memories from Erasure. Science *325*, 1258-1261.
Goldmann, T., Zeller, N., Raasch, J., Kierdorf, K., Frenzel, K., Ketscher, L., Basters, A., Staszewski, O., Brendecke, S.M., Spiess, A.*, et al.* (2015). USP18 lack in microglia causes destructive interferonopathy of the mouse brain. The EMBO journal *34*, 1612-1629.
Gomez Perdiguero, E., Klapproth, K., Schulz, C., Busch, K., Azzoni, E., Crozet, L., Garner, H., Trouillet, C., de Bruijn, M.F., Geissmann, F.*, et al.* (2015). Tissue-resident macrophages originate from yolk-sac-derived erythro-myeloid progenitors. Nature *518*, 547-551.
Gottschall, P.E., and Howell, M.D. (2015). ADAMTS expression and function in central nervous system injury and disorders. Matrix Biology *44-46*, 70-76.
Gottschling, C., Wegrzyn, D., Denecke, B., and Faissner, A. (2019). Elimination of the four extracellular matrix molecules tenascin-C, tenascin-R, brevican and neurocan alters the ratio of excitatory and inhibitory synapses. Scientific Reports *9*, 13939.
Gray, E., Thomas, T.L., Betmouni, S., Scolding, N., and Love, S. (2008a). Elevated Matrix Metalloproteinase-9 and Degradation of Perineuronal Nets in Cerebrocortical Multiple Sclerosis Plaques. Journal of Neuropathology & Experimental Neurology *67*, 888-899.
Gray, M., Shirasaki, D.I., Cepeda, C., Andre, V.M., Wilburn, B., Lu, X.H., Tao, J., Yamazaki, I., Li, S.H., Sun, Y.E.*, et al.* (2008b). Full-length human mutant huntingtin with a stable polyglutamine repeat can elicit progressive and selective neuropathogenesis in BACHD mice. The Journal of neuroscience : the official journal of the Society for Neuroscience *28*, 6182-6195.
Green, K.N., Crapser, J.D., and Hohsfield, L.A. (2020). To Kill a Microglia: A Case for CSF1R Inhibitors. Trends in Immunology *41*, 771-784.
Griciuc, A., Patel, S., Federico, A.N., Choi, S.H., Innes, B.J., Oram, M.K., Cereghetti, G., McGinty, D., Anselmo, A., Sadreyev, R.I.*, et al.* (2019). TREM2 Acts Downstream of CD33 in Modulating Microglial Pathology in Alzheimer's Disease. Neuron *103*, 820-835.e827.
Groc, L., Choquet, D., Stephenson, F.A., Verrier, D., Manzoni, O.J., and Chavis, P. (2007). NMDA receptor surface trafficking and synaptic subunit composition are developmentally regulated by the extracellular matrix protein Reelin. The Journal of neuroscience : the official journal of the Society for Neuroscience *27*, 10165-10175.
Guentchev, M., Groschup, M.H., Kordek, R., Liberski, P.P., and Budka, H. (1998). Severe, Early and Selective Loss of a Subpopulation of GABAergic Inhibitory Neurons in Experimental Transmissible Spongiform Encephalopathies. Brain Pathology *8*, 615-623.
Gunner, G., Cheadle, L., Johnson, K.M., Ayata, P., Badimon, A., Mondo, E., Nagy, M.A., Liu, L., Bemiller, S.M., Kim, K.W.*, et al.* (2019). Sensory lesioning induces microglial synapse elimination via ADAM10 and fractalkine signaling. Nat Neurosci *22*, 1075-1088.

Guttenplan, K.A., Stafford, B.K., El-Danaf, R.N., Adler, D.I., Münch, A.E., Weigel, M.K., Huberman, A.D., and Liddelow, S.A. (2020a). Neurotoxic Reactive Astrocytes Drive Neuronal Death after Retinal Injury. Cell Reports *31*, 107776.
Guttenplan, K.A., Weigel, M.K., Adler, D.I., Couthouis, J., Liddelow, S.A., Gitler, A.D., and Barres, B.A. (2020b). Knockout of reactive astrocyte activating factors slows disease progression in an ALS mouse model. Nature Communications *11*, 3753.
Hagemeyer, N., Hanft, K.M., Akriditou, M.A., Unger, N., Park, E.S., Stanley, E.R., Staszewski, O., Dimou, L., and Prinz, M. (2017). Microglia contribute to normal myelinogenesis and to oligodendrocyte progenitor maintenance during adulthood. Acta neuropathologica *134*, 441-458.
Hamel, M.G., Mayer, J., and Gottschall, P.E. (2005). Altered production and proteolytic processing of brevican by transforming growth factor β in cultured astrocytes. Journal of Neurochemistry *93*, 1533-1541.
Hammond, T.R., Dufort, C., Dissing-Olesen, L., Giera, S., Young, A., Wysoker, A., Walker, A.J., Gergits, F., Segel, M., Nemesh, J.*, et al.* (2019). Single-Cell RNA Sequencing of Microglia throughout the Mouse Lifespan and in the Injured Brain Reveals Complex Cell-State Changes. Immunity *50*, 253-271.e256.
Han, J., Harris, R.A., and Zhang, X.M. (2017). An updated assessment of microglia depletion: current concepts and future directions. Mol Brain *10*, 25.
Han, R.T., Kim, R.D., Molofsky, A.V., and Liddelow, S.A. (2021). Astrocyte-immune cell interactions in physiology and pathology. Immunity *54*, 211-224.
Hansson, O., Petersen, A., Leist, M., Nicotera, P., Castilho, R.F., and Brundin, P. (1999). Transgenic mice expressing a Huntington's disease mutation are resistant to quinolinic acid-induced striatal excitotoxicity. Proceedings of the National Academy of Sciences of the United States of America *96*, 8727-8732.
Hao, H.P., Doh-ura, K., and Nakanishi, H. (2007). Impairment of microglial responses to facial nerve axotomy in cathepsin S–deficient mice. Journal of Neuroscience Research *85*, 2196-2206.
Härtig, W., Mages, B., Aleithe, S., Nitzsche, B., Altmann, S., Barthel, H., Krueger, M., and Michalski, D. (2017). Damaged Neocortical Perineuronal Nets Due to Experimental Focal Cerebral Ischemia in Mice, Rats and Sheep. Frontiers in Integrative Neuroscience *11*.
Hayashi, N., Tatsumi, K., Okuda, H., Yoshikawa, M., Ishizaka, S., Miyata, S., Manabe, T., and Wanaka, A. (2007). DACS, novel matrix structure composed of chondroitin sulfate proteoglycan in the brain. Biochemical and biophysical research communications *364*, 410-415.
Heneka, M.T., Carson, M.J., Khoury, J.E., Landreth, G.E., Brosseron, F., Feinstein, D.L., Jacobs, A.H., Wyss-Coray, T., Vitorica, J., Ransohoff, R.M.*, et al.* (2015). Neuroinflammation in Alzheimer's disease. The Lancet Neurology *14*, 388-405.
Henry, R.J., Ritzel, R.M., Barrett, J.P., Doran, S.J., Jiao, Y., Leach, J.B., Szeto, G.L., Wu, J., Stoica, B.A., Faden, A.I.*, et al.* (2020). Microglial Depletion with CSF1R Inhibitor During Chronic Phase of Experimental Traumatic Brain Injury Reduces Neurodegeneration and Neurological Deficits. The Journal of Neuroscience *40*, 2960-2974.
Herrmann, J.E., Imura, T., Song, B., Qi, J., Ao, Y., Nguyen, T.K., Korsak, R.A., Takeda, K., Akira, S., and Sofroniew, M.V. (2008). STAT3 is a Critical Regulator of Astrogliosis and Scar Formation after Spinal Cord Injury. The Journal of Neuroscience *28*, 7231-7243.
Hijazi, S., Heistek, T.S., Scheltens, P., Neumann, U., Shimshek, D.R., Mansvelder, H.D., Smit, A.B., and van Kesteren, R.E. (2019). Early restoration of parvalbumin interneuron activity prevents memory loss and network hyperexcitability in a mouse model of Alzheimer's disease. Molecular Psychiatry.
Hilbig, H., Bidmon, H.-J., Steingrüber, S., Reinke, H., and Dinse, H.R. (2002). Enriched environmental conditions reverse age-dependent gliosis and losses of neurofilaments and extracellular matrix components but do not alter lipofuscin accumulation in the hindlimb area of the aging rat brain. Journal of Chemical Neuroanatomy *23*, 199-209.
Hobohm, C., Günther, A., Grosche, J., Roßner, S., Schneider, D., and Brückner, G. (2005). Decomposition and long-lasting downregulation of extracellular matrix in perineuronal nets induced by focal cerebral ischemia in rats. Journal of Neuroscience Research *80*, 539-548.
Hodges, A., Strand, A.D., Aragaki, A.K., Kuhn, A., Sengstag, T., Hughes, G., Elliston, L.A., Hartog, C., Goldstein, D.R., Thu, D.*, et al.* (2006). Regional and cellular gene expression changes in human Huntington's disease brain. Human molecular genetics *15*, 965-977.
Hoeffel, G., Chen, J., Lavin, Y., Low, D., Almeida, F.F., See, P., Beaudin, A.E., Lum, J., Low, I., Forsberg, E.C.*, et al.* (2015). C-Myb(+) erythro-myeloid progenitor-derived fetal monocytes give rise to adult tissue-resident macrophages. Immunity *42*, 665-678.
Hohsfield, L.A., Najafi, A.R., Ghorbanian, Y., Soni, N., Crapser, J.D., Figueroa Velez, D.X., Jiang, S., Royer, S.E., Kim, S.J., Anderson, A.J.*, et al.* (2021). Subventricular zone/white matter microglia reconstitute the empty adult microglial niche in a dynamic wave. bioRxiv, 2021.2002.2017.431594.

Hong, S., Beja-Glasser, V.F., Nfonoyim, B.M., Frouin, A., Li, S., Ramakrishnan, S., Merry, K.M., Shi, Q., Rosenthal, A., Barres, B.A.*, et al.* (2016). Complement and microglia mediate early synapse loss in Alzheimer mouse models. Science *352*, 712-716.
Hoshiko, M., Arnoux, I., Avignone, E., Yamamoto, N., and Audinat, E. (2012). Deficiency of the Microglial Receptor CX3CR1 Impairs Postnatal Functional Development of Thalamocortical Synapses in the Barrel Cortex. The Journal of Neuroscience *32*, 15106-15111.
Howell, M.D., Bailey, L.A., Cozart, M.A., Gannon, B.M., and Gottschall, P.E. (2015). Hippocampal administration of chondroitinase ABC increases plaque-adjacent synaptic marker and diminishes amyloid burden in aged APPswe/PS1dE9 mice. Acta Neuropathol Commun *3*, 54.
Hrabětová, S., Masri, D., Tao, L., Xiao, F., and Nicholson, C. (2009). Calcium diffusion enhanced after cleavage of negatively charged components of brain extracellular matrix by chondroitinase ABC. The Journal of Physiology *587*, 4029-4049.
Hsu, J.-Y.C., Bourguignon, L.Y.W., Adams, C.M., Peyrollier, K., Zhang, H., Fandel, T., Cun, C.L., Werb, Z., and Noble-Haeusslein, L.J. (2008). Matrix Metalloproteinase-9 Facilitates Glial Scar Formation in the Injured Spinal Cord. The Journal of Neuroscience *28*, 13467-13477.
Hu, F., Ku, M.C., Markovic, D., Dzaye, O., Lehnardt, S., Synowitz, M., Wolf, S.A., and Kettenmann, H. (2014). Glioma-associated microglial MMP9 expression is upregulated by TLR2 signaling and sensitive to minocycline. International journal of cancer *135*, 2569-2578.
Huang, Y., Happonen, K.E., Burrola, P.G., O'Connor, C., Hah, N., Huang, L., Nimmerjahn, A., and Lemke, G. (2021). Microglia use TAM receptors to detect and engulf amyloid β plaques. Nature Immunology.
Huntley, G.W. (2012). Synaptic circuit remodelling by matrix metalloproteinases in health and disease. Nature reviews Neuroscience *13*, 743-757.
Hyman, B.T., Phelps, C.H., Beach, T.G., Bigio, E.H., Cairns, N.J., Carrillo, M.C., Dickson, D.W., Duyckaerts, C., Frosch, M.P., Masliah, E.*, et al.* (2012). National Institute on Aging-Alzheimer's Association guidelines for the neuropathologic assessment of Alzheimer's disease. Alzheimer's & dementia : the journal of the Alzheimer's Association *8*, 1-13.
Iaccarino, H.F., Singer, A.C., Martorell, A.J., Rudenko, A., Gao, F., Gillingham, T.Z., Mathys, H., Seo, J., Kritskiy, O., Abdurrob, F.*, et al.* (2016). Gamma frequency entrainment attenuates amyloid load and modifies microglia. Nature *540*, 230-235.
Iadarola, N.D., Niciu, M.J., Richards, E.M., Vande Voort, J.L., Ballard, E.D., Lundin, N.B., Nugent, A.C., Machado-Vieira, R., and Zarate, C.A., Jr. (2015). Ketamine and other N-methyl-D-aspartate receptor antagonists in the treatment of depression: a perspective review. Therapeutic advances in chronic disease *6*, 97-114.
Illouz, T., Madar, R., Biragyn, A., and Okun, E. (2019). Restoring microglial and astroglial homeostasis using DNA immunization in a Down Syndrome mouse model. Brain, behavior, and immunity *75*, 163-180.
Jäger, C., Lendvai, D., Seeger, G., Brückner, G., Matthews, R.T., Arendt, T., Alpár, A., and Morawski, M. (2013). Perineuronal and perisynaptic extracellular matrix in the human spinal cord. Neuroscience *238*, 168-184.
Jansen, A.H., van Hal, M., Op den Kelder, I.C., Meier, R.T., de Ruiter, A.A., Schut, M.H., Smith, D.L., Grit, C., Brouwer, N., Kamphuis, W.*, et al.* (2017). Frequency of nuclear mutant huntingtin inclusion formation in neurons and glia is cell-type-specific. Glia *65*, 50-61.
Jawhar, S., Trawicka, A., Jenneckens, C., Bayer, T.A., and Wirths, O. (2012). Motor deficits, neuron loss, and reduced anxiety coinciding with axonal degeneration and intraneuronal Aβ aggregation in the 5XFAD mouse model of Alzheimer's disease. Neurobiology of Aging *33*, 196.e129-196.e140.
Jones, L.L., and Tuszynski, M.H. (2002). Spinal Cord Injury Elicits Expression of Keratan Sulfate Proteoglycans by Macrophages, Reactive Microglia, and Oligodendrocyte Progenitors. The Journal of Neuroscience *22*, 4611-4624.
Ju¨ttner, R., Moré, M.I., Das, D., Babich, A., Meier, J., Henning, M., Erdmann, B., Mu¨ller, E.-C., Otto, A., Grantyn, R.*, et al.* (2005). Impaired Synapse Function during Postnatal Development in the Absence of CALEB, an EGF-like Protein Processed by Neuronal Activity. Neuron *46*, 233-245.
Julien, C., Marcouiller, F., Bretteville, A., El Khoury, N.B., Baillargeon, J., Hebert, S.S., and Planel, E. (2012). Dimethyl sulfoxide induces both direct and indirect tau hyperphosphorylation. PloS one *7*, e40020.
Jüttner, R., Montag, D., Craveiro, R.B., Babich, A., Vetter, P., and Rathjen, F.G. (2013). Impaired presynaptic function and elimination of synapses at premature stages during postnatal development of the cerebellum in the absence of CALEB (CSPG5/neuroglycan C). European Journal of Neuroscience *38*, 3270-3280.
Kana, V., Desland, F.A., Casanova-Acebes, M., Ayata, P., Badimon, A., Nabel, E., Yamamuro, K., Sneeboer, M., Tan, I.-L., Flanigan, M.E.*, et al.* (2019). CSF-1 controls cerebellar microglia and is required for motor function and social interaction. Journal of Experimental Medicine *216*, 2265-2281.

Karch, C.M., Jeng, A.T., Nowotny, P., Cady, J., Cruchaga, C., and Goate, A.M. (2012). Expression of novel Alzheimer's disease risk genes in control and Alzheimer's disease brains. PloS one *7*, e50976.
Karetko-Sysa, M., Skangiel-Kramska, J., and Nowicka, D. (2011). Disturbance of perineuronal nets in the perilesional area after photothrombosis is not associated with neuronal death. Experimental Neurology *231*, 113-126.
Kast, D.J., and Dominguez, R. (2017). The Cytoskeleton-Autophagy Connection. Current biology : CB *27*, R318-r326.
Kelly, E., Russo, A., Jackson, C., Lamantia, C., and Majewska, A. (2015). Proteolytic regulation of synaptic plasticity in the mouse primary visual cortex: analysis of matrix metalloproteinase 9 deficient mice. Frontiers in Cellular Neuroscience *9*.
Keough, M.B., Rogers, J.A., Zhang, P., Jensen, S.K., Stephenson, E.L., Chen, T., Hurlbert, M.G., Lau, L.W., Rawji, K.S., Plemel, J.R.*, et al.* (2016). An inhibitor of chondroitin sulfate proteoglycan synthesis promotes central nervous system remyelination. Nature Communications *7*, 11312.
Keren-Shaul, H., Spinrad, A., Weiner, A., Matcovitch-Natan, O., Dvir-Szternfeld, R., Ulland, T.K., David, E., Baruch, K., Lara-Astaiso, D., Toth, B.*, et al.* (2017). A Unique Microglia Type Associated with Restricting Development of Alzheimer's Disease. Cell *169*, 1276-1290.e1217.
Kierdorf, K., Erny, D., Goldmann, T., Sander, V., Schulz, C., Perdiguero, E.G., Wieghofer, P., Heinrich, A., Riemke, P., Hölscher, C.*, et al.* (2013). Microglia emerge from erythromyeloid precursors via Pu.1- and Irf8-dependent pathways. Nature neuroscience *16*, 273.
Kierdorf, K., and Prinz, M. (2017). Microglia in steady state. The Journal of Clinical Investigation *127*, 3201-3209.
Kim, H.J., Cho, M.H., Shim, W.H., Kim, J.K., Jeon, E.Y., Kim, D.H., and Yoon, S.Y. (2017). Deficient autophagy in microglia impairs synaptic pruning and causes social behavioral defects. Mol Psychiatry *22*, 1576-1584.
Kobayashi, K., Emson, P.C., and Mountjoy, C.Q. (1989). Vicia villosa lectin-positive neurones in human cerebral cortex. Loss in Alzheimer-type dementia. Brain Research *498*, 170-174.
Kobayashi, K., Imagama, S., Ohgomori, T., Hirano, K., Uchimura, K., Sakamoto, K., Hirakawa, A., Takeuchi, H., Suzumura, A., Ishiguro, N.*, et al.* (2013). Minocycline selectively inhibits M1 polarization of microglia. Cell death & disease *4*, e525.
Koga, S., Kouri, N., Walton, R.L., Ebbert, M.T.W., Josephs, K.A., Litvan, I., Graff-Radford, N., Ahlskog, J.E., Uitti, R.J., van Gerpen, J.A.*, et al.* (2018). Corticobasal degeneration with TDP-43 pathology presenting with progressive supranuclear palsy syndrome: a distinct clinicopathologic subtype. Acta neuropathologica *136*, 389-404.
Könnecke, H., and Bechmann, I. (2013). The role of microglia and matrix metalloproteinases involvement in neuroinflammation and gliomas. Clin Dev Immunol *2013*, 914104-914104.
Kraft, A.D., Kaltenbach, L.S., Lo, D.C., and Harry, G.J. (2012). Activated microglia proliferate at neurites of mutant huntingtin-expressing neurons. Neurobiology of aging *33*, 621.e617-633.
Krasemann, S., Madore, C., Cialic, R., Baufeld, C., Calcagno, N., El Fatimy, R., Beckers, L., O'Loughlin, E., Xu, Y., Fanek, Z.*, et al.* (2017). The TREM2-APOE Pathway Drives the Transcriptional Phenotype of Dysfunctional Microglia in Neurodegenerative Diseases. Immunity *47*, 566-581.e569.
Kumar-Singh, S., Cras, P., Wang, R., Kros, J.M., van Swieten, J., Lübke, U., Ceuterick, C., Serneels, S., Vennekens, K., Timmermans, J.P.*, et al.* (2002). Dense-core senile plaques in the Flemish variant of Alzheimer's disease are vasocentric. The American journal of pathology *161*, 507-520.
Kurosawa, M., Matsumoto, G., Kino, Y., Okuno, M., Kurosawa-Yamada, M., Washizu, C., Taniguchi, H., Nakaso, K., Yanagawa, T., Warabi, E.*, et al.* (2015). Depletion of p62 reduces nuclear inclusions and paradoxically ameliorates disease phenotypes in Huntington's model mice. Human molecular genetics *24*, 1092-1105.
Kwok, J.C.F., Carulli, D., and Fawcett, J.W. (2010). In vitro modeling of perineuronal nets: hyaluronan synthase and link protein are necessary for their formation and integrity. Journal of Neurochemistry *114*, 1447-1459.
La Spada, A.R., and Taylor, J.P. (2010). Repeat expansion disease: progress and puzzles in disease pathogenesis. Nature reviews Genetics *11*, 247-258.
Labbadia, J., and Morimoto, R.I. (2013). Huntington's disease: underlying molecular mechanisms and emerging concepts. Trends in biochemical sciences *38*, 378-385.
Lander, C., Zhang, H., and Hockfield, S. (1998). Neurons Produce a Neuronal Cell Surface-Associated Chondroitin Sulfate Proteoglycan. The Journal of Neuroscience *18*, 174-183.
Lau, L.W., Cua, R., Keough, M.B., Haylock-Jacobs, S., and Yong, V.W. (2013). Pathophysiology of the brain extracellular matrix: a new target for remyelination. Nature Reviews Neuroscience *14*, 722-729.
Lau, L.W., Keough, M.B., Haylock-Jacobs, S., Cua, R., Döring, A., Sloka, S., Stirling, D.P., Rivest, S., and Yong, V.W. (2012). Chondroitin sulfate proteoglycans in demyelinated lesions impair remyelination. Annals of Neurology *72*, 419-432.

Lavin, Y., Winter, D., Blecher-Gonen, R., David, E., Keren-Shaul, H., Merad, M., Jung, S., and Amit, I. (2014). Tissue-resident macrophage enhancer landscapes are shaped by the local microenvironment. Cell *159*, 1312-1326.
Lee, H., Noh, J.Y., Oh, Y., Kim, Y., Chang, J.W., Chung, C.W., Lee, S.T., Kim, M., Ryu, H., and Jung, Y.K. (2012). IRE1 plays an essential role in ER stress-mediated aggregation of mutant huntingtin via the inhibition of autophagy flux. Human molecular genetics *21*, 101-114.
Lee, S.W., Park, H.J., Im, W., Kim, M., and Hong, S. (2018). Repeated immune activation with low-dose lipopolysaccharide attenuates the severity of Huntington's disease in R6/2 transgenic mice. Animal cells and systems *22*, 219-226.
Lehrman, E.K., Wilton, D.K., Litvina, E.Y., Welsh, C.A., Chang, S.T., Frouin, A., Walker, A.J., Heller, M.D., Umemori, H., Chen, C.*, et al.* (2018). CD47 Protects Synapses from Excess Microglia-Mediated Pruning during Development. Neuron *100*, 120-134.e126.
Lemarchant, S., Pomeshchik, Y., Kidin, I., Kärkkäinen, V., Valonen, P., Lehtonen, S., Goldsteins, G., Malm, T., Kanninen, K., and Koistinaho, J. (2016). ADAMTS-4 promotes neurodegeneration in a mouse model of amyotrophic lateral sclerosis. Molecular Neurodegeneration *11*, 10.
Lemarchant, S., Pruvost, M., Montaner, J., Emery, E., Vivien, D., Kanninen, K., and Koistinaho, J. (2013). ADAMTS proteoglycanases in the physiological and pathological central nervous system. Journal of neuroinflammation *10*, 133-133.
Lendvai, D., Morawski, M., Brückner, G., Négyessy, L., Baksa, G., Glasz, T., Patonay, L., Matthews, R.T., Arendt, T., and Alpár, A. (2012). Perisynaptic aggrecan-based extracellular matrix coats in the human lateral geniculate body devoid of perineuronal nets. Journal of Neuroscience Research *90*, 376-387.
Lendvai, D., Morawski, M., Négyessy, L., Gáti, G., Jäger, C., Baksa, G., Glasz, T., Attems, J., Tanila, H., Arendt, T.*, et al.* (2013). Neurochemical mapping of the human hippocampus reveals perisynaptic matrix around functional synapses in Alzheimer's disease. Acta Neuropathologica *125*, 215-229.
Lensjø, K.K., Christensen, A.C., Tennøe, S., Fyhn, M., and Hafting, T. (2017a). Differential Expression and Cell-Type Specificity of Perineuronal Nets in Hippocampus, Medial Entorhinal Cortex, and Visual Cortex Examined in the Rat and Mouse. eneuro *4*, ENEURO.0379-0316.2017.
Lensjø, K.K., Lepperød, M.E., Dick, G., Hafting, T., and Fyhn, M. (2017b). Removal of Perineuronal Nets Unlocks Juvenile Plasticity Through Network Mechanisms of Decreased Inhibition and Increased Gamma Activity. The Journal of Neuroscience *37*, 1269-1283.
Li, J.Y., Popovic, N., and Brundin, P. (2005). The use of the R6 transgenic mouse models of Huntington's disease in attempts to develop novel therapeutic strategies. NeuroRx : the journal of the American Society for Experimental NeuroTherapeutics *2*, 447-464.
Li, K.W., Hornshaw, M.P., Van der Schors, R.C., Watson, R., Tate, S., Casetta, B., Jimenez, C.R., Gouwenberg, Y., Gundelfinger, E.D., Smalla, K.-H.*, et al.* (2004). Proteomics Analysis of Rat Brain Postsynaptic Density: IMPLICATIONS OF THE DIVERSE PROTEIN FUNCTIONAL GROUPS FOR THE INTEGRATION OF SYNAPTIC PHYSIOLOGY*. Journal of Biological Chemistry *279*, 987-1002.
Li, M., Li, Z., Ren, H., Jin, W.N., Wood, K., Liu, Q., Sheth, K.N., and Shi, F.D. (2017). Colony stimulating factor 1 receptor inhibition eliminates microglia and attenuates brain injury after intracerebral hemorrhage. Journal of cerebral blood flow and metabolism : official journal of the International Society of Cerebral Blood Flow and Metabolism *37*, 2383-2395.
Li, Q., and Barres, B.A. (2018). Microglia and macrophages in brain homeostasis and disease. Nature reviews Immunology *18*, 225-242.
Li, Q., Cheng, Z., Zhou, L., Darmanis, S., Neff, N.F., Okamoto, J., Gulati, G., Bennett, M.L., Sun, L.O., Clarke, L.E.*, et al.* (2019). Developmental Heterogeneity of Microglia and Brain Myeloid Cells Revealed by Deep Single-Cell RNA Sequencing. Neuron *101*, 207-223.e210.
Liang, X., Song, M.R., Xu, Z., Lanuza, G.M., Liu, Y., Zhuang, T., Chen, Y., Pfaff, S.L., Evans, S.M., and Sun, Y. (2011). Isl1 is required for multiple aspects of motor neuron development. Molecular and cellular neurosciences *47*, 215-222.
Liberatore, G.T., Jackson-Lewis, V., Vukosavic, S., Mandir, A.S., Vila, M., McAuliffe, W.G., Dawson, V.L., Dawson, T.M., and Przedborski, S. (1999). Inducible nitric oxide synthase stimulates dopaminergic neurodegeneration in the MPTP model of Parkinson disease. Nature medicine *5*, 1403.
Liddelow, S.A., and Barres, B.A. (2016). Not everything is scary about a glial scar. Nature *532*, 182-183.
Liddelow, S.A., and Barres, B.A. (2017). Reactive Astrocytes: Production, Function, and Therapeutic Potential. Immunity *46*, 957-967.

Liddelow, S.A., Guttenplan, K.A., Clarke, L.E., Bennett, F.C., Bohlen, C.J., Schirmer, L., Bennett, M.L., Münch, A.E., Chung, W.-S., Peterson, T.C*., et al.* (2017). Neurotoxic reactive astrocytes are induced by activated microglia. Nature *541*, 481-487.
Liddelow, S.A., Marsh, S.E., and Stevens, B. (2020). Microglia and Astrocytes in Disease: Dynamic Duo or Partners in Crime? Trends in Immunology *41*, 820-835.
Lim, S.-H., Park, E., You, B., Jung, Y., Park, A.R., Park, S.G., and Lee, J.-R. (2013). Neuronal synapse formation induced by microglia and interleukin 10. In PloS one, pp. e81218.
Linnartz, B., Kopatz, J., Tenner, A.J., and Neumann, H. (2012). Sialic Acid on the Neuronal Glycocalyx Prevents Complement C1 Binding and Complement Receptor-3-Mediated Removal by Microglia. The Journal of Neuroscience *32*, 946-952.
Liu, Y.-J., Spangenberg, E.E., Tang, B., Holmes, T.C., Green, K.N., and Xu, X. (2021). Microglia Elimination Increases Neural Circuit Connectivity and Activity in Adult Mouse Cortex. The Journal of Neuroscience *41*, 1274-1287.
Liu, Y.U., Ying, Y., Li, Y., Eyo, U.B., Chen, T., Zheng, J., Umpierre, A.D., Zhu, J., Bosco, D.B., Dong, H*., et al.* (2019). Neuronal network activity controls microglial process surveillance in awake mice via norepinephrine signaling. Nature Neuroscience *22*, 1771-1781.
Lund, H., Pieber, M., Parsa, R., Han, J., Grommisch, D., Ewing, E., Kular, L., Needhamsen, M., Espinosa, A., Nilsson, E*., et al.* (2018). Competitive repopulation of an empty microglial niche yields functionally distinct subsets of microglia-like cells. Nature communications *9*, 4845.
Luthi-Carter, R., Apostol, B.L., Dunah, A.W., DeJohn, M.M., Farrell, L.A., Bates, G.P., Young, A.B., Standaert, D.G., Thompson, L.M., and Cha, J.H. (2003). Complex alteration of NMDA receptors in transgenic Huntington's disease mouse brain: analysis of mRNA and protein expression, plasma membrane association, interacting proteins, and phosphorylation. Neurobiology of disease *14*, 624-636.
Ma, X., Chen, K., Cui, Y., Huang, G., Nehme, A., Zhang, L., Li, H., Wei, J., Liong, K., Liu, Q*., et al.* (2020). Depletion of microglia in developing cortical circuits reveals its critical role in glutamatergic synapse development, functional connectivity, and critical period plasticity. J Neurosci Res *98*, 1968-1986.
Maeda, A., and Sobel, R.A. (1996). Matrix Metalloproteinases in the Normal Human Central Nervous System, Microglial Nodules, and Multiple Sclerosis Lesions. Journal of Neuropathology & Experimental Neurology *55*, 300-309.
Mafi, A.M., Hofer, L.N., Russ, M.G., Young, J.W., and Mellott, J.G. (2020). The Density of Perineuronal Nets Increases With Age in the Inferior Colliculus in the Fischer Brown Norway Rat. Frontiers in aging neuroscience *12*, 27.
Mandrekar-Colucci, S., and Landreth, G.E. (2010). Microglia and inflammation in Alzheimer's disease. CNS & neurological disorders drug targets *9*, 156-167.
Mangiarini, L., Sathasivam, K., Seller, M., Cozens, B., Harper, A., Hetherington, C., Lawton, M., Trottier, Y., Lehrach, H., Davies, S.W*., et al.* (1996). Exon 1 of the HD gene with an expanded CAG repeat is sufficient to cause a progressive neurological phenotype in transgenic mice. Cell *87*, 493-506.
Marín-Teva, J.L., Dusart, I., Colin, C., Gervais, A., van Rooijen, N., and Mallat, M. (2004). Microglia Promote the Death of Developing Purkinje Cells. Neuron *41*, 535-547.
Markovic, D.S., Glass, R., Synowitz, M., Rooijen, N.v., and Kettenmann, H. (2005). Microglia Stimulate the Invasiveness of Glioma Cells by Increasing the Activity of Metalloprotease-2. Journal of Neuropathology & Experimental Neurology *64*, 754-762.
Masuda, T., Sankowski, R., Staszewski, O., Böttcher, C., Amann, L., Sagar, Scheiwe, C., Nessler, S., Kunz, P., van Loo, G*., et al.* (2019). Spatial and temporal heterogeneity of mouse and human microglia at single-cell resolution. Nature *566*, 388-392.
Mathys, H., Adaikkan, C., Gao, F., Young, J.Z., Manet, E., Hemberg, M., De Jager, P.L., Ransohoff, R.M., Regev, A., and Tsai, L.H. (2017). Temporal Tracking of Microglia Activation in Neurodegeneration at Single-Cell Resolution. Cell reports *21*, 366-380.
Matsumoto, T., Imagama, S., Hirano, K., Ohgomori, T., Natori, T., Kobayashi, K., Muramoto, A., Ishiguro, N., and Kadomatsu, K. (2012). CD44 expression in astrocytes and microglia is associated with ALS progression in a mouse model. Neuroscience letters *520*, 115-120.
Matthews, R.T., Kelly, G.M., Zerillo, C.A., Gray, G., Tiemeyer, M., and Hockfield, S. (2002). Aggrecan glycoforms contribute to the molecular heterogeneity of perineuronal nets. The Journal of neuroscience : the official journal of the Society for Neuroscience *22*, 7536-7547.

Mauney, S.A., Athanas, K.M., Pantazopoulos, H., Shaskan, N., Passeri, E., Berretta, S., and Woo, T.-U.W. (2013). Developmental Pattern of Perineuronal Nets in the Human Prefrontal Cortex and Their Deficit in Schizophrenia. Biological Psychiatry *74*, 427-435.
McCollum, M.H., Leon, R.T., Rush, D.B., Guthrie, K.M., and Wei, J. (2013). Striatal oligodendrogliogenesis and neuroblast recruitment are increased in the R6/2 mouse model of Huntington's disease. Brain research *1518*, 91-103.
McNamara, C.G., Tejero-Cantero, Á., Trouche, S., Campo-Urriza, N., and Dupret, D. (2014). Dopaminergic neurons promote hippocampal reactivation and spatial memory persistence. Nature neuroscience *17*, 1658-1660.
McRae, P.A., Baranov, E., Rogers, S.L., and Porter, B.E. (2012). Persistent decrease in multiple components of the perineuronal net following status epilepticus. European Journal of Neuroscience *36*, 3471-3482.
McRae, P.A., Rocco, M.M., Kelly, G., Brumberg, J.C., and Matthews, R.T. (2007). Sensory Deprivation Alters Aggrecan and Perineuronal Net Expression in the Mouse Barrel Cortex. The Journal of Neuroscience *27*, 5405-5413.
Medina-Flores, R., Wang, G., Bissel, S.J., Murphey-Corb, M., and Wiley, C.A. (2004). Destruction of extracellular matrix proteoglycans is pervasive in simian retroviral neuroinfection. Neurobiology of disease *16*, 604-616.
Mehta, S.R., Tom, C.M., Wang, Y., Bresee, C., Rushton, D., Mathkar, P.P., Tang, J., and Mattis, V.B. (2018). Human Huntington's Disease iPSC-Derived Cortical Neurons Display Altered Transcriptomics, Morphology, and Maturation. Cell reports *25*, 1081-1096.e1086.
Menalled, L.B., Kudwa, A.E., Miller, S., Fitzpatrick, J., Watson-Johnson, J., Keating, N., Ruiz, M., Mushlin, R., Alosio, W., McConnell, K.*, et al.* (2012). Comprehensive Behavioral and Molecular Characterization of a New Knock-In Mouse Model of Huntington's Disease: zQ175. PloS one *7*.
Milinkeviciute, G., Chokr, S.M., and Cramer, K.S. (2021). Auditory Brainstem Deficits from Early Treatment with a CSF1R Inhibitor Largely Recover with Microglial Repopulation. eNeuro *8*.
Milinkeviciute, G., Henningfield, C.M., Muniak, M.A., Chokr, S.M., Green, K.N., and Cramer, K.S. (2019). Microglia Regulate Pruning of Specialized Synapses in the Auditory Brainstem. Frontiers in neural circuits *13*, 55.
Miller, J.R., Lo, K.K., Andre, R., Hensman Moss, D.J., Trager, U., Stone, T.C., Jones, L., Holmans, P., Plagnol, V., and Tabrizi, S.J. (2016). RNA-Seq of Huntington's disease patient myeloid cells reveals innate transcriptional dysregulation associated with proinflammatory pathway activation. Human molecular genetics *25*, 2893-2904.
Milner, R., Crocker, S.J., Hung, S., Wang, X., Frausto, R.F., and del Zoppo, G.J. (2007). Fibronectin- and Vitronectin-Induced Microglial Activation and Matrix Metalloproteinase-9 Expression Is Mediated by Integrins α₅β₁ and α_vβ₅. The Journal of Immunology *178*, 8158-8167.
Miron, V.E. (2017). Microglia-driven regulation of oligodendrocyte lineage cells, myelination, and remyelination. Journal of Leukocyte Biology *101*, 1103-1108.
Miron, V.E., Boyd, A., Zhao, J.-W., Yuen, T.J., Ruckh, J.M., Shadrach, J.L., van Wijngaarden, P., Wagers, A.J., Williams, A., Franklin, R.J.M.*, et al.* (2013). M2 microglia and macrophages drive oligodendrocyte differentiation during CNS remyelination. Nature Neuroscience *16*, 1211-1218.
Mitlöhner, J., Kaushik, R., Niekisch, H., Blondiaux, A., Gee, C.E., Happel, M.F.K., Gundelfinger, E., Dityatev, A., Frischknecht, R., and Seidenbecher, C. (2020). Dopamine Receptor Activation Modulates the Integrity of the Perisynaptic Extracellular Matrix at Excitatory Synapses. Cells *9*.
Miyamoto, A., Wake, H., Ishikawa, A.W., Eto, K., Shibata, K., Murakoshi, H., Koizumi, S., Moorhouse, A.J., Yoshimura, Y., and Nabekura, J. (2016). Microglia contact induces synapse formation in developing somatosensory cortex. Nat Commun *7*, 12540.
Miyata, S., Komatsu, Y., Yoshimura, Y., Taya, C., and Kitagawa, H. (2012). Persistent cortical plasticity by upregulation of chondroitin 6-sulfation. Nature neuroscience *15*, 414.
Miyata, S., Nishimura, Y., Hayashi, N., and Oohira, A. (2005). Construction of perineuronal net-like structure by cortical neurons in culture. Neuroscience *136*, 95-104.
Miyata, S., Nishimura, Y., and Nakashima, T. (2007). Perineuronal nets protect against amyloid beta-protein neurotoxicity in cultured cortical neurons. Brain Res *1150*, 200-206.
Miyazaki, H., Oyama, F., Inoue, R., Aosaki, T., Abe, T., Kiyonari, H., Kino, Y., Kurosawa, M., Shimizu, J., Ogiwara, I.*, et al.* (2014). Singular localization of sodium channel β4 subunit in unmyelinated fibres and its role in the striatum. Nature communications *5*, 5525.
Moffitt, H., McPhail, G.D., Woodman, B., Hobbs, C., and Bates, G.P. (2009). Formation of polyglutamine inclusions in a wide range of non-CNS tissues in the HdhQ150 knock-in mouse model of Huntington's disease. PloS one *4*, e8025.
Mok, S., Koya, R.C., Tsui, C., Xu, J., Robert, L., Wu, L., Graeber, T., West, B.L., Bollag, G., and Ribas, A. (2014). Inhibition of CSF-1 receptor improves the antitumor efficacy of adoptive cell transfer immunotherapy. Cancer research *74*, 153-161.

Monnier, P.P., Sierra, A., Schwab, J.M., Henke-Fahle, S., and Mueller, B.K. (2003). The Rho/ROCK pathway mediates neurite growth-inhibitory activity associated with the chondroitin sulfate proteoglycans of the CNS glial scar. Molecular and cellular neurosciences *22*, 319-330.
Monteiro, S., Roque, S., Marques, F., Correia-Neves, M., and Cerqueira, J.J. (2017). Brain interference: Revisiting the role of IFNgamma in the central nervous system. Progress in neurobiology *156*, 149-163.
Morawski, M., Brückner, G., Jäger, C., Seeger, G., and Arendt, T. (2010a). Neurons associated with aggrecan-based perineuronal nets are protected against tau pathology in subcortical regions in Alzheimer's disease. Neuroscience *169*, 1347-1363.
Morawski, M., Brückner, G., Jäger, C., Seeger, G., Matthews, R.T., and Arendt, T. (2012). Involvement of perineuronal and perisynaptic extracellular matrix in Alzheimer's disease neuropathology. Brain pathology (Zurich, Switzerland) *22*, 547-561.
Morawski, M., Pavlica, S., Seeger, G., Grosche, J., Kouznetsova, E., Schliebs, R., Brückner, G., and Arendt, T. (2010b). Perineuronal nets are largely unaffected in Alzheimer model Tg2576 mice. Neurobiology of Aging *31*, 1254-1256.
Morawski, M., Reinert, T., Meyer-Klaucke, W., Wagner, F.E., Tröger, W., Reinert, A., Jäger, C., Brückner, G., and Arendt, T. (2015). Ion exchanger in the brain: Quantitative analysis of perineuronally fixed anionic binding sites suggests diffusion barriers with ion sorting properties. Scientific Reports *5*, 16471.
Morikawa, S., Ikegaya, Y., Narita, M., and Tamura, H. (2017). Activation of perineuronal net-expressing excitatory neurons during associative memory encoding and retrieval. Scientific Reports *7*, 46024.
Morozko, E.L., Ochaba, J., Hernandez, S.J., Lau, A., Sanchez, I., Orellana, I., Kopan, L., Crapser, J., Duong, J.H., Overman, J.*, et al.* (2018). Longitudinal Biochemical Assay Analysis of Mutant Huntingtin Exon 1 Protein in R6/2 Mice. Journal of Huntington's disease *7*, 321-335.
Mostafavi, S., Yoshida, H., Moodley, D., LeBoité, H., Rothamel, K., Raj, T., Ye, C.J., Chevrier, N., Zhang, S.Y., Feng, T.*, et al.* (2016). Parsing the Interferon Transcriptional Network and Its Disease Associations. Cell *164*, 564-578.
Mrdjen, D., Pavlovic, A., Hartmann, F.J., Schreiner, B., Utz, S.G., Leung, B.P., Lelios, I., Heppner, F.L., Kipnis, J., Merkler, D.*, et al.* (2018). High-Dimensional Single-Cell Mapping of Central Nervous System Immune Cells Reveals Distinct Myeloid Subsets in Health, Aging, and Disease. Immunity *48*, 380-395.e386.
Murase, S., Lantz, C.L., and Quinlan, E.M. (2017). Light reintroduction after dark exposure reactivates plasticity in adults via perisynaptic activation of MMP-9. eLife *6*, e27345.
Najafi, A.R., Crapser, J., Jiang, S., Ng, W., Mortazavi, A., West, B.L., and Green, K.N. (2018). A limited capacity for microglial repopulation in the adult brain. Glia *66*, 2385-2396.
Nakamura, H., Fujii, Y., Inoki, I., Sugimoto, K., Tanzawa, K., Matsuki, H., Miura, R., Yamaguchi, Y., and Okada, Y. (2000). Brevican Is Degraded by Matrix Metalloproteinases and Aggrecanase-1 (ADAMTS4) at Different Sites*. Journal of Biological Chemistry *275*, 38885-38890.
Nakanishi, H. (2003). Microglial functions and proteases. Molecular Neurobiology *27*, 163-176.
Nakanishi, H. (2020). Cathepsin regulation on microglial function. Biochimica et Biophysica Acta (BBA) - Proteins and Proteomics *1868*, 140465.
Nakanishi, K., Aono, S., Hirano, K., Kuroda, Y., Ida, M., Tokita, Y., Matsui, F., and Oohira, A. (2006). Identification of Neurite Outgrowth-promoting Domains of Neuroglycan C, a Brain-specific Chondroitin Sulfate Proteoglycan, and Involvement of Phosphatidylinositol 3-Kinase and Protein Kinase C Signaling Pathways in Neuritogenesis*. Journal of Biological Chemistry *281*, 24970-24978.
Nakayama, H., Abe, M., Morimoto, C., Iida, T., Okabe, S., Sakimura, K., and Hashimoto, K. (2018). Microglia permit climbing fiber elimination by promoting GABAergic inhibition in the developing cerebellum. Nat Commun *9*, 2830.
Nazmi, A., Field, R.H., Griffin, E.W., Haugh, O., Hennessy, E., Cox, D., Reis, R., Tortorelli, L., Murray, C.L., Lopez-Rodriguez, A.B.*, et al.* (2019). Chronic neurodegeneration induces type I interferon synthesis via STING, shaping microglial phenotype and accelerating disease progression. Glia.
Nguyen, P.T., Dorman, L.C., Pan, S., Vainchtein, I.D., Han, R.T., Nakao-Inoue, H., Taloma, S.E., Barron, J.J., Molofsky, A.B., Kheirbek, M.A.*, et al.* (2020). Microglial Remodeling of the Extracellular Matrix Promotes Synapse Plasticity. Cell.
Nicholson, C., and Syková, E. (1998). Extracellular space structure revealed by diffusion analysis. Trends in Neurosciences *21*, 207-215.
Nimmerjahn, A., Kirchhoff, F., and Helmchen, F. (2005). Resting Microglial Cells Are Highly Dynamic Surveillants of Brain Parenchyma in Vivo. Science *308*, 1314-1318.

Nott, A., Holtman, I.R., Coufal, N.G., Schlachetzki, J.C.M., Yu, M., Hu, R., Han, C.Z., Pena, M., Xiao, J., Wu, Y.*, et al.* (2019). Brain cell type–specific enhancer–promoter interactome maps and disease-risk association. Science *366*, 1134-1139.
O'Rourke, J.G., Gareau, J.R., Ochaba, J., Song, W., Rasko, T., Reverter, D., Lee, J., Monteys, A.M., Pallos, J., Mee, L.*, et al.* (2013). SUMO-2 and PIAS1 modulate insoluble mutant huntingtin protein accumulation. Cell reports *4*, 362-375.
Oakley, H., Cole, S.L., Logan, S., Maus, E., Shao, P., Craft, J., Guillozet-Bongaarts, A., Ohno, M., Disterhoft, J., Van Eldik, L.*, et al.* (2006). Intraneuronal β-Amyloid Aggregates, Neurodegeneration, and Neuron Loss in Transgenic Mice with Five Familial Alzheimer's Disease Mutations: Potential Factors in Amyloid Plaque Formation. The Journal of Neuroscience *26*, 10129-10140.
Ochaba, J., Monteys, A.M., O'Rourke, J.G., Reidling, J.C., Steffan, J.S., Davidson, B.L., and Thompson, L.M. (2016). PIAS1 regulates mutant Huntingtin accumulation and Huntington's disease-associated phenotypes in vivo. Neuron *90*, 507-520.
Ochaba, J., Morozko, E.L., O'Rourke, J.G., and Thompson, L.M. (2018). Fractionation for Resolution of Soluble and Insoluble Huntingtin Species. JoVE, e57082.
Oddo, S., Billings, L., Kesslak, J.P., Cribbs, D.H., and LaFerla, F.M. (2004). Abeta immunotherapy leads to clearance of early, but not late, hyperphosphorylated tau aggregates via the proteasome. Neuron *43*, 321-332.
Oddo, S., Caccamo, A., Shepherd, J.D., Murphy, M.P., Golde, T.E., Kayed, R., Metherate, R., Mattson, M.P., Akbari, Y., and LaFerla, F.M. (2003). Triple-transgenic model of Alzheimer's disease with plaques and tangles: intracellular Abeta and synaptic dysfunction. Neuron *39*, 409-421.
Ohtake, Y., Wong, D., Abdul-Muneer, P.M., Selzer, M.E., and Li, S. (2016). Two PTP receptors mediate CSPG inhibition by convergent and divergent signaling pathways in neurons. Scientific Reports *6*, 37152.
Okunuki, Y., Mukai, R., Pearsall, E.A., Klokman, G., Husain, D., Park, D.H., Korobkina, E., Weiner, H.L., Butovsky, O., Ksander, B.R.*, et al.* (2018). Microglia inhibit photoreceptor cell death and regulate immune cell infiltration in response to retinal detachment. Proceedings of the National Academy of Sciences of the United States of America *115*, E6264-e6273.
Orlando, C., Ster, J., Gerber, U., Fawcett, J.W., and Raineteau, O. (2012). Perisynaptic Chondroitin Sulfate Proteoglycans Restrict Structural Plasticity in an Integrin-Dependent Manner. The Journal of Neuroscience *32*, 18009-18017.
Osipovitch, M., Asenjo Martinez, A., Mariani, J.N., Cornwell, A., Dhaliwal, S., Zou, L., Chandler-Militello, D., Wang, S., Li, X., Benraiss, S.J.*, et al.* (2019). Human ESC-Derived Chimeric Mouse Models of Huntington's Disease Reveal Cell-Intrinsic Defects in Glial Progenitor Cell Differentiation. Cell stem cell *24*, 107-122.e107.
Oyama, F., Miyazaki, H., Sakamoto, N., Becquet, C., Machida, Y., Kaneko, K., Uchikawa, C., Suzuki, T., Kurosawa, M., Ikeda, T.*, et al.* (2006). Sodium channel beta4 subunit: down-regulation and possible involvement in neuritic degeneration in Huntington's disease transgenic mice. Journal of neurochemistry *98*, 518-529.
Paine, S.M., Anderson, G., Bedford, K., Lawler, K., Mayer, R.J., Lowe, J., and Bedford, L. (2013). Pale body-like inclusion formation and neurodegeneration following depletion of 26S proteasomes in mouse brain neurones are independent of alpha-synuclein. PloS one *8*, e54711.
Pantazopoulos, H., and Berretta, S. (2016). In sickness and in health: perineuronal nets and synaptic plasticity in psychiatric disorders. Neural plasticity *2016*.
Pantazopoulos, H., Gisabella, B., Rexrode, L., Benefield, D., Yildiz, E., Seltzer, P., Valeri, J., Chelini, G., Reich, A., Ardelt, M.*, et al.* (2020). Circadian Rhythms of Perineuronal Net Composition. eNeuro *7*.
Pantazopoulos, H., Markota, M., Jaquet, F., Ghosh, D., Wallin, A., Santos, A., Caterson, B., and Berretta, S. (2015). Aggrecan and chondroitin-6-sulfate abnormalities in schizophrenia and bipolar disorder: a postmortem study on the amygdala. Translational psychiatry *5*, e496.
Pantazopoulos, H., Woo, T.-U.W., Lim, M.P., Lange, N., and Berretta, S. (2010). Extracellular Matrix-Glial Abnormalities in the Amygdala and Entorhinal Cortex of Subjects Diagnosed With Schizophrenia. Archives of General Psychiatry *67*, 155-166.
Paolicelli, R.C., Bolasco, G., Pagani, F., Maggi, L., Scianni, M., Panzanelli, P., Giustetto, M., Ferreira, T.A., Guiducci, E., Dumas, L.*, et al.* (2011). Synaptic Pruning by Microglia Is Necessary for Normal Brain Development. Science *333*, 1456-1458.
Park, H., Kim, M., Kim, H.J., Lee, Y., Seo, Y., Pham, C.D., Lee, J., Byun, S.J., and Kwon, M.H. (2017). Heparan sulfate proteoglycans (HSPGs) and chondroitin sulfate proteoglycans (CSPGs) function as endocytic receptors for an internalizing anti-nucleic acid antibody. Scientific Reports *7*, 14373.

Parkhurst, C.N., Yang, G., Ninan, I., Savas, J.N., Yates, J.R., 3rd, Lafaille, J.J., Hempstead, B.L., Littman, D.R., and Gan, W.B. (2013). Microglia promote learning-dependent synapse formation through brain-derived neurotrophic factor. Cell *155*, 1596-1609.
Paschalis, E.I., Lei, F., Zhou, C., Kapoulea, V., Dana, R., Chodosh, J., Vavvas, D.G., and Dohlman, C.H. (2018). Permanent neuroglial remodeling of the retina following infiltration of CSF1R inhibition-resistant peripheral monocytes. Proceedings of the National Academy of Sciences of the United States of America *115*, E11359-e11368.
Patel, A.R., Ritzel, R., McCullough, L.D., and Liu, F. (2013). Microglia and ischemic stroke: a double-edged sword. International journal of physiology, pathophysiology and pharmacology *5*, 73-90.
Pavese, N., Gerhard, A., Tai, Y.F., Ho, A.K., Turkheimer, F., Barker, R.A., Brooks, D.J., and Piccini, P. (2006). Microglial activation correlates with severity in Huntington disease: a clinical and PET study. Neurology *66*, 1638-1643.
Pearson, C.S., Mencio, C.P., Barber, A.C., Martin, K.R., and Geller, H.M. (2018). Identification of a critical sulfation in chondroitin that inhibits axonal regeneration. eLife *7*.
Pendleton, J.C., Shamblott, M.J., Gary, D.S., Belegu, V., Hurtado, A., Malone, M.L., and McDonald, J.W. (2013). Chondroitin sulfate proteoglycans inhibit oligodendrocyte myelination through PTPσ. Experimental Neurology *247*, 113-121.
Petanceska, S., Canoll, P., and Devi, L.A. (1996). Expression of Rat Cathepsin S in Phagocytic Cells (∗). Journal of Biological Chemistry *271*, 4403-4409.
Petkau, T.L., Hill, A., Connolly, C., Lu, G., Wagner, P., Kosior, N., Blanco, J., and Leavitt, B.R. (2019). Mutant huntingtin expression in microglia is neither required nor sufficient to cause the Huntington's disease-like phenotype in BACHD mice. Human molecular genetics.
Pintér, A., Hevesi, Z., Zahola, P., Alpár, A., and Hanics, J. (2020). Chondroitin sulfate proteoglycan-5 forms perisynaptic matrix assemblies in the adult rat cortex. Cellular Signalling *74*, 109710.
Pippucci, T., Parmeggiani, A., Palombo, F., Maresca, A., Angius, A., Crisponi, L., Cucca, F., Liguori, R., Valentino, M.L., Seri, M.*, et al.* (2013). A novel null homozygous mutation confirms CACNA2D2 as a gene mutated in epileptic encephalopathy. PloS one *8*, e82154.
Pirbhoy, P.S., Rais, M., Lovelace, J.W., Woodard, W., Razak, K.A., Binder, D.K., and Ethell, I.M. (2020). Acute pharmacological inhibition of matrix metalloproteinase-9 activity during development restores perineuronal net formation and normalizes auditory processing in Fmr1 KO mice. J Neurochem *155*, 538-558.
Pizzorusso, T., Medini, P., Berardi, N., Chierzi, S., Fawcett, J.W., and Maffei, L. (2002). Reactivation of Ocular Dominance Plasticity in the Adult Visual Cortex. Science *298*, 1248-1251.
Planas, A.M., Solé, S., and Justicia, C. (2001). Expression and Activation of Matrix Metalloproteinase-2 and -9 in Rat Brain after Transient Focal Cerebral Ischemia. Neurobiology of disease *8*, 834-846.
Politis, M., Pavese, N., Tai, Y.F., Kiferle, L., Mason, S.L., Brooks, D.J., Tabrizi, S.J., Barker, R.A., and Piccini, P. (2011). Microglial activation in regions related to cognitive function predicts disease onset in Huntington's disease: a multimodal imaging study. Human brain mapping *32*, 258-270.
Prinz, M., Jung, S., and Priller, J. (2019). Microglia Biology: One Century of Evolving Concepts. Cell *179*, 292-311.
Properzi, F., Carulli, D., Asher, R.A., Muir, E., Camargo, L.M., van Kuppevelt, T.H., ten Dam, G.B., Furukawa, Y., Mikami, T., Sugahara, K.*, et al.* (2005). Chondroitin 6-sulphate synthesis is up-regulated in injured CNS, induced by injury-related cytokines and enhanced in axon-growth inhibitory glia. The European journal of neuroscience *21*, 378-390.
Quattromani, M.J., Pruvost, M., Guerreiro, C., Backlund, F., Englund, E., Aspberg, A., Jaworski, T., Hakon, J., Ruscher, K., Kaczmarek, L.*, et al.* (2018). Extracellular Matrix Modulation Is Driven by Experience-Dependent Plasticity During Stroke Recovery. Molecular Neurobiology *55*, 2196-2213.
Rankin-Gee, E.K., McRae, P.A., Baranov, E., Rogers, S., Wandrey, L., and Porter, B.E. (2015). Perineuronal net degradation in epilepsy. Epilepsia *56*, 1124-1133.
Reed-Geaghan, E.G., Croxford, A.L., Becher, B., and Landreth, G.E. (2020). Plaque-associated myeloid cells derive from resident microglia in an Alzheimer's disease model. Journal of Experimental Medicine *217*.
Reichelt, A.C., Hare, D.J., Bussey, T.J., and Saksida, L.M. (2019). Perineuronal Nets: Plasticity, Protection, and Therapeutic Potential. Trends in Neurosciences *42*, 458-470.
Reichelt, A.C., Lemieux, C.A., Princz-Lebel, O., Singh, A., Bussey, T.J., and Saksida, L.M. (2021). Age-dependent and region-specific alteration of parvalbumin neurons, perineuronal nets and microglia in the mouse prefrontal cortex and hippocampus following obesogenic diet consumption. Scientific Reports *11*, 5593.
Reiner, A., Shelby, E., Wang, H., Demarch, Z., Deng, Y., Guley, N.H., Hogg, V., Roxburgh, R., Tippett, L.J., Waldvogel, H.J.*, et al.* (2013). Striatal parvalbuminergic neurons are lost in Huntington's disease: implications for dystonia. Movement disorders : official journal of the Movement Disorder Society *28*, 1691-1699.

Rice, R.A., Pham, J., Lee, R.J., Najafi, A.R., West, B.L., and Green, K.N. (2017). Microglial repopulation resolves inflammation and promotes brain recovery after injury. Glia *65*, 931-944.
Rice, R.A., Spangenberg, E.E., Yamate-Morgan, H., Lee, R.J., Arora, R.P., Hernandez, M.X., Tenner, A.J., West, B.L., and Green, K.N. (2015). Elimination of Microglia Improves Functional Outcomes Following Extensive Neuronal Loss in the Hippocampus. The Journal of neuroscience : the official journal of the Society for Neuroscience *35*, 9977-9989.
Robinson, M.D., McCarthy, D.J., and Smyth, G.K. (2010). edgeR: a Bioconductor package for differential expression analysis of digital gene expression data. Bioinformatics (Oxford, England) *26*, 139-140.
Rodrigues, F.B., Byrne, L.M., McColgan, P., Robertson, N., Tabrizi, S.J., Zetterberg, H., and Wild, E.J. (2016). Cerebrospinal Fluid Inflammatory Biomarkers Reflect Clinical Severity in Huntington's Disease. PloS one *11*, e0163479.
Rogers, S.L., Rankin-Gee, E., Risbud, R.M., Porter, B.E., and Marsh, E.D. (2018). Normal Development of the Perineuronal Net in Humans; In Patients with and without Epilepsy. Neuroscience *384*, 350-360.
Rojo, R., Raper, A., Ozdemir, D.D., Lefevre, L., Grabert, K., Wollscheid-Lengeling, E., Bradford, B., Caruso, M., Gazova, I., Sanchez, A.*, et al.* (2019). Deletion of a Csf1r enhancer selectively impacts CSF1R expression and development of tissue macrophage populations. Nat Commun *10*, 3215.
Romberg, C., Yang, S., Melani, R., Andrews, M.R., Horner, A.E., Spillantini, M.G., Bussey, T.J., Fawcett, J.W., Pizzorusso, T., and Saksida, L.M. (2013). Depletion of perineuronal nets enhances recognition memory and long-term depression in the perirhinal cortex. The Journal of neuroscience : the official journal of the Society for Neuroscience *33*, 7057-7065.
Rosell, A., Ortega-Aznar, A., Alvarez-Sabín, J., Fernández-Cadenas, I., Ribó, M., Molina, C.A., Lo, E.H., and Montaner, J. (2006). Increased Brain Expression of Matrix Metalloproteinase-9 After Ischemic and Hemorrhagic Human Stroke. Stroke *37*, 1399-1406.
Ross, C.A., and Tabrizi, S.J. (2011). Huntington's disease: from molecular pathogenesis to clinical treatment. The Lancet Neurology *10*, 83-98.
Rossier, J., Bernard, A., Cabungcal, J.H., Perrenoud, Q., Savoye, A., Gallopin, T., Hawrylycz, M., Cuénod, M., Do, K., Urban, A.*, et al.* (2015). Cortical fast-spiking parvalbumin interneurons enwrapped in the perineuronal net express the metallopeptidases Adamts8, Adamts15 and Neprilysin. Molecular Psychiatry *20*, 154-161.
Rothhammer, V., Borucki, D.M., Tjon, E.C., Takenaka, M.C., Chao, C.-C., Ardura-Fabregat, A., de Lima, K.A., Gutiérrez-Vázquez, C., Hewson, P., Staszewski, O.*, et al.* (2018). Microglial control of astrocytes in response to microbial metabolites. Nature *557*, 724-728.
Rowlands, D., Lensjo, K.K., Dinh, T., Yang, S., Andrews, M.R., Hafting, T., Fyhn, M., Fawcett, J.W., and Dick, G. (2018). Aggrecan Directs Extracellular Matrix-Mediated Neuronal Plasticity. The Journal of neuroscience : the official journal of the Society for Neuroscience *38*, 10102-10113.
Rubino, S.J., Mayo, L., Wimmer, I., Siedler, V., Brunner, F., Hametner, S., Madi, A., Lanser, A., Moreira, T., Donnelly, D.*, et al.* (2018). Acute microglia ablation induces neurodegeneration in the somatosensory system. Nature Communications *9*, 4578.
Runne, H., Regulier, E., Kuhn, A., Zala, D., Gokce, O., Perrin, V., Sick, B., Aebischer, P., Deglon, N., and Luthi-Carter, R. (2008). Dysregulation of gene expression in primary neuron models of Huntington's disease shows that polyglutamine-related effects on the striatal transcriptome may not be dependent on brain circuitry. The Journal of neuroscience : the official journal of the Society for Neuroscience *28*, 9723-9731.
Ryan, R.E., Sloane, B.F., Sameni, M., and Wood, P.L. (1995). Microglial Cathepsin B: An Immunological Examination of Cellular and Secreted Species. Journal of Neurochemistry *65*, 1035-1045.
Safaiyan, S., Besson-Girard, S., Kaya, T., Cantuti-Castelvetri, L., Liu, L., Ji, H., Schifferer, M., Gouna, G., Usifo, F., Kannaiyan, N.*, et al.* (2021). White matter aging drives microglial diversity. Neuron *109*, 1100-1117.e1110.
Safaiyan, S., Kannaiyan, N., Snaidero, N., Brioschi, S., Biber, K., Yona, S., Edinger, A.L., Jung, S., Rossner, M.J., and Simons, M. (2016). Age-related myelin degradation burdens the clearance function of microglia during aging. Nature Neuroscience *19*, 995-998.
Saiz-Sanchez, D., De La Rosa-Prieto, C., Ubeda-Bañon, I., and Martinez-Marcos, A. (2013). Interneurons and Beta-Amyloid in the Olfactory Bulb, Anterior Olfactory Nucleus and Olfactory Tubercle in APPxPS1 Transgenic Mice Model of Alzheimer's Disease. The Anatomical Record *296*, 1413-1423.
Salter, Michael W., and Beggs, S. (2014). Sublime Microglia: Expanding Roles for the Guardians of the CNS. Cell *158*, 15-24.
Salter, M.W., and Stevens, B. (2017). Microglia emerge as central players in brain disease. Nature Medicine *23*, 1018-1027.

Sánchez-Ventura, J., Giménez-Llort, L., Penas, C., and Udina, E. (2021). Voluntary wheel running preserves lumbar perineuronal nets, enhances motor functions and prevents hyperreflexia after spinal cord injury. Exp Neurol *336*, 113533.
Sandvig, I., Augestad, I.L., Haberg, A.K., and Sandvig, A. (2018). Neuroplasticity in stroke recovery. The role of microglia in engaging and modifying synapses and networks. The European journal of neuroscience *47*, 1414-1428.
Sapp, E., Kegel, K.B., Aronin, N., Hashikawa, T., Uchiyama, Y., Tohyama, K., Bhide, P.G., Vonsattel, J.P., and DiFiglia, M. (2001). Early and progressive accumulation of reactive microglia in the Huntington disease brain. Journal of neuropathology and experimental neurology *60*, 161-172.
Schafer, D.P., Lehrman, E.K., Kautzman, A.G., Koyama, R., Mardinly, A.R., Yamasaki, R., Ransohoff, R.M., Greenberg, M.E., Barres, B.A., and Stevens, B. (2012). Microglia sculpt postnatal neural circuits in an activity and complement-dependent manner. Neuron *74*, 691-705.
Schafer, D.P., Lehrman, E.K., and Stevens, B. (2013). The "quad-partite" synapse: Microglia-synapse interactions in the developing and mature CNS. Glia *61*, 24-36.
Schafer, D.P., and Stevens, B. (2015). Microglia Function in Central Nervous System Development and Plasticity. Cold Spring Harbor perspectives in biology *7*, a020545.
Schäfer, M.K.E., and Tegeder, I. (2018). NG2/CSPG4 and progranulin in the posttraumatic glial scar. Matrix biology : journal of the International Society for Matrix Biology *68-69*, 571-588.
Schecter, R.W., Maher, E.E., Welsh, C.A., Stevens, B., Erisir, A., and Bear, M.F. (2017). Experience-Dependent Synaptic Plasticity in V1 Occurs without Microglial CX3CR1. The Journal of neuroscience : the official journal of the Society for Neuroscience *37*, 10541-10553.
Seidenbecher, C.I., Richter, K., Rauch, U., Fässler, R., Garner, C.C., and Gundelfinger, E.D. (1995). Brevican, a Chondroitin Sulfate Proteoglycan of Rat Brain, Occurs as Secreted and Cell Surface Glycosylphosphatidylinositol-anchored Isoforms (*). Journal of Biological Chemistry *270*, 27206-27212.
Selkoe, D.J., and Hardy, J. (2016). The amyloid hypothesis of Alzheimer's disease at 25 years. EMBO Molecular Medicine *8*, 595-608.
Serrano-Pozo, A., Muzikansky, A., Gómez-Isla, T., Growdon, J.H., Betensky, R.A., Frosch, M.P., and Hyman, B.T. (2013). Differential relationships of reactive astrocytes and microglia to fibrillar amyloid deposits in Alzheimer disease. Journal of neuropathology and experimental neurology *72*, 462-471.
Shemer, A., Grozovski, J., Tay, T.L., Tao, J., Volaski, A., Süß, P., Ardura-Fabregat, A., Gross-Vered, M., Kim, J.-S., David, E.*, et al.* (2018). Engrafted parenchymal brain macrophages differ from microglia in transcriptome, chromatin landscape and response to challenge. Nature Communications *9*, 5206.
Shen, Y., Tenney, A.P., Busch, S.A., Horn, K.P., Cuascut, F.X., Liu, K., He, Z., Silver, J., and Flanagan, J.G. (2009). PTPσ Is a Receptor for Chondroitin Sulfate Proteoglycan, an Inhibitor of Neural Regeneration. Science *326*, 592-596.
Shi, W., Wei, X., Wang, X., Du, S., Liu, W., Song, J., and Wang, Y. (2019a). Perineuronal nets protect long-term memory by limiting activity-dependent inhibition from parvalbumin interneurons. Proceedings of the National Academy of Sciences *116*, 27063-27073.
Shi, Y., Manis, M., Long, J., Wang, K., Sullivan, P.M., Remolina Serrano, J., Hoyle, R., and Holtzman, D.M. (2019b). Microglia drive APOE-dependent neurodegeneration in a tauopathy mouse model. The Journal of experimental medicine *216*, 2546-2561.
Shigemoto-Mogami, Y., Hoshikawa, K., Goldman, J.E., Sekino, Y., and Sato, K. (2014). Microglia Enhance Neurogenesis and Oligodendrogenesis in the Early Postnatal Subventricular Zone. The Journal of Neuroscience *34*, 2231-2243.
Sierksma, A., Lu, A., Mancuso, R., Fattorelli, N., Thrupp, N., Salta, E., Zoco, J., Blum, D., Buée, L., De Strooper, B.*, et al.* Novel Alzheimer risk genes determine the microglia response to amyloid-β but not to TAU pathology. EMBO Molecular Medicine *n/a*, e10606.
Sierra, A., Encinas, J.M., Deudero, J.J., Chancey, J.H., Enikolopov, G., Overstreet-Wadiche, L.S., Tsirka, S.E., and Maletic-Savatic, M. (2010). Microglia shape adult hippocampal neurogenesis through apoptosis-coupled phagocytosis. Cell stem cell *7*, 483-495.
Siew, J.J., Chen, H.-M., Chen, H.-Y., Chen, H.-L., Chen, C.-M., Soong, B.-W., Wu, Y.-R., Chang, C.-P., Chan, Y.-C., Lin, C.-H.*, et al.* (2019). Galectin-3 is required for the microglia-mediated brain inflammation in a model of Huntington's disease. Nature communications *10*, 3473.
Sieweke, M.H., and Allen, J.E. (2013). Beyond Stem Cells: Self-Renewal of Differentiated Macrophages. Science (New York, NY) *342*, 1242974.
Silver, J., and Miller, J.H. (2004). Regeneration beyond the glial scar. Nature Reviews Neuroscience *5*, 146-156.
Silvestri, L., Baker, J.R., Rodén, L., and Stroud, R.M. (1981). The C1q inhibitor in serum is a chondroitin 4-sulfate proteoglycan. Journal of Biological Chemistry *256*, 7383-7387.

Simmons, D.A., Casale, M., Alcon, B., Pham, N., Narayan, N., and Lynch, G. (2007). Ferritin accumulation in dystrophic microglia is an early event in the development of Huntington's disease. Glia *55*, 1074-1084.
Sims, R., van der Lee, S.J., Naj, A.C., Bellenguez, C., Badarinarayan, N., Jakobsdottir, J., Kunkle, B.W., Boland, A., Raybould, R., Bis, J.C.*, et al.* (2017). Rare coding variants in PLCG2, ABI3, and TREM2 implicate microglial-mediated innate immunity in Alzheimer's disease. Nature genetics *49*, 1373-1384.
Sipe, G.O., Lowery, R.L., Tremblay, M.È., Kelly, E.A., Lamantia, C.E., and Majewska, A.K. (2016). Microglial P2Y12 is necessary for synaptic plasticity in mouse visual cortex. Nature Communications *7*, 10905.
Siri, A., Knäuper, V., Veirana, N., Caocci, F., Murphy, G., and Zardi, L. (1995). Different Susceptibility of Small and Large Human Tenascin-C Isoforms to Degradation by Matrix Metalloproteinases *. Journal of Biological Chemistry *270*, 8650-8654.
Smith, A.M., Gibbons, H.M., Oldfield, R.L., Bergin, P.M., Mee, E.W., Faull, R.L., and Dragunow, M. (2013). The transcription factor PU.1 is critical for viability and function of human brain microglia. Glia *61*, 929-942.
Smith, D.L., Woodman, B., Mahal, A., Sathasivam, K., Ghazi-Noori, S., Lowden, P.A., Bates, G.P., and Hockly, E. (2003). Minocycline and doxycycline are not beneficial in a model of Huntington's disease. Annals of neurology *54*, 186-196.
Sobel, R.A., and Ahmed, A.S. (2001). White Matter Extracellular Matrix Chondroitin Sulfate/Dermatan Sulfate Proteoglycans in Multiple Sclerosis. Journal of Neuropathology & Experimental Neurology *60*, 1198-1207.
Song, I., and Dityatev, A. (2018). Crosstalk between glia, extracellular matrix and neurons. Brain Research Bulletin *136*, 101-108.
Sorg, B.A., Berretta, S., Blacktop, J.M., Fawcett, J.W., Kitagawa, H., Kwok, J.C., and Miquel, M. (2016). Casting a Wide Net: Role of Perineuronal Nets in Neural Plasticity. The Journal of neuroscience : the official journal of the Society for Neuroscience *36*, 11459-11468.
Spangenberg, E., Severson, P.L., Hohsfield, L.A., Crapser, J., Zhang, J., Burton, E.A., Zhang, Y., Spevak, W., Lin, J., Phan, N.Y.*, et al.* (2019). Sustained microglial depletion with CSF1R inhibitor impairs parenchymal plaque development in an Alzheimer's disease model. Nature Communications *10*, 3758.
Spangenberg, E.E., Lee, R.J., Najafi, A.R., Rice, R.A., Elmore, M.R., Blurton-Jones, M., West, B.L., and Green, K.N. (2016). Eliminating microglia in Alzheimer's mice prevents neuronal loss without modulating amyloid-beta pathology. Brain : a journal of neurology *139*, 1265-1281.
Stafford, J.H., Hirai, T., Deng, L., Chernikova, S.B., Urata, K., West, B.L., and Brown, J.M. (2016). Colony stimulating factor 1 receptor inhibition delays recurrence of glioblastoma after radiation by altering myeloid cell recruitment and polarization. Neuro-oncology *18*, 797-806.
Stanek, L.M., Bu, J., and Shihabuddin, L.S. (2019). Astrocyte transduction is required for rescue of behavioral phenotypes in the YAC128 mouse model with AAV-RNAi mediated HTT lowering therapeutics. Neurobiology of disease.
Stelzmann, R.A., Norman Schnitzlein, H., and Reed Murtagh, F. (1995). An english translation of alzheimer's 1907 paper, "über eine eigenartige erkankung der hirnrinde". Clinical Anatomy *8*, 429-431.
Sterling, J.K., Adetunji, M.O., Guttha, S., Bargoud, A.R., Uyhazi, K.E., Ross, A.G., Dunaief, J.L., and Cui, Q.N. (2020). GLP-1 Receptor Agonist NLY01 Reduces Retinal Inflammation and Neuron Death Secondary to Ocular Hypertension. Cell Reports *33*, 108271.
Stevens, B., Allen, N.J., Vazquez, L.E., Howell, G.R., Christopherson, K.S., Nouri, N., Micheva, K.D., Mehalow, A.K., Huberman, A.D., Stafford, B.*, et al.* (2007). The Classical Complement Cascade Mediates CNS Synapse Elimination. Cell *131*, 1164-1178.
Stowell, R.D., Sipe, G.O., Dawes, R.P., Batchelor, H.N., Lordy, K.A., Whitelaw, B.S., Stoessel, M.B., Bidlack, J.M., Brown, E., Sur, M.*, et al.* (2019). Noradrenergic signaling in the wakeful state inhibits microglial surveillance and synaptic plasticity in the mouse visual cortex. Nature Neuroscience *22*, 1782-1792.
Stowell, R.D., Wong, E.L., Batchelor, H.N., Mendes, M.S., Lamantia, C.E., Whitelaw, B.S., and Majewska, A.K. (2018). Cerebellar microglia are dynamically unique and survey Purkinje neurons in vivo. Dev Neurobiol *78*, 627-644.
Stoyanov, S., Sun, W., Düsedau, H.P., Cangalaya, C., Choi, I., Mirzapourdelavar, H., Baidoe-Ansah, D., Kaushik, R., Neumann, J., Dunay, I.R.*, et al.* (2021). Attenuation of the extracellular matrix restores microglial activity during the early stage of amyloidosis. Glia *69*, 182-200.
Strand, A.D., Aragaki, A.K., Shaw, D., Bird, T., Holton, J., Turner, C., Tapscott, S.J., Tabrizi, S.J., Schapira, A.H., Kooperberg, C.*, et al.* (2005). Gene expression in Huntington's disease skeletal muscle: a potential biomarker. Human molecular genetics *14*, 1863-1876.
Svensson, M.N., Andersson, K.M., Wasén, C., Erlandsson, M.C., Nurkkala-Karlsson, M., Jonsson, I.M., Brisslert, M., Bemark, M., and Bokarewa, M.I. (2015). Murine germinal center B cells require functional Fms-like tyrosine kinase

3 signaling for IgG1 class-switch recombination. Proceedings of the National Academy of Sciences of the United States of America *112*, E6644-6653.
Syková, E. (1997). The Extracellular Space in the CNS: Its Regulation, Volume and Geometry in Normal and Pathological Neuronal Function. The Neuroscientist *3*, 28-41.
Szalay, G., Martinecz, B., Lenart, N., Kornyei, Z., Orsolits, B., Judak, L., Csaszar, E., Fekete, R., West, B.L., Katona, G.*, et al.* (2016). Microglia protect against brain injury and their selective elimination dysregulates neuronal network activity after stroke. Nature communications *7*, 11499.
Szklarczyk, A., Lapinska, J., Rylski, M., McKay, R.D.G., and Kaczmarek, L. (2002). Matrix Metalloproteinase-9 Undergoes Expression and Activation during Dendritic Remodeling in Adult Hippocampus. The Journal of Neuroscience *22*, 920-930.
Tai, Y.F., Pavese, N., Gerhard, A., Tabrizi, S.J., Barker, R.A., Brooks, D.J., and Piccini, P. (2007). Microglial activation in presymptomatic Huntington's disease gene carriers. Brain : a journal of neurology *130*, 1759-1766.
Takahashi, H., Brasnjevic, I., Rutten, B.P.F., Van Der Kolk, N., Perl, D.P., Bouras, C., Steinbusch, H.W.M., Schmitz, C., Hof, P.R., and Dickstein, D.L. (2010). Hippocampal interneuron loss in an APP/PS1 double mutant mouse and in Alzheimer's disease. Brain Struct Funct *214*, 145-160.
Takeuchi, H., Jin, S., Wang, J., Zhang, G., Kawanokuchi, J., Kuno, R., Sonobe, Y., Mizuno, T., and Suzumura, A. (2006). Tumor Necrosis Factor-α Induces Neurotoxicity via Glutamate Release from Hemichannels of Activated Microglia in an Autocrine Manner*. Journal of Biological Chemistry *281*, 21362-21368.
Tap, W.D., Anthony, S.P., Chmielowski, B., Staddon, A.P., Cohn, A.L., Shapiro, G., Puzanov, I., Kwak, E.L., Wagner, A.J., Peterfy, C.*, et al.* (2014). A pilot study of PLX3397, a selective colony-stimulating factor 1 receptor (CSF1R) kinase inhibitor, in pigmented villonodular synovitis (PVNS). Journal of Clinical Oncology *32*, 10503-10503.
Tap, W.D., Wainberg, Z.A., Anthony, S.P., Ibrahim, P.N., Zhang, C., Healey, J.H., Chmielowski, B., Staddon, A.P., Cohn, A.L., Shapiro, G.I.*, et al.* (2015). Structure-Guided Blockade of CSF1R Kinase in Tenosynovial Giant-Cell Tumor. The New England journal of medicine *373*, 428-437.
Tay, T.L., Sagar, Dautzenberg, J., Grün, D., and Prinz, M. (2018). Unique microglia recovery population revealed by single-cell RNAseq following neurodegeneration. Acta Neuropathologica Communications *6*, 87.
Tewari, B.P., Chaunsali, L., Campbell, S.L., Patel, D.C., Goode, A.E., and Sontheimer, H. (2018). Perineuronal nets decrease membrane capacitance of peritumoral fast spiking interneurons in a model of epilepsy. Nat Commun *9*, 4724.
Tewari, B.P., and Sontheimer, H. (2019). Protocol to Quantitatively Assess the Structural Integrity of Perineuronal Nets ex vivo. Bio-protocol *9*, e3234.
Thompson, E.H., Lensjø, K.K., Wigestrand, M.B., Malthe-Sørenssen, A., Hafting, T., and Fyhn, M. (2018). Removal of perineuronal nets disrupts recall of a remote fear memory. Proceedings of the National Academy of Sciences *115*, 607-612.
Tortorella, M.D., Burn, T.C., Pratta, M.A., Abbaszade, I., Hollis, J.M., Liu, R., Rosenfeld, S.A., Copeland, R.A., Decicco, C.P., Wynn, R.*, et al.* (1999). Purification and Cloning of Aggrecanase-1: A Member of the ADAMTS Family of Proteins. Science *284*, 1664-1666.
Tremblay, M.-È., Lowery, R.L., and Majewska, A.K. (2010). Microglial interactions with synapses are modulated by visual experience. In PLoS Biol, pp. e1000527.
Tremblay, M., Stevens, B., Sierra, A., Wake, H., Bessis, A., and Nimmerjahn, A. (2011). The role of microglia in the healthy brain. The Journal of neuroscience : the official journal of the Society for Neuroscience *31*, 16064-16069.
Tremblay, M., Zettel, M.L., Ison, J.R., Allen, P.D., and Majewska, A.K. (2012). Effects of aging and sensory loss on glial cells in mouse visual and auditory cortices. Glia *60*, 541-558.
Trias, E., King, P.H., Si, Y., Kwon, Y., Varela, V., Ibarburu, S., Kovacs, M., Moura, I.C., Beckman, J.S., Hermine, O.*, et al.* (2018). Mast cells and neutrophils mediate peripheral motor pathway degeneration in ALS. JCI insight *3*.
Tsien, R.Y. (2013). Very long-term memories may be stored in the pattern of holes in the perineuronal net. Proceedings of the National Academy of Sciences *110*, 12456-12461.
Ueno, H., Fujii, K., Takao, K., Suemitsu, S., Murakami, S., Kitamura, N., Wani, K., Matsumoto, Y., Okamoto, M., and Ishihara, T. (2019). Alteration of parvalbumin expression and perineuronal nets formation in the cerebral cortex of aged mice. Molecular and Cellular Neuroscience *95*, 31-42.
Vainchtein, I.D., Chin, G., Cho, F.S., Kelley, K.W., Miller, J.G., Chien, E.C., Liddelow, S.A., Nguyen, P.T., Nakao-Inoue, H., Dorman, L.C.*, et al.* (2018). Astrocyte-derived interleukin-33 promotes microglial synapse engulfment and neural circuit development. Science *359*, 1269-1273.
Vainchtein, I.D., and Molofsky, A.V. (2020). Astrocytes and Microglia: In Sickness and in Health. Trends in Neurosciences *43*, 144-154.
Van Cauwenberghe, C., Van Broeckhoven, C., and Sleegers, K. (2016). The genetic landscape of Alzheimer disease: clinical implications and perspectives. Genetics in Medicine *18*, 421-430.

Varol, C., Mildner, A., and Jung, S. (2015). Macrophages: Development and Tissue Specialization. Annual Review of Immunology *33*, 643-675.
Vashishtha, M., Ng, C.W., Yildirim, F., Gipson, T.A., Kratter, I.H., Bodai, L., Song, W., Lau, A., Labadorf, A., Vogel-Ciernia, A.*, et al.* (2013). Targeting H3K4 trimethylation in Huntington disease. Proceedings of the National Academy of Sciences of the United States of America *110*, E3027-3036.
Végh, M.J., Heldring, C.M., Kamphuis, W., Hijazi, S., Timmerman, A.J., Li, K.W., van Nierop, P., Mansvelder, H.D., Hol, E.M., Smit, A.B.*, et al.* (2014). Reducing hippocampal extracellular matrix reverses early memory deficits in a mouse model of Alzheimer's disease. Acta Neuropathologica Communications *2*, 76.
Verret, L., Mann, E.O., Hang, G.B., Barth, A.M., Cobos, I., Ho, K., Devidze, N., Masliah, E., Kreitzer, A.C., Mody, I.*, et al.* (2012). Inhibitory interneuron deficit links altered network activity and cognitive dysfunction in Alzheimer model. Cell *149*, 708-721.
Virgintino, D., Perissinotto, D., Girolamo, F., Mucignat, M.T., Montanini, L., Errede, M., Kaneiwa, T., Yamada, S., Sugahara, K., Roncali, L.*, et al.* (2009). Differential distribution of aggrecan isoforms in perineuronal nets of the human cerebral cortex. Journal of cellular and molecular medicine *13*, 3151-3173.
Vita, S.M., Grayson, B.E., and Grill, R.J. (2020). Acute damage to the blood–brain barrier and perineuronal net integrity in a clinically-relevant rat model of traumatic brain injury. NeuroReport *31*.
Vitellaro-Zuccarello, L., De Biasi, S., and Spreafico, R. (1998). One hundred years of Golgi's "perineuronal net": history of a denied structure. The Italian Journal of Neurological Sciences *19*, 249.
Waisman, A., Ginhoux, F., Greter, M., and Bruttger, J. (2015). Homeostasis of Microglia in the Adult Brain: Review of Novel Microglia Depletion Systems. Trends Immunol *36*, 625-636.
Wake, H., Moorhouse, A.J., Jinno, S., Kohsaka, S., and Nabekura, J. (2009). Resting Microglia Directly Monitor the Functional State of Synapses In Vivo and Determine the Fate of Ischemic Terminals. The Journal of Neuroscience *29*, 3974-3980.
Wake, H., Moorhouse, A.J., Miyamoto, A., and Nabekura, J. (2013). Microglia: actively surveying and shaping neuronal circuit structure and function. Trends in Neurosciences *36*, 209-217.
Wang, C., Yue, H., Hu, Z., Shen, Y., Ma, J., Li, J., Wang, X.-D., Wang, L., Sun, B., Shi, P.*, et al.* (2020). Microglia mediate forgetting via complement-dependent synaptic elimination. Science *367*, 688-694.
Wang, D., and Fawcett, J. (2012). The perineuronal net and the control of CNS plasticity. Cell and Tissue Research *349*, 147-160.
Wegner, F., Härtig, W., Bringmann, A., Grosche, J., Wohlfarth, K., Zuschratter, W., and Brückner, G. (2003). Diffuse perineuronal nets and modified pyramidal cells immunoreactive for glutamate and the GABAA receptor α1 subunit form a unique entity in rat cerebral cortex. Experimental Neurology *184*, 705-714.
Weinhard, L., di Bartolomei, G., Bolasco, G., Machado, P., Schieber, N.L., Neniskyte, U., Exiga, M., Vadisiute, A., Raggioli, A., Schertel, A.*, et al.* (2018). Microglia remodel synapses by presynaptic trogocytosis and spine head filopodia induction. Nature Communications *9*, 1228.
Welser-Alves, J.V., Crocker, S.J., and Milner, R. (2011). A dual role for microglia in promoting tissue inhibitor of metalloproteinase (TIMP) expression in glial cells in response to neuroinflammatory stimuli. Journal of neuroinflammation *8*, 61.
Welsh, C.A., Stephany, C., Sapp, R.W., and Stevens, B. (2020). Ocular Dominance Plasticity in Binocular Primary Visual Cortex Does Not Require C1q. The Journal of neuroscience : the official journal of the Society for Neuroscience *40*, 769-783.
Wen, T.H., Afroz, S., Reinhard, S.M., Palacios, A.R., Tapia, K., Binder, D.K., Razak, K.A., and Ethell, I.M. (2018a). Genetic Reduction of Matrix Metalloproteinase-9 Promotes Formation of Perineuronal Nets Around Parvalbumin-Expressing Interneurons and Normalizes Auditory Cortex Responses in Developing Fmr1 Knock-Out Mice. Cerebral cortex (New York, NY : 1991) *28*, 3951-3964.
Wen, T.H., Binder, D.K., Ethell, I.M., and Razak, K.A. (2018b). The Perineuronal 'Safety' Net? Perineuronal Net Abnormalities in Neurological Disorders. Frontiers in Molecular Neuroscience *11*.
Werneburg, S., Jung, J., Kunjamma, R.B., Ha, S.-K., Luciano, N.J., Willis, C.M., Gao, G., Biscola, N.P., Havton, L.A., Crocker, S.J.*, et al.* (2020). Targeted Complement Inhibition at Synapses Prevents Microglial Synaptic Engulfment and Synapse Loss in Demyelinating Disease. Immunity *52*, 167-182.e167.
Wiley, C.A., Bissel, S.J., Lesniak, A., Dixon, C.E., Franks, J., Beer Stolz, D., Sun, M., Wang, G., Switzer, R., Kochanek, P.M.*, et al.* (2016). Ultrastructure of Diaschisis Lesions after Traumatic Brain Injury. Journal of neurotrauma *33*, 1866-1882.
Wisniewski, H.M., Wen, G.Y., and Kim, K.S. (1989). Comparison of four staining methods on the detection of neuritic plaques. Acta Neuropathologica *78*, 22-27.

Wlodarczyk, A., Holtman, I.R., Krueger, M., Yogev, N., Bruttger, J., Khorooshi, R., Benmamar-Badel, A., de Boer-Bergsma, J.J., Martin, N.A., Karram, K.*, et al.* (2017). A novel microglial subset plays a key role in myelinogenesis in developing brain. The EMBO Journal *36*, 3292-3308.
Wong, B.K.Y., Ehrnhoefer, D.E., Graham, R.K., Martin, D.D.O., Ladha, S., Uribe, V., Stanek, L.M., Franciosi, S., Qiu, X., Deng, Y.*, et al.* (2015). Partial rescue of some features of Huntington Disease in the genetic absence of caspase-6 in YAC128 mice. Neurobiology of disease *76*, 24-36.
Wood, T.E., Yang, Z., Gray, M., Cepeda, C., Barry, J., and Levine, M.S. (2018). Mutant huntingtin reduction in astrocytes slows disease progression in the BACHD conditional Huntington's disease mouse model. Human molecular genetics *28*, 487-500.
Xu, Z.-X., Kim, G.H., Tan, J.-W., Riso, A.E., Sun, Y., Xu, E.Y., Liao, G.-Y., Xu, H., Lee, S.-H., Do, N.-Y.*, et al.* (2020). Elevated protein synthesis in microglia causes autism-like synaptic and behavioral aberrations. Nature Communications *11*, 1797.
Yang, H.M., Yang, S., Huang, S.S., Tang, B.S., and Guo, J.F. (2017). Microglial Activation in the Pathogenesis of Huntington's Disease. Frontiers in aging neuroscience *9*, 193.
Yi, J.H., Katagiri, Y., Susarla, B., Figge, D., Symes, A.J., and Geller, H.M. (2012). Alterations in sulfated chondroitin glycosaminoglycans following controlled cortical impact injury in mice. The Journal of comparative neurology *520*, 3295-3313.
Yin, Z., Raj, D., Saiepour, N., Van Dam, D., Brouwer, N., Holtman, I.R., Eggen, B.J.L., Möller, T., Tamm, J.A., Abdourahman, A.*, et al.* (2017). Immune hyperreactivity of Aβ plaque-associated microglia in Alzheimer's disease. Neurobiology of Aging *55*, 115-122.
Yiu, G., and He, Z. (2006). Glial inhibition of CNS axon regeneration. Nature Reviews Neuroscience *7*, 617-627.
Yong, V.W., Power, C., Forsyth, P., and Edwards, D.R. (2001). Metalloproteinases in biology and pathology of the nervous system. Nature Reviews Neuroscience *2*, 502-511.
Yu, P., Wang, H., Katagiri, Y., and Geller, H.M. (2012). An in vitro model of reactive astrogliosis and its effect on neuronal growth. Methods in molecular biology (Clifton, NJ) *814*, 327-340.
Yun, S.P., Kam, T.-I., Panicker, N., Kim, S., Oh, Y., Park, J.-S., Kwon, S.-H., Park, Y.J., Karuppagounder, S.S., Park, H.*, et al.* (2018). Block of A1 astrocyte conversion by microglia is neuroprotective in models of Parkinson's disease. Nature Medicine *24*, 931-938.
Yutsudo, N., and Kitagawa, H. (2015). Involvement of chondroitin 6-sulfation in temporal lobe epilepsy. Experimental neurology *274*, 126-133.
Zallo, F., Gardenal, E., Verkhratsky, A., and Rodríguez, J.J. (2018). Loss of calretinin and parvalbumin positive interneurones in the hippocampal CA1 of aged Alzheimer's disease mice. Neuroscience Letters *681*, 19-25.
Zamanian, J.L., Xu, L., Foo, L.C., Nouri, N., Zhou, L., Giffard, R.G., and Barres, B.A. (2012). Genomic Analysis of Reactive Astrogliosis. The Journal of Neuroscience *32*, 6391-6410.
Zhan, Y., Paolicelli, R.C., Sforazzini, F., Weinhard, L., Bolasco, G., Pagani, F., Vyssotski, A.L., Bifone, A., Gozzi, A., Ragozzino, D.*, et al.* (2014). Deficient neuron-microglia signaling results in impaired functional brain connectivity and social behavior. Nature Neuroscience *17*, 400-406.
Zhang, H., Yan, S., Khambu, B., Ma, F., Li, Y., Chen, X., Martina, J.A., Puertollano, R., Li, Y., Chalasani, N.*, et al.* (2018). Dynamic MTORC1-TFEB feedback signaling regulates hepatic autophagy, steatosis and liver injury in long-term nutrient oversupply. Autophagy *14*, 1779-1795.
Zhang, J., and Dong, X.P. (2012). Dysfunction of microtubule-associated proteins of MAP2/tau family in Prion disease. Prion *6*, 334-338.
Zhang, Y., Chen, K., Sloan, S.A., Bennett, M.L., Scholze, A.R., O'Keeffe, S., Phatnani, H.P., Guarnieri, P., Caneda, C., Ruderisch, N.*, et al.* (2014). An RNA-Sequencing Transcriptome and Splicing Database of Glia, Neurons, and Vascular Cells of the Cerebral Cortex. The Journal of Neuroscience *34*, 11929-11947.
Zielonka, D., Piotrowska, I., Marcinkowski, J.T., and Mielcarek, M. (2014). Skeletal muscle pathology in Huntington's disease. Frontiers in physiology *5*, 380.